Fakultät für Medizin

Klinikum rechts der Isar

Novel model for *in vivo* imaging of large arteries in steady state and atherosclerosis using 2 photon microscopy

A comparison of the role of Mac-1 integrin in leukocyte crawling in steady state or inflammation in small vessels and carotid arteries

Raffaele Coletti

Vollständiger Abdruck der von der Fakultät für Medizin der Technischen Universität München zur
Erlangung des akademischen Grades eines

Doctor of Philosophy (Ph.D.)

genehmigten Dissertation.

Betreuer: Univ.-Prof. Dr. Steffen Maßberg

Vorsitzende: Univ.-Prof. Dr. Agnes Görlach

Prüfer der Dissertation:

1. Univ.-Prof. Dr. Jürgen Ruland

2. Univ.-Prof. Dr. Dr. Stefan Engelhardt

Die Dissertation wurde am 24.01.2014 bei der Fakultät für Medizin der Technischen Universität München eingereicht und durch die Fakultät für Medizin am 18.03.2014 angenommen.

Contents

1. Introduction

Inflammation is defined as a complex physiological biological process during which the host raises defence mechanisms against harmful stimuli such as irritants, damaged cells and pathogens. Cells of the myeloid leukocyte lineage (monocytes – neutrophils) play a pivotal role in this process by accumulating in the affected area and eliminating the factors that lead to the inflammatory response[1,2]. In order to arrive at the site of inflammation leukocytes are following a multistep cascade for their migration to sites of inflammation. According to this cascade the cells initially tether and passively roll on the activated endothelium, subsequently they adhere stronger and finally transmigrate in the tissue[3]. Recently neutrophil intraluminal crawling, an additional post adhesion step of leukocyte recruitment on the endothelium was discovered and therefore the classical migration cascade was updated[3,4]. Crawling was proven to be an essential dynamic step in the process of leukocyte migration into inflamed tissues. The previously published data suggest that the molecules that regulate leukocyte adhesion and crawling are the beta-2 integrin family members LFA-1 (CD11a/CD18) and Mac-1 (CD11b/CD18), expressed on leukocytes, and their cognate ligands (cell adhesion molecules-CAMS) expressed on the endothelium[5-7] . However, the exact role of beta2 integrins and their interplay in these processes are not fully investigated so far. The basic approaches addressed to analyse the mechanisms of crawling, were based either on the use of Mac-1 or LFA-1 deficient mice or on injection of function blocking antibodies prior to *in vivo* imaging [4,8]. However, since both these integrins have been shown to be involved in previous steps of the migration cascade such as slow rolling and firm adhesion[8-10], the lack of their expression or the early injection of blocking antibodies against them could influence steps of the migration cascade precedent to crawling. Therefore, following these approaches, it could not be excluded that the effect detected on crawling is a secondary phenomenon.

Apart from leukocyte recruitment through post-capillary venules in the case of acute inflammation, monocytes and neutrophils are also recruited in conditions of chronic inflammation such as atherosclerosis and vasculitis in the vessel wall of large arteries[11,12]. In the case of atherosclerosis, the inflamed arterial wall develops gradually an atherosclerotic plaque (containing lipids, leukocytes and necrotic

cells)[13]. This can eventually lead to life threatening conditions, such as myocardial infarction, due to stenosis and complete occlusion of the affected vessel. The leukocyte migration cascade in that case was only partially analysed due to limitations of the available intravital techniques. Thus, leukocyte crawling and transmigration in atherosclerotic vessels was never detected *in vivo* so far.

Recent *in vivo* data proved that crawling can occur also under physiological steady state conditions. A specific subset of non inflammatory ("patrolling") monocytes was shown to be able to crawl on the non stimulated endothelium of murine venules and arterioles[14]. In this way monocytes are thought to patrol the endothelium of blood vessels and clear it from adhering molecules that could eventually lead to an inflammatory reaction. The crawling process of patrolling monocytes in the micro-vasculature is thought to be regulated by LFA-1 while Mac-1 is thought to be dispensable. Crawling of patrolling monocytes in the case of large arteries was never studied so far[14].

This dissertation provides a study of the direct effect of blocking of beta-2 integrins in the process of leukocyte crawling in the microvasculature under steady state and acute inflammatory conditions. Furthermore a novel model for long-term *in vivo* imaging of large vessels by the use of two photon microscopy will be presented. Based on this model the effect of blocking of the beta-2 integrins (with a major focus on Mac-1) on leukocyte crawling will be studied under steady state and inflammatory conditions in large arteries (carotid artery) and will be compared with the case of small vessels (post-capillary venules, arterioles) under the same conditions.

2. Leukocytes subsets recruited in the tissue during inflammation and steady state

2.1 Neutrophils

Neutrophil granulocytes (also known as polymorphonuclear leukocytes – PMNs) are the most abundant immune cell type in human blood[15] and play a pivotal role in the responses of the innate immune system. Together with monocytes neutrophils are thought to derive from the granulocyte – monocyte precursor (GMP)[16]. Action of M-CSF leads towards a monocyte differentiation while action of G-CSF leads to

granulocyte development[17]. The chemokine receptors CXCR2 (responsible for mobilization) and CXCR4 (responsible for retention and homing), expressed on the surface of neutrophils, are the key players for their homeostasis in the bone marrow[18]. Under steady state conditions only a small proportion of cells is released from a neutrophil pool in the bone marrow while their half-life in circulation is 6-8 hours[19]. Polymorphonuclear leukocytes are considered to be phagocytes that act in the front line of the immune responses. Upon recruitment in areas of inflammation or injury they contribute to the host defence by phagocytosing pathogens and by releasing reactive oxygen species as well as granule proteins such as elastase, myeloperoxidase and metalloproteinases which have hydrolytic and bactericidal functions[20]. Furthermore, through the release of cathelcidins they are thought to regulate the recruitment of other types of leukocytes such as monocytes[21]. An additional mechanism through which neutrophils are thought to fight bacteria is by releasing their DNA which creates traps for these pathogens[22]. These are widely known as neutrophils extracellular traps and have recently gained a lot of attention. Neutrophils are also thought to produce pro-angiogenic molecules such as VEGF and MMP9 that contribute to tissue restitution [23]. Interestingly however, the release of factors such as ROS and proteases apart from contributing to the host defence is also involved in various pathologic conditions through damage of the host tissue[24,25]. In that context apart to their involvement in acute conditions such as acute lung injury and myocardial ischemia reperfusion injury[26], neutrophils are also thought to be involved in chronic conditions such as rheumatoid arthritis, chronic obstructive pulmonary disease (COPD), asthma and atherosclerosis[27-29].

2.2 Monocytes

Monocytes are white blood cells that also constitute an important part of the innate immune system. They are produced in the bone marrow and derive from a monocyte, macrophage and dendritic cell precursor (MDP) which derives from the granulocyte – monocyte precursor (GMP)[16]. They represent the 10% of leukocytes in human blood and the 4% of leukocytes in mouse blood[30]. Three types of monocytes have been

detected in humans: 1) classical-inflammatory monocytes which represent the 80% to 90% of blood monocytes and are characterized by high expression of CD14 and no expression of CD16, 2) non classical-non inflammatory monocytes (also known as resident) which represent the 10-15% of blood monocytes and are characterized by low expression of CD14 and high expression of CD16, 3) intermediate monocytes which are characterized by an intermediate expression of CD14 and high expression of CD16[30,31].

In mice two types of monocytes were described so far: the classical monocytes and the non classical monocytes [32].

2.2.1 Classical (inflammatory) monocytes

The first mouse subset of monocytes (also known as classical or inflammatory monocytes) is equivalent to the classical $CD14^{high}$ human monocytes [32]. The classical monocytes are phenotypically characterized by high expression of the granulocyte differentiation antigen 1 (Gr1), the chemokine receptor CCR2, and the cell adhesion molecule L-selectin, while the chemokine receptor CX3CR1 (fraktalkine) is expressed in low levels. Therefore, they are characterized as $CX3Cr1^{low}CCr2+GR1+$ cells[14,30]. As their name suggests inflammatory monocytes are recruited in areas of inflammation [2]. This process implicates the chemokine receptor CCR2 via binding of chemotactic cytokines such as CCL2 and CCL7[2]. Furthermore, it was shown that neutrophils (which provide a fast initial immune response) can also regulate the recruitment of inflammatory monocytes by secretion of granule proteins such as LL37 in areas of transmigration [33].These factors activate formyl peptide receptors (FPR) on inflammatory monocytes stimulating further their recruitment [33]. Once extravasated, inflammatory monocytes produce inflammatory factors such as reactive oxygen species, complement factors, prostaglandins, cytokines (such as TNF-α, IL-1β, CXCL8, IL-6, and IL-10) and proteolytic enzymes [30,34,35], and can further differentiate in macrophages and dendritic cells [30,34,36,37]. The inflammatory monocytes contribute to the host defence both in the case of tissue damage (myocardial infarction) and bacterial or viral infections[38-40].

2.2.2 Non classical (non inflammatory, patrolling, resident) monocytes

The second subset of monocytes (equivalent to the $CD14^{low}$ human monocytes, also known as “patrolling” or “resident”) is characterized by a smaller size but higher expression of the chemokine receptor CX3CR1 as well as expression of the beta2 integrin LFA-1. However, they do not express Gr1, CCR2, or L-selectin[30]. Therefore they are generally identified as $CX3Cr1^{high}$CCr2-GR1- cells. The non classical monocytes are found in both inflamed and non inflamed tissues. In steady state conditions they are thought to be responsible for the renewal of tissue resident macrophages, dendritic cells and osteoclasts[32,41]. However, there are also studies suggesting that the renewal of tissue resident macrophages is independent from the circulating monocytes and rely on the ability of tissue resident monocytes for self-renewal [42]. Interestingly, it was recently shown that the non classical monocytes are able to intravascularly actively migrate for long distances along the non activated endothelium of post-capillary venules and arterioles during steady state[43]. In addition, it was shown that through this active dynamic behaviour patrolling monocytes are able to clear the microvasculature of the mouse kidney from foreign bodies such as adherent fluorescent beads (injected during the experiment) and furthermore to recruit neutrophils in a Toll like receptor 7 (TLR7) dependent manner. This process leads to neutrophil dependent endothelial cell necrosis and to further removal of cellular debris by the non classical monocytes[44]. Therefore, apart from populating the tissue with resident macrophages or dendritic cells, non classical monocytes are also thought to patrol (therefore they are also known as “patrolling” monocytes) the endothelium during steady state and clear it from possible infectious agents.

3. Basic mechanisms of leukocyte migration during inflammation and steady state

In the case of an immune reaction leukocytes (mainly neutrophils and inflammatory monocytes) are generally thought to follow a multistep cascade for their migration to the sites of inflammation[3]. In the first step of this cascade circulating leukocytes are loosely tethered and start to roll on the activated endothelium following the direction of the blood flow in a fast and passive way[3]. The rolling process becomes eventually

slower and subsequently firm adhesion occurs[3]. In a next step, leukocytes actively move on the activated endothelium being able to follow the blood flow but also to move against it[3]. This process is named crawling and it is significantly slower than rolling. Subsequently, transcellular or paracellular transmigration takes place and leukocytes reach the interstitium through gaps between the pericytes[45] (Figure 1). These sequential steps required for extravasation to areas of inflammation are known as “leukocyte migration cascade”.

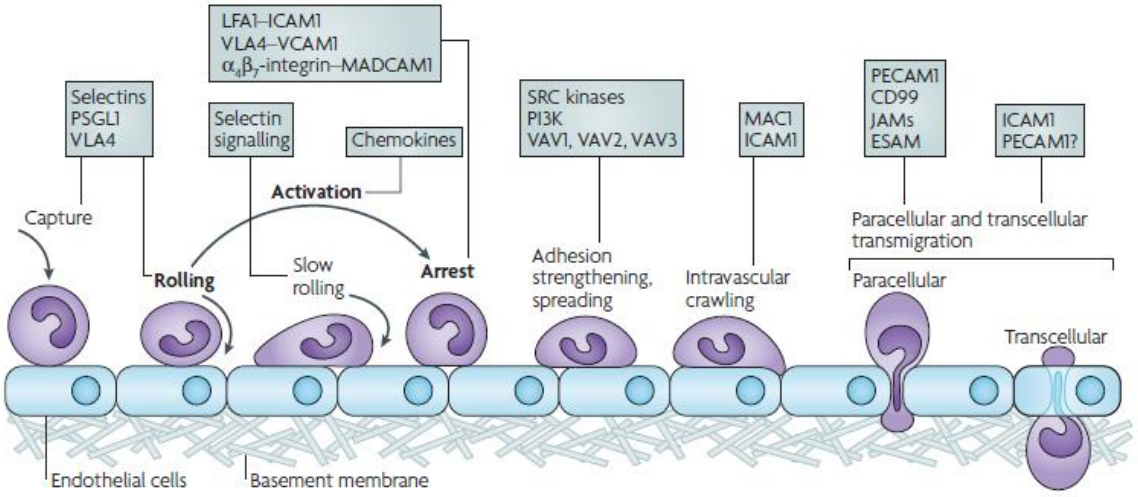

Taken from *Ley K et al, Nat Rev Immunol, 2007*

Figure 1. Leukocytes migration cascade in sites of inflammation[3]. Detailed information is provided in the text.

Interestingly however, the dynamic process of crawling was shown to take place not only in inflammation but also during steady state conditions in venules and arterioles by a specific subset of non inflammatory monocytes. In that way, this subset of monocytes is thought to patrol and clear the endothelium from pathogens that could eventually lead in an inflammatory reaction.

3.1 Steps of leukocyte migration to the tissue

3.1.1 Rolling on activated endothelium in inflammation

Rolling is mainly regulated by a group of proteins that are called selectins. These are carbohydrate-binding molecules that bind to fucosylated and sialylated glycoprotein ligands, and are found on endothelial cells, leukocytes and platelets[46]. There are three major types of selectins: a) L-selectin which is expressed by granulocytes, monocytes and lymphocytes, b) P-selectin which is expressed by endothelial cells and platelets and c) E-selectin which is expressed by activated endothelial cells. The major ligand of all the types of selectins is P-selectin glycoprotein ligand -1 (PSGL-1) which is expressed by both endothelial cells and leukocytes. Apart from PSGL1, E-selectin can also bind to CD 44 and E-selectin ligand 1 (ESL-1)[3].

Apart from selectins it was also reported that certain types of integrins play role in the process of rolling[9,10,47]. Integrins are a large family of transmembrane heterodimeric glycoprotein receptors. They consist of paired alpha (at least 18 types are known) and beta subunits (8 types are known), which form 24 distinct integrin heterodimers (Figure 2)[48]. During steady state the integrins are inactive and adopt a bent conformation that leads to low affinity bonds with adhesion molecules such as ICAM-1 and VCAM-1 expressed on the activated endothelium. However, upon activation they adopt an extended high affinity conformation[3,49,50].

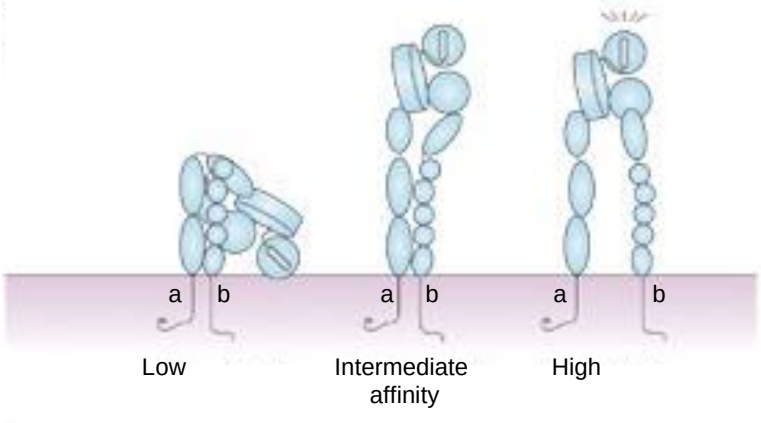

Taken from: *Tatsuo Kinashi et al, Nat Rev Immunol, 2005*

Figure 2. Integrin activation state[50].

One of these types of molecules, the α4β1 integrin very late antigen 4 (VLA-4), can interact upon activation with vascular cell adhesion molecule 1 (VCAM 1) and also with P-selectin supporting the process of rolling in post-capillary venules[47]. Furthermore rolling of leukocytes on E-selectin but also ICAM-1 induces an intermediate affinity conformation of the αLβ2-integrin lymphocyte function-associated antigen 1 (LFA-1, CD11a/CD18, αLβ2) for its endothelial ligands which leads to a process of slow rolling[3]. Further studies implicate in the process of slow rolling also macrophage -1 antigen integrin (Mac-1, CD11b/CD18)[9].

3.1.2 Activation and arrest on activated endothelium in inflammation

Cells in the interstitial tissue at sites of inflammation release cytokines which in their turn lead to the activation of the endothelial cell layer of post-capillary venules. This results apart from the expression of selectins and adhesion molecules (CAMs) also in the presentation of chemokines by endothelial cells. These are small proteins produced and released upon action of inflammatory cytokines, able to regulate the directed recruitment of leukocytes to areas of inflammation[51-53]. Chemokines such as CCL5, CXCL4, CXCL5 are thought to be involved in these processes and are presented on glycosaminoglycans (GAGs) on the endothelial-cell surface[54]. Through the processes of rolling and slow rolling of leukocytes, chemokines present on the endothelial cell layer bind to G–protein coupled receptors (GPCRs) expressed on leukocytes[55]. These interactions lead to an activation of integrins which is mediated by bidirectional integrin signalling. During an initial so called ‘‘inside out’’ signalling intracellular ligands such as talin or kindlin bind to the beta subunit of the integrins. Through this binding integrins transit from a bent low‐affinity conformation to extended intermediate-and high-affinity conformations, which allow firm binding to adhesion molecules such as ICAM1 and VCAM1 and results in the firm adhesion of leukocytes[56]. The high affinity binding of integrins to their extracellular ligands has as a result an outside– in signalling which leads to integrins clustering[3,56] (Figure 3). This is achieved by an increase in tyrosine phosphorylation and to second messengers such as phosphatidylinositol-4,5 biphosphate[53], which can regulate the

rearrangement of the cytoskeleton allowing leukocytes to adhere stronger on the endothelium and to migrate. Research regarding the mechanism of leukocytes adhesion has mainly focused in the last years on the role of the beta 2 integrins LFA-1 and Mac-1.

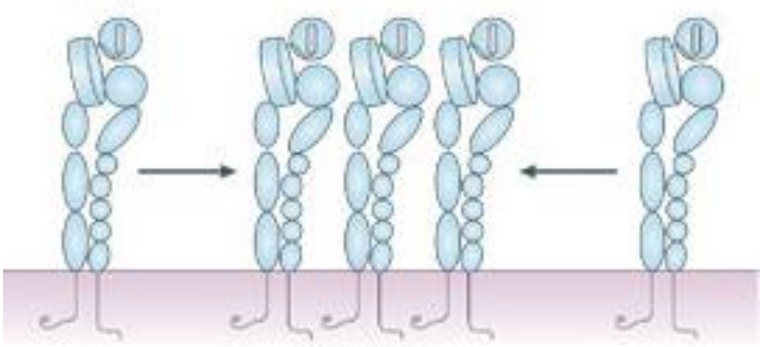

Clustering

Taken from*: Tatsuo Kinashi et al, Nat Rev Immunol, 2005*

Figure 3. Integrins clustering due to outside in signalling[50].

Data from experiments performed *in vivo* in the microvasculature of the murine cremaster muscle under conditions of acute inflammation appear to be controversial regarding the role of these two beta 2 integrins in this process. Initially it was suggested that leukocytes imply mainly LFA-1 in order to firmly adhere on the activated endothelium upon stimulation with TNF-a[57]. Interestingly however, further experiments showed that the role of the beta-2 integrins LFA-1 and Mac-1 in leukocytes adhesion can be stimulus dependent[58]. In that case adhesion of leukocytes was again LFA-1 dependent upon treatment with fMLP. In contrast fMLP stimulation in addition to TNF-α resulted in a Mac-1 dependent adhesion while LFA-1 was dispensable[58]. Apart from *in vivo* experiments also *in vitro* studies indicate that not only LFA-1 but also Mac-1 can mediate adhesion of neutrophils on the activated endothelium[59]. Furthermore recent findings indicate that the role of LFA-1 and Mac-1 in the process of adhesion depends on the type of tissue where the process of migration cascade takes place. *In vivo* experiments performed in mouse liver upon

thermal tissue injury revealed that the adhesion of neutrophils in the vicinity of sites of inflammation was Mac-1 dependent and LFA-1 independent[60]. All these controversial findings clearly show that there is still a need for a better understanding regarding the role of these beta 2 integrins in this process of adhesion.

3.1.3 Crawling along the endothelium during inflammation and steady state

3.1.3.1 Inflammation

Data from in vitro studies in 2004 suggested that monocytes are able to actively move from a site of firm adhesion to the nearest junction and transmigrate. This active movement was named initially “locomotion” [61]. Later studies[57] confirmed that leukocytes are able to actively move on the activated endothelium upon adhesion, a process which is widely characterized now as “crawling”. The reason why neutrophils and leukocytes in general crawl is thought to be that in that way they reach the most favourable areas for their migration which are the endothelial junctions. This active and dynamic behaviour of leukocytes is thought to be mainly regulated by the beta 2 integrin Mac-1 [57] since injection of blocking antibodies against it or the use of Mac-1 knockout mice leads to a decreased ratio of crawling / adhering cells[4]. The previously used approaches to test the role of beta-2 integrins on leukocyte crawling *in vivo* (except from the use of KO mice) included the following steps: a) performing initial baseline *in vivo* imaging without application of blocking antibody, where a number of leukocytes are detected adhering and crawling, b) stop of the recording and application of blocking antibody against Mac-1 and finally c) secondary *in vivo* imaging [62]. The number of crawling cells as well as the general crawling behaviour of leukocytes in the secondary recording was compared with the crawling leukocytes detected in the initial recording. An additional approach in this type of studies is to inject blocking antibodies against Mac-1 prior to the intravital imaging[4,57]. The majority of the data from the experiments performed following these approaches indicate that leukocytes were still able to adhere but unable to crawl on the activated endothelium[4,57]. These approaches however, did not permit for analysis of the direct effect of blocking of Mac-1in the crawling process of leukocytes. In addition, it cannot be excluded that precedent steps of the migration cascade such as rolling and

adhesion are already influenced and therefore the effect detected on crawling could be a secondary phenomenon. Regarding the role of LFA-1 in adhesion and crawling processes the same experimental approaches were followed. However, its role in crawling could not be so far analysed in details *in vivo* (especially in the case of neutrophil recruitment in inflammation) following these experimental protocols since only small numbers of cells adhered upon application of blocking antibodies against LFA-1[57]. In the case of LFA-1 deficient mice, leukocytes failed anyway to initially adhere and thus to subsequently crawl, although the few cells that managed to adhere could crawl in a normal way[4]. Again in that case however, the direct effect of blocking of LFA-1 on crawling was not studied. Thus, it cannot be excluded that this molecule apart from adhesion plays a role also in the crawling process of leukocytes.
Further *in vitro* results showed that neutrophils are able to crawl in every direction after application of shear stress conditions while interestingly the majority of neutrophils crawl perpendicular or upstream to the blood flow *in vivo*[63]. In these studies only a percentage of about 30% of neutrophils crawl downstream to the direction of the blood flow[63]. Under flow conditions the endothelial cells are elongated and aligned to the blood stream. Therefore, it is hypothesized that through perpendicular crawling leukocytes reach within shorter distances endothelial cell junctions which are thought to be favourable areas for transmigration and extravasation[4].
In vitro studies indicate that this perpendicular or upstream crawling is rather a mechanotactic dynamic behaviour than a chemotactic since neutrophils were still able to crawl *in vitro* perpendicularly and upstream to the flow direction upon application of shear forces even in the absence of chemotactic gradients[63]. *In vivo* experiments performed in VAV1-/- mice revealed that neutrophils were not able to crawl perpendicularly to the blood flow and presented ability only for passive downstream crawling[63]. Additionally they failed to reach and strongly adhere to endothelial junctions thus showing limited migratory potential. VAV-1 mediates intercellular activation downstream to LFA-1 in all types of leukocytes and is responsible for cytoskeleton reorganization and cellular polarization during migration[64]. Although previous studies revealed a crucial role of Mac-1 in the process of crawling in general, blocking of Mac-1 had no effect in the downstream crawling of

the VAV-1 deficient neutrophils. This finding could imply that the Mac-1 beta-2 integrin could also participate in the regulation of the upstream and perpendicular crawling of neutrophils. Apart from VAV-1, also HPK1 (hematopoietic progenitor kinase 1) is thought to play a role in the mechanotactic behaviour of neutrophils. HPK1 co- immunoprecipitates with the actin binding protein mApB1 which is an adaptor protein that regulates activation of neutrophils downstream to LFA-1. Again in that case *in vivo* experiments performed in HPK1$^{-/-}$ mice showed that the mechanotactic perpendicular crawling of neutrophils was significantly reduced[65]. These observations are also supported by studies performed *in vitro* which suggest that LFA-1 supports the mechanotactic perpendicular crawling of neutrophils[64]. Additionally further studies in regard to lymphoid cells (T cells) reveal that LFA-1 plays an important role in T lymphocytes crawling[66].

These data in total underline the significance of both beta-2 integrins in the process of leukocyte crawling. However, they do not provide clear information regarding their role especially in regard to the direction of crawling. Furthermore, the way that these studies were performed cannot exclude the possibility that the detected effects on crawling upon blocking of Mac-1 or LFA-1 are secondary phenomena. Finally, it should be also underlined that leukocyte crawling has been studied so far only in the case of postcapillary venules under acute inflammatory conditions. Whether this process takes place in large inflamed arteries was never studied so far.

3.1.3.2 Steady state

As discussed neutrophils are able to adhere and crawl on the activated endothelium during inflammatory reactions. However, there is no evidence provided in the literature regarding neutrophil recruitment and crawling in unstimulated vessels during steady state[57]. In contrast, recent *in vivo* data show that the CX3CR1^{high}CCr2-GR1- subset of monocytes (patrolling monocytes) are able to adhere and actively crawl on unstimulated venules and arterioles in mice[14]. Patrolling monocytes follow crawling paths that are characterized as hairpin, wavy, loop and mixed being in general able to move also against the blood flow in post-capillary venules and arterioles[14]. Interestingly under steady state conditions it was shown that blocking of Mac-1 had no effect on the crawling behaviour (crawling velocity, distance and

number of crawling cells) of patrolling monocytes. In contrast, blocking selectively only of LFA-1 significantly reduced monocytes adhesion and crawling on the endothelium.

Therefore, it was proposed that LFA-1 regulates the crawling of these cells under steady state while Mac-1 was considered to be dispensable in that case[14,57]. However, the experimental procedure followed in these studies again did not allow for analysis of the exact direct effect of blocking of beta-2 integrins in the crawling process of patrolling monocytes. Additionally, whether this process takes place also in large arteries under steady state conditions and which are the mechanisms that regulate it was also not analysed so far.

3.1.4 Transmigration during inflammation

In the case of inflammation the subsequent step of the migration cascade of leukocytes upon crawling regards their transmigration through the endothelial cell layer of the vessel. Leukocytes generally have to overcome three layers upon crawling in order to transmigrate through the venular wall. These layers are the endothelial cells, the endothelial cell basement membrane and pericytes[45]. The migration through the endothelial cells can occur either in a paracellular (which is the most common) or transcellular way[3]. Binding of leukocyte integrins to endothelial cell adhesion molecules (ICAM-1, VCAM-1) leads to formation of docking structures from the endothelial cell layer[3,67]. These are projections of the endothelial cells rich in ICAM-1, VCAM-1, cytoplasmic molecules such as esrin and cytoskeletal components such as vinculin, a-actinin and talin–1[3,67]. Subsequently these docking structures cluster and associate with cytoplasmic proteins related to phosphatidylinositol 4,5-bisphosphate and Rho family GTPases[68]. This process finally leads to the activation of the myosin light chain kinase and subsequently to endothelial contraction and opening of interendothelial contacts. Through these areas leukocytes are able to leave the lumen of the vessel and reach the subendothelial region[3]. Additionally an active redistribution of junctional endothelial molecules occurs, during which molecules that do not favour transmigration (pe VE cadherin) are distributed away from the junction. In contrast, the molecules that facilitate the transmigration such as

PECAM-1 and JAM-A, are mobilised to the luminal side of the endothelium[3,69]. The endothelial molecules that are involved in this type of paracellular transmigration are the PECAM-1, ICAM-1, ICAM-2, JAM-A, JAM-B, JAM- C, and CD99.The beta 2 integrin LFA-1 is highly involved in this process through interactions with junctional ICAM-1 and ICAM-2[3].

Leukocyte transcellular migration is based on the presence of “vesiculo-vacuolar organelles “(VVOs) within the endothelial cells. These VVOs are clusters of vesicles within the cytoplasm of endothelial cells which function as intracellular channels through which leukocyte can migrate[70]. Once present in the subendothelial area of the vessels leukocytes were reported to be still able for motility in order to find gaps between adjacent pericytes through which they reach the interstitial tissue[45,71].

4. Leukocyte recruitment under conditions of sterile inflammation in the micro-vasculature and macrovasculature

4.1 Leukocyte recruitment in the microvasculature during acute sterile inflammation

The term sterile inflammation describes the inflammatory reaction that develops in the absence of an infectious signal or agent and usually is triggered by the necrosis of cells of the organism. According to the danger hypothesis which was proposed in 1994 by Matzinger the immune system can respond not only to infection per se but also to non physiological cell death, damage or stress[72]. Conditions that include trauma, ischemia reperfusion injury, chronic inflammatory reactions in large arteries (atherosclerosis) or even cancer are related to sterile inflammatory conditions through cellular necrotic processes. Living cells contain factors that can lead to an inflammatory reaction upon release. These factors are called “danger associated molecular patterns” (DAMPs) and examples of these are HMGB1 (high mobility group box 1 protein), heat shock proteins, uric acid ,genomic DNA, and ADP[73]. The plasma membrane in living cells does not allow to these intracellular molecules to come in contact with the cells of the innate immune system. However, when cells undergo necrosis they lose the integrity of their plasma membrane and release their

intracellular contents, including DAMPs. This can also occur when apoptotic cells aren't rapidly cleared undergoing a process of secondary necrosis[74] (Figure 4).

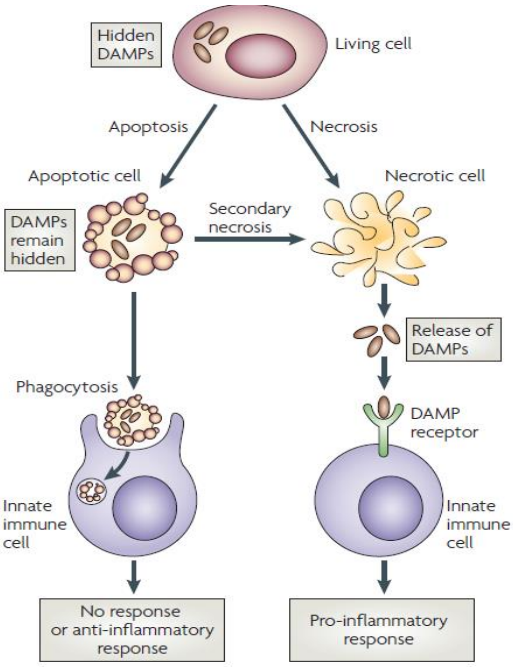

Taken from: *Kono,H & Rock,K.L. Nat Rev Immunol, 2008*

Figure 4. Danger associated patterns released from necrotic but not apoptotic cells lead to inflammatory responses[74].

Upon release, DAMPS are recognised by a variety of receptors expressed on leukocytes and endothelial cells such as the purinergic receptors P2X7 and P2X2, the toll-like receptors TLR2 and 4, CD91, CD24, the formyl peptide receptors FPR1 and FPR2 and the receptor for advanced glycation end-products (RAGE)[75]. The exact mechanisms through which the binding of several DAMPs to their receptors leads to an inflammatory reaction remain to be fully elucidated. However, the alarmin HMGB1 (that in living cells acts as a non-histone nuclear protein that binds to DNA and facilitates gene transcription) gained a lot of attention over the last years. Research in that field revealed that its binding to TLR 2,TLR 4 and RAGE leads to activation of the NFkB transcription factor and subsequently to an inflammatory reaction[76].

A key player in the triggering of the inflammatory response induced by sterile inflammation is interleukin 1 (IL1) which is thought to derive mainly from tissue resident macrophages. Once released IL1 (including both IL1α and IL1β) leads to the upregulation of endothelial adhesion molecules and the production of additional inflammatory factors. Mice deficient for IL1 show reduced neutrophil recruitment in sterile inflammation[77]. Recently, spinning disk confocal intravital microscopy was applied in order to investigate molecular mechanisms of neutrophil recruitment to sites of focal hepatic necrosis which resembled an area of sterile inflammation. In this context the major DAMP that was analysed was ATP which was proposed to bind to the purinergic P2X7-receptor thereby inducing the Nlrp3 inflammasome activation which finally leads to the production and secretion of IL1[75].This created an intravascular inflammatory microenvironment which resulted in adhesion of neutrophils on the activated endothelium. Interestingly enough, this adhesion was Mac-1 dependent (through binding to ICAM1) and LFA-1 independent. Furthermore it was proposed that neutrophils reach the area of sterile inflammation through a process that involves the initial step of adhesion which is followed by directed migration towards chemotactic gradients initially and subsequently towards "necrotactic" stimuli (dependent on release of N-formyl peptides from necrotic cells) in the vicinity of the sterile injury[75]. This process was named necrotaxis.

The recruitment of leukocytes to sites of sterile inflammation is thought to follow the updated multistep migration cascade. However the exact role of LFA-1 and Mac-1 during leukocyte migration especially in the context of sterile cell necrosis was not fully analysed so far.

4.2 Leukocyte recruitment in large arteries during atherosclerosis

4.2.1 Atherosclerosis: chronic sterile arterial inflammation

Atherosclerosis is a chronic inflammatory disease of the medium and large sized arteries of the body which is characterised by a thickening of the affected area of the vessel wall[13]. This eventually leads to formation of atherosclerotic plaques which are responsible for reduction in the diameter of the lumen and eventually for complete occlusion of the vessel upon plaque rupture due to thrombotic effects[78].

Subsequently, this condition can have as a final result the infarction of the organ that it is supplied with blood from this vessel. In the case of coronary artery disease this is often manifested as a myocardial infarction. The arterial wall consists of three layers. The *tunica adventitia* is the outermost layer and it is composed of connective tissue and collagen. The *tunica media* is the middle layer and it is composed of smooth muscle cells and elastic tissue. Finally, the *tunica intima* is the innermost layer and consists of a single layer of endothelial cells (Figure 5).

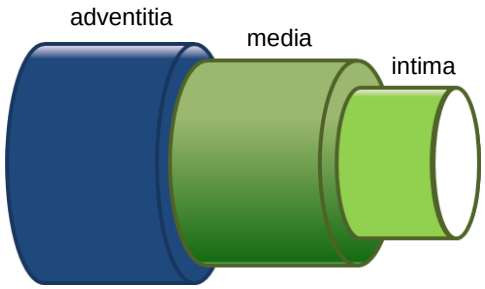

Figure 5. Layers of arterial wall

Atherosclerosis is a disease that develops gradually in sequential stages and involves all the layers of the arterial wall[13,79]. A very early triggering step in the atherosclerotic plaque formation is considered to be the endothelial denudation as this is proposed in the response to injury theory [80]. Additionally apart to the endothelial injury per se also endothelial dysfunction (impaired arterial vasodilation) is thought to contribute in the very early stages of the plaque formation[81-83]. These alterations in the endothelial function and homeostasis lead to increased permeability of the endothelial cell layer to lipoproteins (LDL)[84]. The trapped LDL particles undergo a process of oxidation by myeloperoxidase, lipoxygenase and reactive oxygen species which has as a final result the activation of the endothelial cells and the up regulation of leukocyte adhesion molecules[85-87]. Additionally oxidized LDL is phagocytosed by monocytes and macrophages (transforming subsequently in foam cells) which together with T cells contribute to the development of fatty streaks which resemble the initial form of the plaques[78]. During this initial period of ongoing chronic inflammation cytokines produced in this inflammatory environment such as TNF-a and IL-2 lead to T cell activation[87]. Furthermore, factors such as PDGF (platelet

derived growth factor) or TGFβ (transforming growth factor b) lead to the proliferation and migration of smooth muscle cells[78]. This migration of smooth muscle cells from the *tunica media* to the endothelial cell layer is responsible for the formation of a fibrous cap which is characteristic of an advanced atherosclerotic lesion. This fibrous cap covers a mixture of leukocytes, lipids and debris (Figure 6).

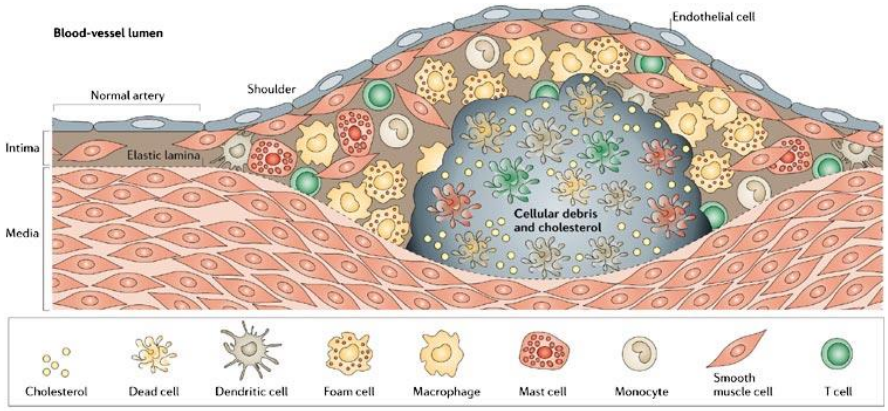

Taken from: *Hansson GK, Libby P, Nat. Rev. Immunol 2006*

Figure 6. The atherosclerotic plaque contains leukocytes, cellular debris and cholesterol[12].

In a final stage it is possible that the fibrous cap ruptures leading to acute atherothrombotic effects. This phenomenon has been attributed so far to the activation of macrophages which release metalloproteinases and proteolytic enzymes at the sites of rupture. Additionally through this mechanism the activated macrophages can also lead to a rupture of microvessels within the atherosclerotic plaque leading to intraplaque haemorrhage[78].

During the process of atherosclerotic plaque development the endothelial cell layer which under steady state conditions is very thin becomes thickened and contains a big number of immune cells and lipids. Interestingly, leukocyte accumulation is observed not only in the intimal but also in the adventitial side of the plaque raising the so far unanswered question for the major entrance pathway of these cells into the arterial wall[13]. T cells and macrophages are the most abundant cellular component of the developing atherosclerotic plaque and have been studied extensively. However, different types of monocytes as well as neutrophils are also involved in the process of

atheroprogression and gained attention over the last years[29]. Primarily macrophages but possibly also neutrophils are thought to be responsible for phagocytic clearance of apoptotic cells (such as foam cells) through a process which is termed efferocytosis[88]. In advanced atherosclerotic plaques however, efferocytosis is not efficient enough to clear apoptotic cells. Whether this is a result of defective efferocytosis or extensive apoptosis is not clear, however the outcome remains an increase in secondary necrosis of apoptotic cells leading to formation of large necrotic cores within the plaques[88]. Thus, there is a direct link of atherosclerosis with the condition of sterile inflammation (mediated by cellular necrosis) which was mainly analysed so far *in vivo* only in small vessels. One of the better studied DAMPS in the case of atherosclerosis is HMGB1[89]. Studies performed both in humans and mice reveal its indispensable role in the process of atherosclerotic plaque formation[90]. Neutralization of HMGB1 in hypercholesterolemic mice leads to reduced development of atherosclerosis[91]. Interestingly in humans it was shown that simvastatin (which is administered to patients in order to reduce cholesterol levels) supresses the HMGB1/RAGE axis reducing in that way leukocyte recruitment and subsequently the formation of atherosclerotic plaques[92].

4.2.2 Myeloid subsets in atherosclerosis

4.2.2.1 Neutrophils

In contrast to other subsets of leukocytes such as T cells, macrophages, dendritic cells and monocytes, neutrophils did not initially gain attention in the context of atherosclerosis. To this contributed also the fact that they could be detected only with difficulty within atherosclerotic lesions with *ex vivo* techniques such as immunohistochemistry[29]. However, over the last years a lot of attention was drawn on them in the context of atherosclerosis since several data indicate that they decisively contribute in the process of atherogenesis and atheroprogression[93]. Advances of labelling techniques confirmed their presence within human atherosclerotic lesions post mortem[94] but also within mouse lesions. Neutrophils account for the 1,8% of the CD45 positive leukocytes in the aortic wall of ApoE deficient mice (hypercholesterolemic mice that develop atherosclerotic plaques upon feeding with a high

cholesterol diet) and accumulate mainly in the shoulder regions of atherosclerotic lesions[95]. Hyperlipidemia per se, has as a result monocytosis but also neutrophilia due to enhanced granulopoiesis and mobilisation from the bone marrow while depletion of neutrophils leads to reduced plaque size at early stages of atherosclerosis revealing their detrimental role in the process of atherogenesis[93]. Disruption of the CXCL12/CXCR4 axis which provides a retention signal for neutrophils in the bone marrow leads to a significant increase of neutrophil counts in blood (while the increase in monocytes count is moderate) of ApoE$^{-/-}$ mice and subsequently to an aggravation of atherosclerotic plaque formation highlighting further the indispensable contribution of neutrophils in atherosclerosis[96].

The exact way through which neutrophils contribute to the atherosclerotic plaque development is not fully understood so far although several different hypotheses have been raised regarding this issue[97]. *In vivo* experiments performed in the microvasculature of the cremaster muscle of mice upon stimulation with PAF (Platelet activating factor) revealed that neutrophils regulate the recruitment and extravasation of inflammatory monocytes. Neutrophils succeed in this role by releasing granule proteins such as LL-37 and azurocidin which in their turn activate formyl peptide receptors expressed on the surface of inflammatory monocytes[33]. In addition, it was shown that proteins that reside in secondary granules of neutrophils play a role in monocytes recruitment also in the case of atherosclerosis in mice[98]. Apart to the recruitment to early stages of atherosclerotic plaque formation it was further demonstrated that neutrophils accumulate in the lesions at later time points mainly in the highly inflammatory shoulders of the plaques. In the case of humans, presence of neutrophils within the atherosclerotic arterial wall was correlated to instability of the plaques implying high possibility of plaque rupture[94,99].

4.2.2.2 Monocytes

Increasing evidence suggests a correlation between increased monocyte blood counts and atherosclerotic plaque formation in different animal models and in humans [100].As it was shown administration of high cholesterol diet to ApoE deficient mice leads to an increased number of circulating monocytes in the blood stream[100]. Additionally, it was described that monocyte accumulation in mouse atherogenesis is

proportional to the extent of the plaque formation[101]. Clinical studies in humans also correlate the peripheral monocyte blood count with cardiovascular diseases like atherosclerosis[102]. Furthermore it was shown that depletion of monocytes by application of chlodronate leads to a decreased atherosclerotic plaque formation in rabbits[103].

Both classical and non classical monocytes are thought to play a role in atherosclerotic plaque formation. However, the different role of each subset of monocytes in atherosclerosis as well as their recruitment mechanisms are not analysed in an exhausted way. Interestingly, monocytosis in hypercholesterolemic mice is attributed mainly to an increase of the classical inflammatory subset of monocyte [100]. An interesting study based on depletion of monocytes and subsequent reconstitution with either the classical or non classical subset highlighted the pivotal role of the classical population during atheroprogression [104]. In this study it was suggested that the non classical monocytes play only a minor role in atherosclerosis. Further analysis however, suggested that this type of monocytes is also able to infiltrate the plaques revealing a possible role also for them in the arterial inflammation[105]. In general the classical monocytes are thought to differentiate mainly into macrophages within the plaque while the non classical mainly into dendritic cells[106].

Regarding the recruitment of monocytes in atherosclerotic plaques the recent interest was focused in the role of chemokine receptors expressed on different monocyte subsets. CX3CL1 is expressed in early and advanced atherosclerotic lesions and mediates recruitment of monocytes via binding to the chemokine receptor CX3CR1[107]. Additionally absence of CX3CL1 or of its receptor leads to reduced atherosclerotic plaques formation in mice[108-110]. In the case of classical monocytes it was shown that apart from CCR2 and CCR5 these cells interestingly require CX3CR1 for recruitment in atherosclerotic regions although they express it in low levels[106]. In contrast, CX3CR1 was dispensable for the migration of non classical monocytes in the atherosclerotic arterial wall. The recruitment of this subset of monocytes was mainly dependent on the CCR5 chemokine receptor which is upregulated in the ApoE deficient mice mice[106].

Mechanistically, as in the case of neutrophils, monocytes are thought to follow the multistep cascade for their migration into atherosclerotic arterial walls. *Ex vivo*

experiments in excised carotid arteries from ApoE deficient mice highlighted the role of VLA-4 integrin and VCAM-1 adhesion molecule in the process of rolling of monocytes while VLA4-1 was also shown to mediate firm adhesion[111-113] . Although rolling and adhesion were analysed in the case of atherosclerosis the subsequent step of crawling in the emigration cascade was never reported and analysed *in vivo* in large inflamed vessels and therefore it remains still a hypothesis.

4.2.3 Leukocyte recruitment in atherosclerotic plaques

The study of leukocytes recruitment during the initiation and progression of the atherosclerotic disease was based for a lot of years in *in vitro* and *ex vivo* techniques. These included immunohistochemistry on sections of extracted tissue, flow cytometric quantification of the leukocyte counts in atherosclerotic plaques and *ex vivo* imaging of interactions of leukocytes with the endothelium of atherosclerotic arteries under shear stress conditions[112,114,115]. Additionally advanced imaging techniques such as SPECT/CT[116] were recently used in order to detect *in vivo* leukocyte trafficking in murine atherosclerotic plaques. These techniques provided us with important knowledge regarding the cellular composition of the plaques and with indirect information regarding the basic mechanisms of leukocyte recruitment into the inflamed arterial wall. However, they did not succeed in providing direct real time *in vivo* information regarding the dynamic behaviour of leukocytes (which includes intraluminal leukocyte crawling and transmigration) in large inflamed arteries.

4.2.4 Leukocyte migration cascade in presence of atherosclerotic plaques

The first attempt to overcome the limitations of the previously described techniques was performed in 2001 with the use of conventional epi-fluorescence microscopy in the abdominal aorta of hypercholesterolemic ApoE deficient mice[114]. This type of microscopy provides only limited imaging penetration depth and thus, cannot be used for direct *in vivo* imaging within well established dense atherosclerotic plaques. It allowed however to detect interactions of circulating leukocytes (*in vivo* stained with injection of rhodamine 6g) with the inflamed endothelium in adjacent areas to the atherosclerotic lesion. Following this approach the researchers were able for the first

time to observe and analyse in real time leukocyte rolling on the endothelium of large atherosclerotic vessels which refers to one of the initial steps of the leukocyte migration cascade. In that case it was shown that mainly P-selectin but also E-selectin are mainly responsible for leukocyte rolling in atherosclerosis. Interestingly, in contrast with studies in post-capillary venules, blocking of the integrin VLA-4 had no effect in the rolling behaviour of leukocytes although its ligand (VCAM1) is expressed also by the arterial endothelial cells. Furthermore, it was shown that the majority of cells interacting with the endothelium were neutrophils and this was the first indication for luminal recruitment of this type of cells in atherosclerosis. Notably, firm adhesion was rarely observed in that study. Further steps of the migration cascade such as crawling and transmigration were also not detected. This can be attributed to the absence of firm leukocyte adhesion on the endothelium but even more to the fact that the abdominal aorta and in general large arteries are pulsating organs and this instable nature does not allow for long-term *in vivo* imaging applications without losing the imaging focus. However, analysis of processes such as crawling demand long-term tracking of single cells and therefore stable imaging is a prerequisite. As it matters transmigration the limitations of this type of microscopy (low imaging depth and low resolution) are not allowing for detection of such phenomena. Later studies in established atherosclerotic plaques in abdominal aortas of ApoE deficient mice following the same approach revealed that microvessels on the external part of the plaque (vasa vasorum) also contribute to leukocyte recruitment in the adventitial area of atherosclerotic plaques[117]. In that case P-selectin, L-selectin as well as PSGL1 were recognised as key players in the process of rolling of leukocytes. Furthermore, firm adhesion was significant and was attenuated upon blocking of rolling which is the precedent step of adhesion in leukocyte migration cascade. However, once again a prominent imaging instability was present and did not allow for stable long-term tracking of single cells.

These experiments showed that conventional bright field and fluorescence microscopy techniques can be used for analysis of blood cells interactions with endothelial cells in large arteries, however, imaging quality is decreased in deeper layers in the presence of a plaque[118]. Therefore, these approaches are not suitable for real time *in vivo* detection of subcellular structures within the vessel wall of large

arteries. Additionally, the lack of adequate models for stable long-term *in vivo* imaging of large vessels does not allow for detection and analysis of processes such as crawling or transmigration. Therefore, only initial steps of the migration cascade (rolling, adhesion) were analysed so far in the case of atherosclerosis.

4.2.5 Imaging of large arteries with two photon laser scanning microscopy

The low image quality of conventional intravital microscopy (due to limited penetration depth and loss of resolution with increasing tissue depth) can be circumvented by the application of two photon laser scanning microscopy (TPLSM). Interestingly ex vivo experiments in excised murine carotid arteries revealed that the use of 2 photon technology can provide information about the histology of large arteries even without prior staining of the vessels. In that sense *tunica media* with its elastic bands can be imaged even without labelling due to its auto-fluorescence signal (detected by the two photon microscopy)[119,120]. On the other hand adventitia is rich in collagen fibers which can be visualised by the two photon microscopy due to non-linear scattering processes (known as “second harmonic generation”)[119-122]. These unique advantages of two photon microscopy in the case of imaging of large arteries in addition to its great resolution (0,3µm in XY direction and 0,7 µm in Z direction) and the possibility for imaging in 4 dimensions (XYZ spatial axis, T temporal axis)[123] rendered TPLSM ideal for *in vivo* imaging of big vessels and atherosclerotic plaques. However, instability of the vessel due to the motion related to the mouse heart cycle and respiration led to extreme imaging artifacts and prominent loss of imaging focus[118]. Two photon microscopes are generally obtaining images by scanning the tissue point by point in the XY axis. When this 2 dimensional scanning is completed the same procedure is taking place in a predetermined different level of the Z axis in the tissue. This scanning procedure in the XY and Z axis can be repeated in sequential time points allowing 4 dimensional analysis (XYZ spatial axis, T temporal axis). However, this is a relatively slow process while the mouse heart beats in a very fast rhythm (300 – 500 beats per minute). For that reason different parts of the pulsating arteries are scanned and imaged in different periods of the heart cycle (either in systole or diastole) during the same imaging time and therefore significant imaging distortion is present[118]. This is described as “in frame loss of

focus". Additionally, the normal movement of the mouse due to respiration leads to further loss of focus which is described as "out of frame loss of focus". The first attempts to overcome these limitations were based on surgical approaches in order to stabilise the carotid arteries. These approaches were successful in stabilising the vessel and detecting cells adhering on atherosclerotic endothelium and even present within the atherosclerotic plaques. However, they were based in cessation of the blood flow altering in that way the physiological conditions of the vessels[124]. Later approaches included triggered image acquisition by electrocardiographic and intubating devices[118]. In that case the 2 photon microscope was triggered to acquire images always in the same step of the heart and respiratory cycle greatly reducing in that way the in and out of frame loss of focus without cessation of the blood flow. This approach however, was applied for short periods of time and demanded very fast imaging acquisition processes to overcome especially the in frame loss of focus. In order to achieve a fast imaging procedure short acquisition times were necessary and this resulted in non optimal pixel resolution. Furthermore the analysis was performed only in two dimensions (XY axis). Since then this approach has been used for in vivo imaging of atherosclerotic arteries providing information mainly about luminal leukocyte adhesion in inflamed vessels[125]. However, the information that was provided regarded mainly static and not dynamic phenomena. Thus, there was no advance in the research regarding the mechanistic process of leukocytes migration in atherosclerotic plaques in large arteries. The real time in vivo information that is currently known about the migration cascade of leukocytes in atherosclerotic plaques is restricted up to the point of rolling and adhesion. Whether and how leukocytes crawl and transmigrate into the inflamed arterial wall was never analysed *in vivo* in real time in large vessels and the only available information regarding the dynamic behaviour of leukocytes during immune responses derives from experiments performed in post-capillary venules during acute inflammation. Therefore, the dynamic behaviour of leukocytes during their recruitment in atherosclerosis remains elusive.

5. Objectives

Crawling is a decisive step during the migration of leukocytes to sites of inflammation. Through this active process leukocytes reach endothelial cell junctions which are thought to be favourable areas for transmigration. In order to analyse in detail this dynamic process, *in vivo* real time experiments are required. The molecules that are thought to be involved in leukocyte crawling are the beta 2 integrins Mac-1 and LFA-1. Their contribution in the crawling process was analysed so far in vivo only under conditions of acute inflammation in post capillary venules. These experiments were performed either by the use of knockout mice or by function blocking of Mac-1 or LFA-1 and subsequently imaging after relatively long periods of time. Therefore, the direct effect of blocking of these molecules in leukocyte crawling process was not analysed so far. Thus, it cannot be excluded that the observed effect is secondary due to influence in the preceding steps of the migration cascade.

Additionally, presence of leukocytes has been reported within the vessel wall of large arteries under conditions of chronic inflammation which refers to atherosclerosis. Although it was assumed that leukocytes follow the same migration cascade (analysed in post-capillary venules) for their migration in atherosclerotic plaques, only the initial steps of rolling and adhesion were analysed *in vivo* so far in atherosclerosis. This is a consequence of the lack of suitable imaging models for stable long term *in vivo* imaging of big vessels. Therefore, apart from the initial steps (rolling, adhesion) of the migration cascade the subsequent steps of crawling and transmigration as well as the motility of leukocytes within the inflamed arterial wall has not been so far analysed.

Apart from crawling under conditions of inflammation, a specific subset of monocytes (non classical-patrolling monocytes) was found to be able to crawl also under steady state conditions. The beta 2 integrin LFA-1 is thought to be mediating this process while Mac-1 is considered to be dispensable. However, as in the case of the experiments performed under inflammatory conditions the direct effect of blocking of beta 2 integrins was not analysed. Furthermore crawling of patrolling monocytes was not examined in large arteries due to the mentioned lack of imaging models that would be suitable for long-term stable imaging of large vessels.

In this study we focus on the *in vivo* analysis of crawling behaviour of leukocytes during conditions of steady state and inflammation in the microvasculature and we provide for the first time a comparison with the leukocyte crawling behaviour in large arteries.

Our objectives are:

1. Establishment of a novel model for long term stable in vivo imaging of large arteries during steady state and atherosclerosis using the two photon microscopy technology. This model will provide us the possibility of analysis of dynamic leukocytes processes with a focus on leukocyte crawling.

2. Application of an alternative way of analysis of crawling in the microvasculature based on continuous tracking of single crawling cells before, during and immediately after the application of blocking antibodies. This approach will permit us to analyse the direct effect of blocking of beta-2 integrins in the crawling behaviour of leukocytes in real time and compare it with the conventional ways of analysis regarding the long-term effect. In our experiments different types of leukocytes are analysed under steady state (monocytes) and acute sterile inflammation (neutrophils) in the microvasculature.

3. Analysis of the role of Mac-1 in the crawling of leukocytes in large vessels during steady state (monocytes) and atherosclerosis (neutrophils) and comparison with the crawling behaviour in the microvasculature under the same conditions.

6. Material and methods

The experiments were performed at the, German Heart Center ("Deutsches Herzzentrum" Technical university of Munich- TUM) and the Walter Brendel Centre of Experimental Medicine (Ludwig Maximilians University of Munich- LMU), according to German legislation on the protection of animals.

6.1 Reagents and antibodies

Table 1. List of reagents and antibodies

Anti Ly-6G/Ly6C (GR-1) Clone RB6-8C5, PE conjugated	Biolegend
Anti mouse CD11a PE or FITC conjugated, Clone M17/4	Affymetrix eBioscience
Anti mouse CD11b PE or FITC conjugated, Clone M1/70	Affymetrix eBioscience
Anti mouse Ly6G Clone 1A8 , PE conjugated	Biolegend
Biozym LE Agarose	Biozym, Oldendorf, Germany
BSA	PAA Laboratories GMbH, Pasching, Germany
DNeasy Blood & Tissue Kit	Qiagen, Hilden, Germany
dNTP-Mix	Thermo Scientific, Bremen, Germany
EDTA	Sigma-Aldrich Chemie GmbH, Steinheim, Germany
Ethanol	Merck Schuchardt OHG, Hohenbrunn,Germany
Ethidium bromide	Sigma-Aldrich, Taufkirchen, Germany
FITC dextran	4,000 MW, Sigma-Aldrich
KHCO3	Sigma-Aldrich Chemie GmbH, Steinheim, Germany
NaCl	Diaco, Naila, Deutschland
NH4Cl	Sigma-Aldrich Chemie GmbH, Steinheim, Germany

PBS	Sigma-Aldrich Chemie GmbH, Steinheim, Germany
PRIMERS	Eurofins MWG Operon (Ebersberg, Germany)
Rat IgG2a K Isotype Control Alexa Fluor® 488 or PE conjugated	Affymetrix eBioscience
Rat IgG2b K Isotype Control PE or FITC conjugated	Affymetrix eBioscience
Rhodamine 6G Chloride	Molecular probes, Eugen Oregon, USA
Taq DNA Polymerase	Qiagen , Hilden
TBE	Life Technologies, Darmstadt, Germany
TRITC dextran	2,000,000 MW, invitrogen

6.2 Animals

Female and male C57BL/6J wild-type, ApoE deficient, LysM^{eGFP}, CX3CR1^{eGFP} and MHCII^{eGFP} mice with C57BL/6J background were used. The mice were held under control of day/night cycle in groups from 3 to 5 animals in Makrolon-cages and had free access to tap water and pellet food (ssniff special diets, Soest, Germany). The C57Bl/6J, LysM^{eGFP} and CX3CR1^{eGFP} mice were fed with a standard chow while the ApoE deficient mice were fed with a high cholesterol diet (1,25% Cholesterin, Altromin) for a time period of 14-16 weeks starting at the age of 4 weeks.

6.2.1 C57Bl/6J

The C57BL/6J is the most widely used inbred strain of mice. It has been used as a wild type background for genetical modifications and production of transgenic strains. Furthermore these mice are commonly used as native control animals in experiments that include the use of transgenic mice or of mice treated with several factors that could alter the physiological conditions of the organism. The C57Bl/6J mice were purchased from Charles River laboratories.

6.2.2 ApoE deficient mice

Apolipoprotein E is a glycoprotein which is synthetized mainly by the liver and is a structural component of different types of lipoproteins except from low density lipoproteins (LDL). This glycoprotein mediates the binding of chylomicrons and vLDL to the LDL receptor in the liver and therefore plays a predominant role in the clearance of chylomicrons and vLDL from blood. By that way hypercholesterolemia is prevented[126,127]. Although C57Bl/6J wild type mice do not develop atherosclerotic plaques in their vessels, the ApoE deficient mice develop hypercholesterolemia and therefore are susceptible to the development of atherosclerotic plaques upon feeding with high cholesterol diet with increasing age. Furthermore, as humans, they develop atherosclerotic plaques of all phases (including the initial stage of fatty streak) in different parts of the arterial tree (such as aortic arch and the bifurcation of the carotid arteries[128].

6.2.3 CXC3R1^{eGFP} mice

CX3CR1 receptor is a seven transmembrane receptor present mainly in the membrane of monocytes and dendritic cells that binds to the chemokine fractalkine (CX3CL1, FKN, neuroactin). Binding of fractalkine to its receptor promotes cell adhesion while its soluble form acts in a chemotactic way[129]. In order to investigate the physiological role of the fractalkine receptor a mouse strain was generated by insertion of green fluorescent protein reporter gene in the locus of the CX3CR1 gene [130]. Knock-in/knock-in mice for GFP (GFP/GFP) are characterised by a targeted deletion of the receptor while heterozygote (GFP/+) mice express both GFP and CX3CR1. In that way heterozygotes mice contain monocytes and dendritic cells which are fluorescent but at the same time preserve the functionality of the fraktalkine receptor. These mice were originally generated by Prof. Steffen Jung and kindly provided to us by Prof. F. Krombach, (Walter Brendel center for experimental medicine, Ludwig-Maximilian University).

6.2.4 LysM^{eGFP} mice

The insertion of green fluorescent protein in the murine lysozyme M locus provided us the possibility for *in vivo* imaging of leukocytes that express this protein. In this kind of mice mainly mature neutrophils are fluorescent (98%) and a very small proportion of monocytes (2%) [131]. In addition the highest intensity of fluorescence is detected in the mature subset of neutrophils followed by their progenitors and monocytes. This mouse strain was used in order to *in vivo* visualize neutrophils recruitment in areas of inflammation. These mice were kindly provided us from Professor M. Sperandio (Walter Brendel center for experimental medicine, Ludwig-Maximilian University).

6.2.5 MHCII^{eGFP} mice

The major histocompatibility complex (MHC II) locus is expressed by antigen presenting cells such as dendritic cells and macrophages (APCs). The MHC II molecule is indispensable for adaptive immune responses since it is recognized by the T cell receptor of the CD4+ T helper cells. Through this interaction T cells bind on APCs mainly in the lymph nodes in a process that leads to the priming (activation) of the CD 4+ T cells, which is a decisive step for the development of adaptive immunity. Apart from lymph nodes the APCs are also found in peripheral lymphoid tissues such as spleen where they additionally present phagocytic behaviour. Moreover they are detected in sites of chronic inflammatory responses such as atherosclerosis in the large arteries. In the MHCII eGFP mouse strain the MHC class II gene (expressed in antigen presenting cells- “APCs”) is replaced by a version that codes for a class II molecule, tagged with enhanced green fluorescent protein (eGFP)[132]. Therefore antigen presenting cells can be visualized *in vivo* or *ex vivo* by application of techniques that are based in detection of fluorescence.

6.2.6 Production of bone marrow chimeras

One of our goals was to investigate *in vivo* the presence and motility of different subsets of leukocytes intraluminal but also inside the atherosclerotic plaques that

develop in large arteries. To achieve this it is essential to perform experiments in mice that, on one hand, develop atherosclerotic plaques and, on the other hand, also contain already fluorescent naïve leukocytes. The analysis of leukocyte adhesion and intravascular crawling is possible via simple *in vivo* labelling of different subsets of leukocytes with fluorescent antibodies and does not need the usage of chimeras. However, the *in vivo* imaging and analysis of already emigrated leukocytes in the body of the atherosclerotic plaques is not possible via labelling antibodies, since these cannot penetrate the mass of the plaque and therefore cannot stain cells within the lesion. This limitation is overcome by using ApoE deficient mice that contain cells that express intrinsically green fluorescent protein (GFP). The first approach to achieve that is to cross ApoE deficient mice with strains that express GFP selectively in different subtypes of leukocytes such as LysM^{eGFP} (predominantly neutrophils express eGFP), CX3CR1^{eGFP} (monocytes and macrophages express eGFP) or MHCII^{eGFP} (APCs express eGFP). The second approach is to lethally irradiate ApoE deficient mice and perform bone marrow transplantations using as donors the previously mentioned fluorescent strains. However, ApoE deficient mice present an impaired plaque formation when irradiated and transplanted with bone marrow cells from donors of no ApoE deficient background[133]. Therefore, the irradiation of these mice and the subsequent bone marrow transplantation was performed at 16-18 weeks of age when atherosclerotic plaques are expected to be already developed in atherosclerosis-prone areas including the carotid bifurcation.

6.2.6.1 Irradiation

In order to perform bone marrow transplantation ApoE deficient mice were used as recipients while LysM^{eGFP} and CX3CR1$^{GFP/+}$ mice were used as donors. The recipient mice were placed in a sterile glass beaker (one to two mice per beaker) which was covered with autoclaved filter paper (Tecniplast, Hohenpeissenberg). Subsequently the recipient ApoE deficient mice were transferred to the irradiation unit (OB29 irradiation system BA, Buchler, Braunschweig) and treated with 6,5 Gray of irradiation. This process was repeated two times with a time interval of at least 12 hours. Upon the second dose of irradiation the isolated bone marrow cells of the donors were injected in the tail vein of the irradiated mice via tail vein injection.

6.2.6.2 Isolation of bone marrow cells

Donor mice were introduced in anaesthesia with Isofluran (Isofluran Delta Select, Delta Select GmbH, Deieich) and oxygen and were euthanized by acute dislocation of the cervical spine. After disinfection of the mouse hair with 70% ethanol (Merck Schuchardt OHG, Hohenbrunn,Germany), the skin of the arms and legs was cut and deducted by the use of a scalpel (Pfm Medical AG, Köln, Germany). In a next step the arms and legs were amputated at the level of shoulder joint and the musculature was removed by the use of the scalpel. The bones were placed in a petri dish containing 10ml of pre warmed puffer: PBS (Sigma Aldricht Chemie GmbH, Steinheim, Germany), + 5% Fetal Bovine Serum-FBS (Invitrogen, Carlsbad, USA) + 2 mM EDTA (Sigma Aldrich, Steinheim, Germany). Under a sterile cabinet (Typ HS12, Heraeus, Hanau, Germany) the epiphysis of bones were carefully separated and cut on their top side with a scalpel. The bone marrow was flushed out of the bones by using a puffer containing syringe (B. Braun, Melsungen, Germany) with a canula (26G, BD Microlance, Becton Dickinson Labware, Franklin Lakes, USA) inserted in this area of the bones. The bone marrow cells were gathered in a 50 ml Falcon tube that had a 40 µm filter mesh adapted on its top side. The falcon tube was filled up to 30 ml with puffer and then was centrifuged at 612g and 4° C for 5 minutes (Megafuge 1.0 R, Heraeus Instruments, Hanau, Germany). A vacuum pump (Vacuubrand GmbH + CO KG, Wertheim, Germany) was used in order to discard the supernatant. Erythrocyte lysis was performed by resuspending the pellet in 2,5 ml of 8% hypotonic Ammonium chloride solution (1,5 M NH4Cl + 0,1 M KHCO3+ 10 mM EDTA, all from Sigma-Aldrich, Steinheim, Germany) and incubating for 4 minutes at 4° C. Subsequently the Falcon tube was filled with puffer up to 30 ml and a further step of centrifugation (612g, 4° C, 5min) was performed. After this final step of centrifugation the cells were resuspended in 2-4 ml PBS and were counted in a Neubauer counting chamber.

6.2.6.3 Injection of bone marrow cells

Each recipient mouse received approximately $5x10^6$ cells in a final volume of 300µl of PBS. The injection of isolated bone marrow cells was performed via an inserted

catheter (Portex®, Polythene Tubing, 0,28mmID, Smiths Medical, St. Paul, USA) to the tail vein of the mouse. In order to accomplish the injection of the bone marrow cells to the tail vein an injection stage (Broome HAR5204, Föhr Medical Instruments GmbH, Germany, see Figure 7) was used which reduced the motility of the mouse but at the same time left the mouse tail free for handling.

Figure 7. Injection stage for performance of tail vein injection

6.2.7 Cross breeding of ApoE$^{-/-}$ with MHCII^{eGFP} mice

In order to analyse the presence and behaviour of dendritic cells within the plaque, the ApoE deficient mice were crossed with MHCII^{eGFP} mice. The mice were mated after 9 weeks of age. During this procedure one male of one strain was placed in the same cage with two females of the other strain. The genotype of the infants was analysed by PCR.

6.2.7.1 Genotyping of crossed mice

For genotyping ApoE deficient mice, genomic DNA was extracted and purified from earmarks or tail tip cuts using the DNeasy Tissue & Blood kit from Qiagen (Hilden, Germany) according to the manufacturer's protocol. In brief, tissue biopsies were first lysed in a tissue lysing buffer containing proteinase K at 56°C for at least 3 hours, but preferably overnight. Buffering conditions were adjusted to provide optimal DNA

binding conditions and the lysate was loaded onto a spin column. During centrifugation DNA was selectively bound to the silica membrane in the column while contaminants passed through. Remaining contaminants and enzyme inhibitors were removed in two efficient wash steps and DNA was then eluted in buffer, ready for use. The following oligonucleotides were used for genotyping of ApoE deficient mice: oIMR180 (GCCTAGCCGAGGGAG AGCCG, common primer), oIMR181 (TGTGACT-TGGGAGCTCTGCAGC, wild type reverse), oIMR182 (GCCGCC-CCGACTGCATCT, mutant reverse). The expected amplicon sizes were 245 bp for the mutant allele and 155 bp for the wild type allele.

In short 2µl of purified genomic DNA (about 100ng) were added to a PCR reaction mix with a total volume of 25µl consisting of 1/10 final volume 10x PCR Buffer, $MgCl_2$ 1.5 mM, dNTP-Mix 0.2 mM, the oligonucleotides oIMR180, oIMR181 and oIMR182 in a final concentration of 0,5µM and Taq Polymerase 0.05U/µl. The following PCR program and cycling conditions were used for the confirmation of ApoE wild type and knock out alleles: 95°C for 3 min, repeat 35 times 95°C for 30 sec, 68°C for 40 sec, 72°C for 1min followed by 72°C for 2 min then holding for 4°C. The PCR products were analysed on 2% TBE-agarose gels containing 0,5µg/ml ethidium bromide and were visualized by exposure to ultraviolet light on a UV transilluminator.

The following oligonucleotides were used for genotyping $MHCII^{eGFP}$ mice: H2_AB1_f (CCTTGTCCACCACTGTCACTG) and H2_AB1_E6_rev (TCAGGAATTCGGAGC-AGAGAC) for the wild type allele, CEST#140_fw (TCAT-CTGCACCACCGGCAAGC) and CEST#66_rev (AGCAGGACCATGTGATC-GCGC) for the mutant allele. The expected amplicon sizes were 525 bp for the mutant allele and 949 bp for the wild type allele. Finally, both bands should be present in heterozygous animals.

In short 2µl of purified genomic DNA (about 100ng) were added to two separate PCR reaction mixes with a total volume of 25µl consisting of 1/10 final volume 10x PCR Buffer, $MgCl_2$ 1.5 mM, dNTP-Mix 0.2 mM, the oligonucleotides H2_AB1_fw and H2_AB1_E6_rev or CEST#140_fw and CEST#66_rev in a final concentration of 0,5µM and Taq Polymerase 0.05U/µl. The following PCR program and cycling conditions were used for the confirmation of MHCII wild type and knock in alleles: 95°C for 3 min, repeat 35 times 95°C for 1 min, 64°C for 30 sec, 72°C for 1min

followed by 72°C for 7 min then holding for 4°C. The PCR products were analysed on 1.5% TBE-agarose gels containing 0,5µg/ml ethidium bromide and were visualized as in the previous case by exposure to ultraviolet light on a UV trans-illuminator.

6.3 Mouse handling prior to the *in vivo* imaging

6.3.1 Anaesthesia

The *in vivo* experiments performed required the use of non invasive (ear model, see 6.4.1) but also invasive (carotid artery model, see 6.4.2) procedures. In order to ensure that the mice suffered no pain during the experiments a coctail of anaesthetics and analgesics has been used in both types of preparation. This offered the desired sedation for long periods of time. The medicaments that were used included (table 2): Isofluran (Forene®, Abbott GmBH, Wiesbaden), Metedomidine (Domitor®, Pfizer GmbH, Karlsruhe), Midazolam (Midazolam-ratiopharm ®, CuraMED Pharma GmbH, Karlsruhe), Fentanyl (Fentanyl Curamed®, CuraMED Pharma GmbH, Karlsruhe)

Table 2. Medicaments used in order to achieve mouse sedation.

Isofluran	Halogenated ether used for inhalational anesthesia	
Metedomidine	Alpha two adrenergic agonist used for anesthesia and analgesia	0,5 mg/kg
Midazolam	Benzodiazepine with hypnotic, anticonvulsant, skeletal muscle relaxant and sedative properties	5 mg/kg
Fentanyl	Synthetic opioid analgesic with a rapid onset and short duration of action	0,05 mg/kg

The mice were anaesthetized by inhalation of a mixture of oxygen and isofluran through an evaporator (Ohmeda Isotec 3, Fa. Eickmeyer, Tuttlingen, set by Völker Vet, Völker GmbH, Kalten-kirchen,Germany) that was connected in a body chamber. The mice were gently placed in the chamber and isofluran was administrated in a mixture of 2-3% with oxygen. Subsequently a coctail of metedomidine, midazolam and fentanyl was injected intraperitoneally (IP) in order to achieve deeper hypnosis, analgesia and muscle relaxation. Using this mixture, a surgical tolerance is achieved after a period of time of 10–20 minutes during which the mouse was kept in a box free of light. Before initiating the operation we confirmed the pain tolerance of the mice by checking the flexor withdrawal reflex. The induction of anaesthesia that was just described offers a surgical tolerance for 45 minutes. After this period of time additional half dose of the anaesthetic coctail was injected succeeding in that way to preserve the desired surgical tolerance for bigger periods. Additionally the flexor withdrawal reflex was checked in regular time points and more anaesthesia was supplied if needed.

6.3.2 Catheterization of the mouse

During our experiments labelling or blocking antibodies and fluorescent dextrans, were injected through a catheter inserted in the tail vein of mice. In some cases of ApoE deficient mice the insertion of the catheter was not possible in the tail vein due to thickening of the skin as a consequence of the accumulation of lipids and fat tissue in the area. In these cases a catheter was injected in the femoral artery of the mice.

6.3.2.1 Tail vein catheterisation

The anaesthetized mice were placed on a heating pad (Thermo Lux- heating pad, Fa. Dehner, Germany) and with the help of warm water, the vessels were dilated. Subsequently we used our index and middle fingers to apply pressure on the basis of the tail and accumulate the vein blood proximal to this area. Before injection we disinfected the region of puncture (with Octeniderm ® Schulke & Mayr GmbH, Norderstedt, Germany). In order to stabilise the catheter on the tail and to avoid its accidental removal from the tail vein, a tissue glue (histoacryl, B/BRAUN) was used.

The injection was performed in one of the two lateral tail veins. To prepare the catheter we used a plastic tube (Portex®, Polythene Tubing, 0,28mmID, Smiths Medical, St. Paul, USA), two needles (30G, BD Microlance, Becton Dickinson Labware, Franklin Lakes, USA) and a 1 ml syringe (B. Braun, Melsungen). One of the needles was removed from its plastic basis and was plugged into the front end of the tube. In the other edge of the tube the second needle was plugged and the syringe was adapted on it. Curved forceps were used to insert the catheter with the attached needle in the vein of the mouse tail (Figure 8). As previously described (6.2.6.3) in the case of injection of bone marrow cells into the tail vein the mice were not anaesthetized and an injection cage (Broome HAR5204, Föhr Medical Instruments GmbH, Germany) was used in order to immobilize them. This reduced the motility of the mouse but at the same time left the tail free for handling. The rest procedure regarding the tail vein injection was the same as previously described.

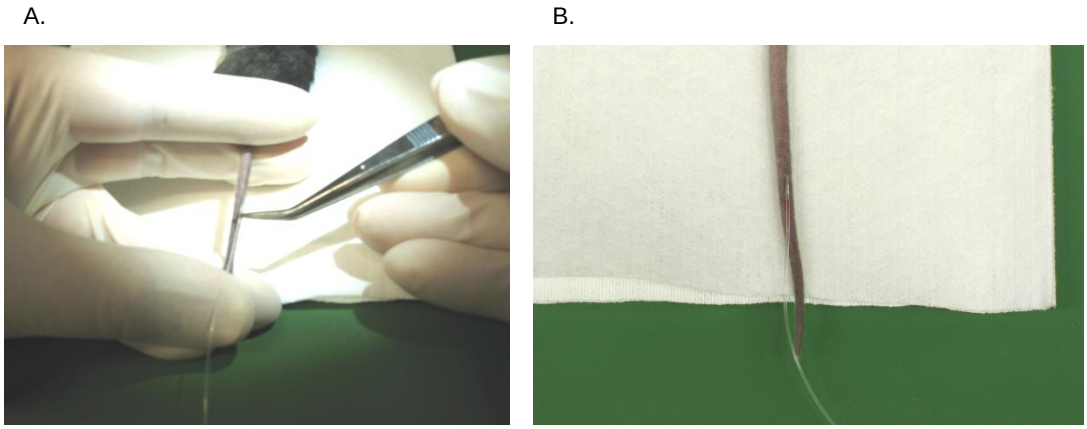

Figure 8. Tail vein catheter. **A.** Insertion of catheter to the tail vein. **B.** Catheter inserted in the tail vein.

6.3.2.2 Femoral catheter

The surgical process for the insertion of the catheter into the femoral artery was performed under a stereo microscope (Stemi 2000, Zeiss, Jena) and a gooseneck lamp (Schott Cold light source KL200, goose neck light guide, Zeiss, Jena) was used in order to illuminate the field of surgery. During the process of microsurgery sterile instruments were used (Micro2000, Medicon, Tuttlingen, see Figure 9).

Figure 9. Microsurgery instruments used for our surgical interventions

In a first step the left foot of the mouse was fixed with a small piece of tape (Transpore TM, 3M Health Care, Neuss). The hair was shaved and the skin was disinfected (Cutasept®F, Fa.Bode Chemie, Hamburg). Subsequently a small incision on the skin was performed approximately 2 cm proximal from the knee joint of the mouse and this allowed the identification of the femoral vein, artery and nerve. Typically the femoral artery is found between the nerve and the vein. The artery was very gently separated from the surrounding tissue and structures, including the nerve and the vein, by the use of forceps. Two threads (Pearsalls Limited, Taunton, england) were placed gently under the prepared artery in a distal and proximal area. The thread in the distal area was further ligated and its free edge was fixed on the pad with tape in order to stay stable during the following surgical procedure. In the next step a folded needle was used in order to make a small whole in the central part of the prepared artery through which a catheter (Catheter tube Portex®, Polythene Tubing, 0,28mm ID, Smiths Medical, Keene, USA) could be inserted. The catheter was then stabilised by being ligated with the non previously ligated thread and the non fixed edge of the previously ligated thread (Figure 10). The incision in the skin was finally stitched with surgical threads (Prolene® Polypropylen, 7-0 metric, Fa. Ethicon, Norderstedt). During the process of microsurgery the tissue was regularly superfused with isotonic natrium chloride solution (Diaco Naila, Deutschland).

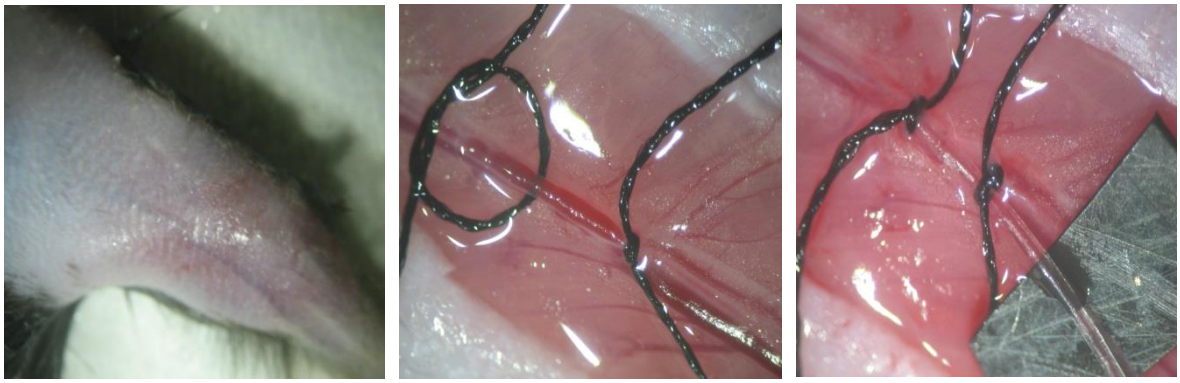

Figure 10. Femoral catheter.

6.4 Models for in vivo imaging of microvasculature and large arteries using TPLSM

6.4.1 Ear model

The model of mouse ear is one of the classical models for analysis of the microcirculation and has been widely used in the past[134-137]. Particularly, this model was also used as a model for *in vivo* analysis of the interstitial migration of leukocytes upon induction of acute sterile inflammation via laser-ablation in the interstitial area[134,136]. The ear of the mice is easily accessible without any need for surgery and contains vessels that are anatomically superficial and can be imaged *in vivo* with two photon or confocal microscopy. Additionally the ear itself is free of motion distortion due to the cardiac or respiratory cycle of the mouse allowing stable long-term video recordings of its micro-vessels. In our experiments we used two photon laser scanning microscopy in order to visualise leukocyte firm adhesion and intraluminal crawling in the microvasculature of the mouse ear. The mice were sedated as previously described (6.3.1), a catheter was placed and fixed in their tail vein and the eyes were covered with a protective cream (Bepanthen® eyes and nasal ointment, Hoffmann La Roche AG, GrenzachWyhlen). Subsequently the mice were placed in a supine position on a heating pad that was developed in our laboratory in order to keep the body temperature at 37°C. The ear was fixed in a special stage in the center of the pad. This stage consists of 2 rings (Figure 11A). A metallic external one

and an adjacent internal which is filled with silicon (Baysilone Paste, GE Bayer Silicones, Leverkusen, Germany). The periphery of the ear was fixed on the internal ring (Figure 11b) by the use of 5 needles (30G, BD Microlance, Becton Dickinson Labware, Franklin Lakes, USA). Finally before placing the mouse under the microscope the stage was filled with 0,9% NaCl buffer saline that covered the ear.

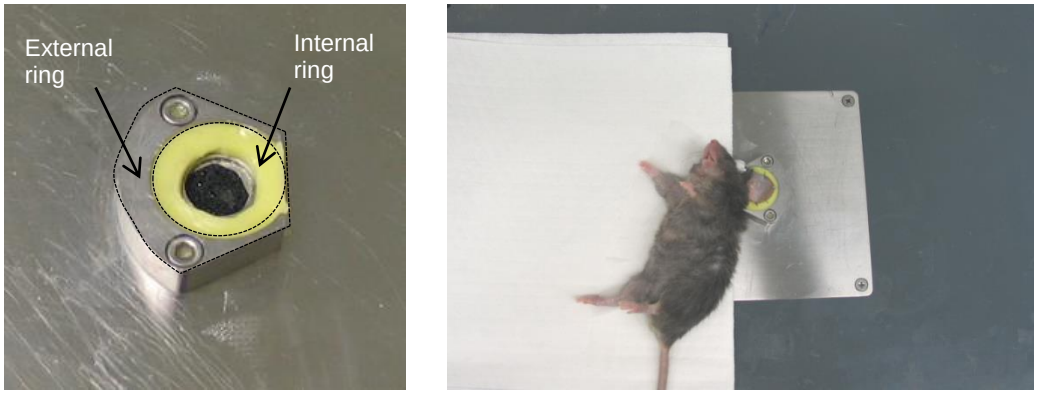

Figure 11. Stage for intravital microscopy in the mouse ear

6.4.1.1 Induction of the acute sterile inflammation in the mouse ear

One of the objectives of our experiments was to analyse the recruitment of leukocytes in the context of acute sterile inflammation in the post capillary venules of the mouse ear. Therefore, we induced necrosis of the interstitial area in the vicinity of post capillary vessels as described in the literature[136]. During this procedure the laser of our two photon microscope was focused in a small region of interest (30x30 μm) in a distance of about 30 micro-meters from the external border of a post capillary venule with diameter between 25 and 40μm. The excitation wavelength was set to 800nm and the laser power that was used was increased to 15-20%. The number of scanned pixels for this region of interest was set to 515x515 and the treatment was performed using a time lapse mode. In that way the scanning was taking place only in two dimensions (XY, axis). The line average chosen was equal to 1 and the number of treatments performed (which represents the number of scans in this ROI) was equal to 10. Special care was taken in order not to influence the blood flow and the shear stress of the adjacent vessel. After the induction of the laser injury and

during the different steps of the experiment the blood flow was checked (by detection of freely flowing fluorescent cells) through the CCD fluorescence camera of our microscope. In the case of absent or disturbed flow a different vessel with normal flow conditions was chosen and the procedure of laser induced injury was repeated as described. At the end of each experiment 30 µl of fluorescent beads (1 µm nominal diameter polystyrene fluorospheres, 505/ 515 spectra, Invitrogen) were injected to the mouse through the tail vein in order to confirm the directionality of the blood flow.

6.4.2 Carotid artery model

In vivo imaging of large vessels with two photon microscopy suffers from prominent imaging distortion and loss of focus. To overcome these limitations and perform stable long term imaging in carotid arteries in mice we have established a new surgical approach for stabilization of the vessels. The general steps for preparation and imaging of the large vessels include: intubation, preparation and stabilization of the carotid artery and electrocardiographic analysis and triggering for image acquisition.

6.4.2.1 Ventilation

Upon sedation and insertion of a catheter in the tail vein or the femoral artery (6.3.2.2), the mice were placed in a supine position on a heating pad (TKM-0904, Föhr Medical Instruments, GmbH). The surgical procedure was performed under a stereo microscope (Stemi 2000, Zeiss, Jena) and a goose neck lamp (Schott Cold light source KL200, goose neck light guide, Zeiss, Jena) was used to illuminate the surgical field. During the process of microsurgery sterile instruments were used (Micro2000, Medicon, Tuttlingen, see figure 9). Subsequently the fur of the neck was shaved (Figure 12A). An 1ml syringe (b.Braun, Melsungen) was placed under the neck of the anaesthetized mouse in order to lift its internal anatomical structures and provide an easier access to the trachea and the carotid artery. Subsequently a 2,5 cm incision was performed in the skin following the path of the trachea (Figure 12B). The submaxillary gland together with the adjacent sublingual gland were carefully

exteriorised bilaterally (Figure 12C). This allowed us to access the sternohyoid muscles that cover the trachea. In the next step a thread (Pearsalls Limited, Taunton, England) was placed under each muscle and each of their free edges were gently pooled and fixed using tape (TransporeTM, 3M Health Care, Neuss) in the adjacent lateral sides of the mouse (Figure 12D). In that way the left sternohyoid muscle was pooled to the left side and the right sternohyoid to the right allowing free access to the trachea. Two additional threads were gently placed under the trachea proximal to the cricotracheal ligament. Subsequently an incision of 0.5 cm was performed between the thyroid and cricoid cartiladge (Figure 12E). Through this incision a metallic tube connected to the ventilator device (minivent type 845, Hugo Sachs Elektronik, Harvard apparatus D-79232, Germany,see figure 13) was gently inserted in the trachea. The tube was fixed by ligation with the two threads that were previously placed under the trachea (Figure 12F). The respiration rate was set in the ventilation device to 160 breaths/minute with a 500µl air volume/breath, mimicking the physiological aspects of the mouse respiration.

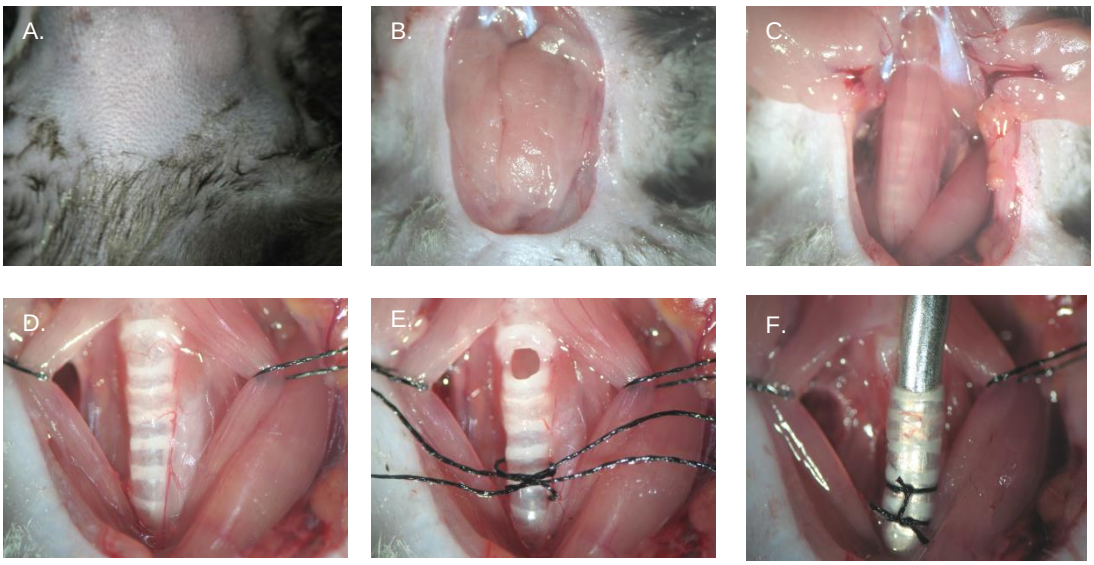

Figure 12. Surgical process for insertion of the intubation tube in the mouse trachea. A detailed description of the process is provided in the text.

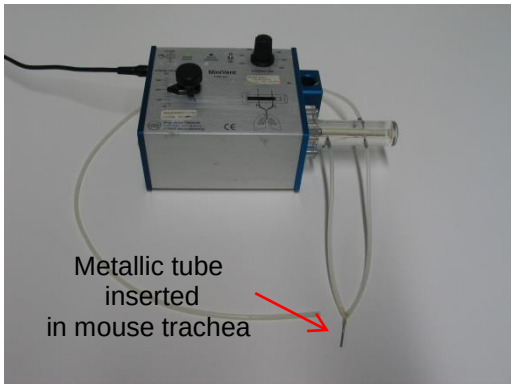

Figure 13. Device used for ventilation.

6.4.2.2 Preparation of the carotid artery

The cervical part of the carotid artery consists of the common carotid artery which is bifurcated in the level of 4th cervical vertebra in the internal carotid artery and the external carotid artery. The internal carotid artery follows a deeper path that leads to the skull in order to provide oxygenated blood to the brain while the external carotid artery follows a more superficial path providing with blood the neck and the face. The area of the carotid bifurcation as well as the external and internal carotid arteries are regions prone to atherosclerotic plaque formation[128,138,139]. In order to visualise the carotid bifurcation and the atherosclerotic plaques that developed in this region we changed the position of the intubated mice from supine to lateral. Upon dissection of the sternocleidomastoid and digasterius muscles the biggest part of the cervical common carotid artery with the adjacent vague nerve was revealed (Figure 14). Furthermore this intervention allowed us to access the carotid bifurcation and parts of the internal and external carotid artery. During this procedure care was taken in order to superfuse regularly the tissue with NaCl.

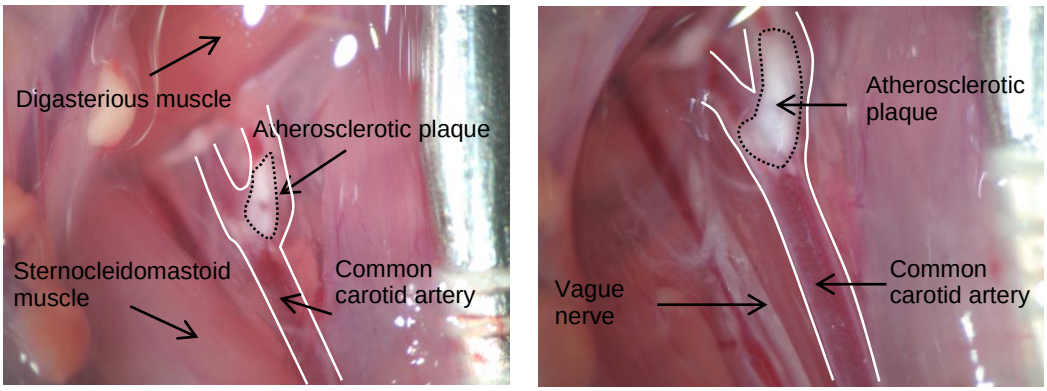

Figure 14. Surgical field in the area of the carotid artery. **A.** Before the incision of the sternocleidomastoid and digasterius muscles. **B.** Upon the incision of the sternocleidomastoid and digasterius muscles. The vague nerve is also visible in the second case. In In this example a well established atherosclerotic plaque is visible in the area of carotid bifurcation and external carotid artery.

6.4.2.3 Stabilisation of the carotid artery

As mentioned before arteries are pulsating organs. This characteristic in addition to the normal respiratory movement of the mouse raises great obstacles to the *in vivo* imaging of large vessels especially in the case of two photon microscopy. In order to achieve maximum stability for our experiments we established a novel approach for stabilisation of the large vessels. The basic principle of our model is to construct a stable micro-environment by separating the vessel from the adjacent tissue and by applying a very small pressure on the top of it in order to minimize the imaging distortion due to the pulsation along the vertical axis. In order to accomplish this goal we have developed a new stage which consists of a metal ring (1.2 cm diameter, and 0,3 cm thick) that is connected through a metal wire at a base. This can be adapted on a heating pad (figure 15). The height of the ring as well as its angle from the level of ground can be modified according to the anatomy of each mouse individually.

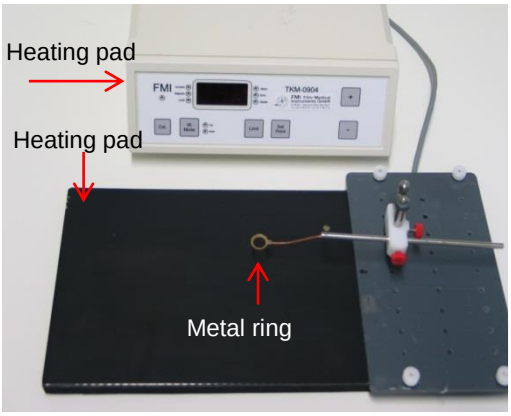

Figure 15. Custom made stage for stabilization of carotid arteries and TPLSM, adjusted on a heating pad.

At the bottom of the ring a circular cover glass was glued, which could be replaced after each experiment. Upon preparation of the carotid artery as it was previously described the vessel was very gently separated from the adjacent vague nerve by the use of forceps. The adjacent vagus nerve (pneumonogastric) nerve innervates the sinoatrial node of the heart and therefore controls the heart rate by lowering it. Parasympathetic hyper-stimulation can lead to bradycardias and fatal arrhythmias and for that reason special care was taken in order not to dissect or injure the nerve during preparation[140]. After separating the carotid artery from the nerve, one piece of thin plastic sheet was placed under the carotid artery in the level of the carotid bifurcation (Figure 16). This procedure was performed in a very gentle way in order to avoid injury or bleeding of the vessel which could alter the physiologic cellular processes intraluminally. Upon separation of the carotid artery from the surrounding tissue, the ring was adapted under the stereo microscope on the top of the carotid artery in order that the glued cover glass slightly touched the artery (Figure 16). During this procedure special care was taken not to press the vessel since this could lead in altered flow conditions intralluminally. The ring was subsequently filled with Nacl in order to perform our experiments with the upright water immersion objective of our two photon microscope.

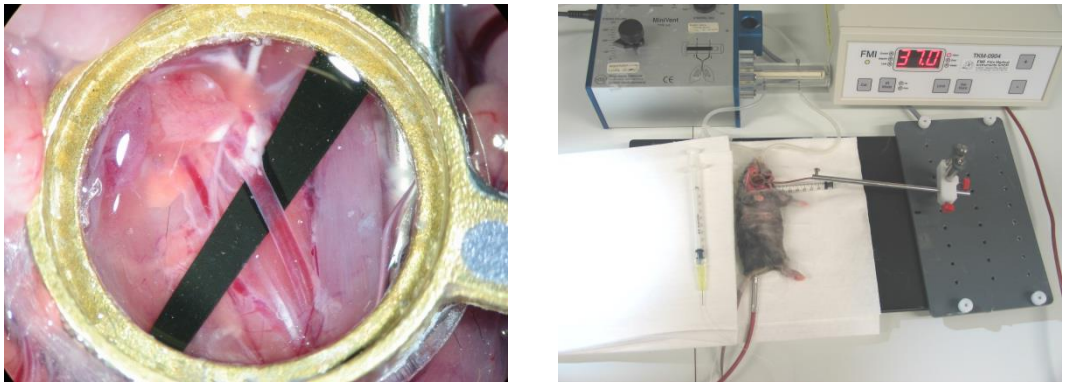

Figure 16. A. Placement of the stabilizing stage on the carotid artery. **B.** Mouse prepared for TPLSM.

6.4.2.4 Monitoring of the heart rate during the experiment and electrocardiographically triggered imaging acquisition.

The area of the carotid bifurcation is characterised by the presence of the carotid sinus which is a region that contains various baroreceptors which are sensitive to changes in the blood pressure of the vessel. The application of pressure on the carotid sinus leads to bradycardia and is used in human medicine in order to differentiate different types of tachycardia (supra-ventricular from ventricular tachycardia). Additionally manipulation of this area can lead to cardiac arrest and death (carotid sinus reflex death)[141,142]. In order to insure that the heart rate of the mouse was not influenced by the application of our stabilizing stage on the carotid bifurcation the electric activity of the heart was continuously monitored through an electrocardiographic device (Animal bio Amp, AD instuments). In order to obtain the electrocardiographic analysis 3 electrodes were connected subcutaneously to the mouse. One was used as a ground electrode and was inserted close to one of the feet of the mouse while the other two were inserted in the thoracic area in such a way that the heart was located between them. The continuous electrocardiographic monitoring confirmed that there was no significant change in the heart rhythm upon

the application of the stabilizing (see 7.1.3.1.1). Furthermore the electrocardiographic triggering unit propagated an output signal to our two photon system activating the acquisition of images. This signal was set to coincide with the peak of the electrocardiographic QRS complex which represents the systole of the heart.

6.5 *In vivo* imaging of immune cell migration using TPLSM

6.5.1 Basic principles of fluorescence and two photon microscopy

Intravital microscopy of leukocyte recruitment in the microvasculature mainly, but also in big vessels (carotid artery) has been performed in the past by means of epi-fluorescence or trans-illumination microscopy[4,114]. However it`s low tissue penetration and low resolution did not allow for analysis of several cellular processes specially in the case of atherosclerosis in large arteries. Confocal laser scanning microscopy has also been used for in vivo imaging in several tissues and offers several advantages in comparison with the conventional techniques. These refer mainly to deeper imaging penetration and significantly higher resolution[143]. The general basic concept of fluorescence is that single photons emitted from a laser source interact with chemical compounds (fluorophores) on the tissue which emit light upon excitation[144]. Fluorophores interacting with photons leave their ground energy state and reach an excited one. While the fluorophore returns to its ground state it releases energy that can be detected as light[144]. In the case of confocal microscopy fluorescence occurs also in out of focus regions resulting thus in higher photobleaching (reduced signal intensity) and increased phototoxicity (tissue damage due to interaction with photons) [145]. The basic principle of two photon microscopy was first described by Maria Goeppert Mayer (1906–1972)[146]. According to this concept two photons (of approximately half the energy of the one photon used in confocal microscopy) interact simultaneously (within ~0.5 fs) with a fluorophore (Figure 17)[144,147]. The simultaneous interaction of two photons with fluorophores is an extremely rare event. To increase the frequency of this phenomenon, infrared lasers which emit very short (~10–13 sec) but high-energy (~2 kW) pulses are used[148]. This process leads to an in focus excitation and emission of fluorescence reducing by this way the levels of phototoxicity and photobleaching. Furthermore, it allows for deep penetration imaging

without damaging the tissue. These characteristics render the two photon microscopy the most suitable technique for long-term *in vivo* imaging of the tissue [148]. A further interesting aspect of two photon microscopy is the "second harmonic generation" (Figure16)[144,147]. This is a fluorescent signal produced when two or more photons are simultaneously scattered from the tissue, generating a single photon of exactly twice the initial excitation energy.

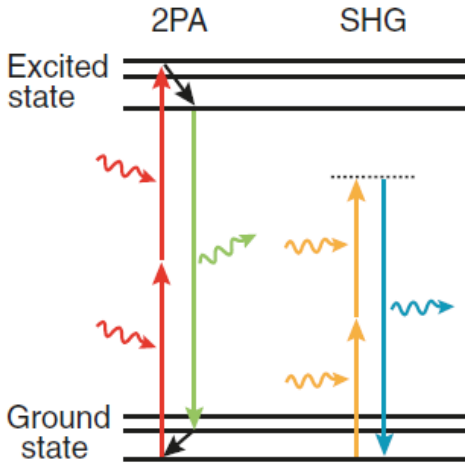

Taken from Helmhen et al, Nat meth, 2005

Figure 17. Jablonski diagram regarding the basic principles of two photon excitation and emission[147].

In the present study we used an excitation wavelength of 800nm and therefore the second harmonic effect resulted in an emission wavelength of about 400 nm, which corresponds to blue light. Second-harmonic generation occurs mainly upon interactions of photons with structures such as collagen fibers or microtubules. Therefore, it provides us with great anatomical information regarding the respective tissue during our experiments.

6.5.2 Technical characteristics of the two photon microscope

For our experiments we used a BioTech TriM Scope system (LaVision Biotech, Bielefeld, Germany see Figure 18). The system was equipped with a Ti:Sa laser (MaiTai, Spectra Physics, Darmstadt, Germany) and with a TriM Scope Scan-head

(LaVision BioTec, Bielefeld, Germany). An Olympus microscope has been used with a 20× water immersion objective lens with NA=0.95 (Olympus, Hamburg, Germany. Furthermore a CCD (charge coupled device) camera was adapted on the microscope in order to acquire images only with epi-fluorescence.

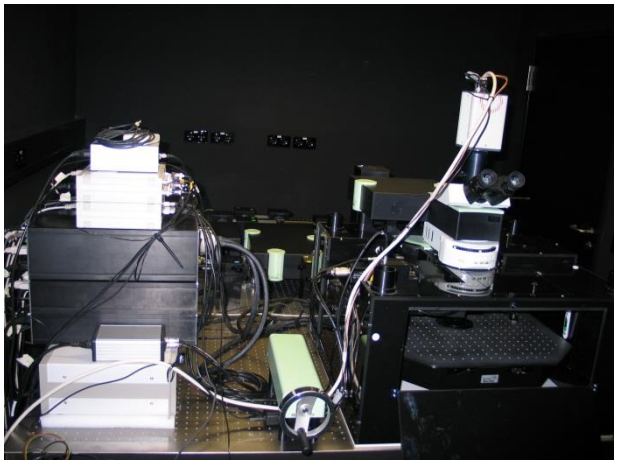

Figure 18. Two photon microscope unit.

The images were normally acquired by unilateral horizontal scanning on the tissue in the XY spatial axis, however depending on the experiment it was possible to perform also bidirectional scans decreasing the image acquisition time by nearly one-half. In our experiments we focused our imaging on a region of interest along the XY axis. Subsequently a range was set in the Z axis allowing us to perform optical tomographies (stacks) in different depths in the tissue. The reconstruction of these scans in the velocity software provided us with a 3 dimensional image of the tissue in a specific time point. This process could be repeated after predetermined time periods (named “wait time”), (Figure19). In a next step we selected a wait time between each scanning as well as the desired number of scans to be performed (“number of steps”). This permitted us to acquire 4 dimensional information regarding the tissue in the X,Y,Z (spatial) as well as T (temporal) axes. The software that was used for regulating the settings regarding the described parameters was the “ImSpector” software (LaVision BioTec, Bielefeld, Germany).

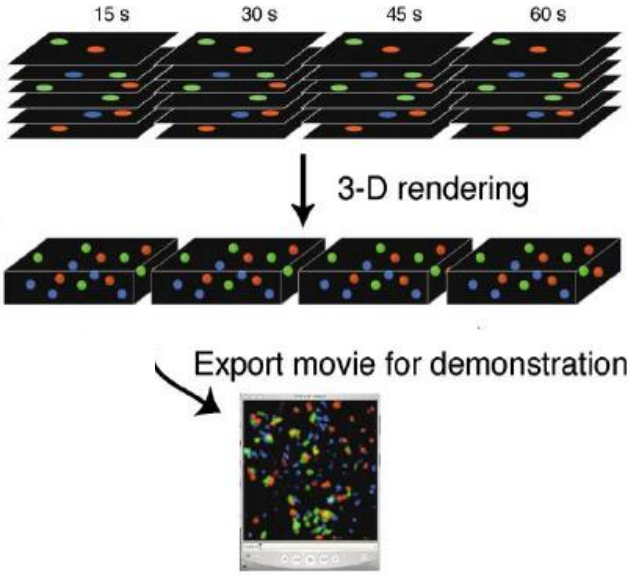

Taken from *Sumen et al. Immunity 2004*

Figure 19. Process for imaging acquisition and demonstration of data that were obtained by two photon microscopy. Modified from Sumen et al[149].

6.5.3 Image acquisition settings for in vivo imaging with TPLSM

6.5.3.1 In vivo imaging in the microvasculature of the mouse ear

For imaging of the microvasculature in the mouse ear a region of interest of 300x300 μm was chosen in the in the XY axis and the pixels were set to 515x515. In the Z axis we defined a range of 15μm while each optical tomography was acquired in an axial (Z) distance of 3-5 μm. The 3dimensional scanning was repeated every 15 seconds for a total time period of 15 minutes. This procedure was repeated 4 times in order to reach a total imaging duration of 1 hour (4 videos of 15 minutes each) or more depending on the needs of each experiment. The 3D image stacks were truncated in order to obtain flattened images along the z axis as maximum intensity projections representing a total X–Y view of the volume. Movies with different time point frames were constructed and exported as avi files using the imspector software.

6.5.3.2 In vivo imaging in carotid arteries

The vessels of the mouse ear are characterised by a small diameter (25-40 μm)[150] and thus deep scanning ranges in the Z axis are not required for their visualization. They are further characterized by a mainly 2-dimensional structure which allows us to image the bigger part of these vessels in the XY axis. Therefore, flattened timeframe images can be used in order to perform cell tracking and further quantitative analysis in two dimensions. In contrast the carotid artery follows progressively deeper paths in the tissue especially in the area distal to the carotid bifurcation (internal-external carotid artery), the area where atherosclerotic plaques will usually develop. Additionally imaging of all the three layers of the arterial wall (adventitia, media, intima) is required in order to analyse the interactions of leukocytes with the endothelium and also their motility within the vessel wall. For these reasons a bigger range of scanning in the Z axis is required in order to visualize simultaneously all the compartments of the wall as well as processes taking place in the luminal area. In the case of carotid arteries the range depending on the experiment and the anatomy of the vessel varied from 30μm to 100μm. Therefore, analysis in flattened images along the Z axis would lead to incorrect estimations regarding factors such as the dimension of the frames. This could lead as a consequence in false quantitative analysis. Thus, a 3 dimensional reconstruction is preferable for the analysis of dynamic cellular processes such as migration in these vessels. For these reasons we have used the professional analysis Software “Velocity” instead of the routinely used “Image j” in order to reconstruct the three dimensional image of the vessel and perform analysis directly in this optical volume.

6.6 Image processing and analysis

6.6.1 “Image j” analysis

In order to analyse the flattened timeframe images obtained from the experiments in the mouse ear we used the image j software (Java-based image processing program,

National Institutes of Health, USA). The 2-dimensional timeframe images were imported in the image j software and a new number of pixels was provided. We next manually calibrated the dimensions of the imported "AVI" movie by dividing the X or Y actual dimension of the frames (as they were set by the Imspector software during our experiments) with the number of pixels given for these frames by the image J software. Furthermore, in the case of time lapses, the time interval between each frame (given in seconds) was divided with 60 in order to obtain quantitative analysis corresponding in minutes/frame. Each cell was tracked manually by the use of the *manual tracking* plugin. The excel files obtained from image j upon tracking were further analysed with the *chemotaxis and migration tool* software (ibidi). The information acquired regarded crawling distance (given in micrometers- μm), velocity (given in μm/min), linearity and forward migration index in x and y axis.

6.6.1.1 Accumulated and euklidean distance

The linear distance that a cell crawls from it`s startpoint to its endpoint is called euklidean distance. The accumulated distance represents the total distance that a cell crawled following it`s actual crawling path (Figure 20).

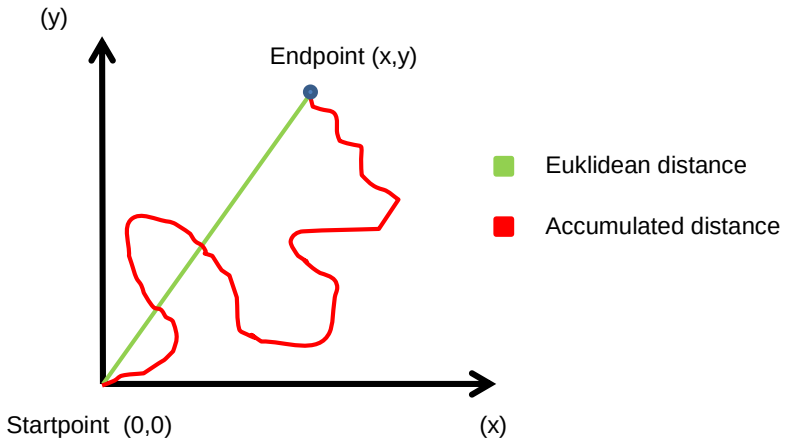

Figure 20. Euklidean and accumulated distance regarding leukocytes crawling from a startpoin (0,0) to an end point (x,y).

6.6.1.2 Velocity

The crawling velocity was automatically provided from the software upon division of the accumulated distance (µm) with the crawling time (min).

6.6.1.3 Linearity

The value of linearity is given by dividing the euklidean with the accumulated distance and is an indicator of how linear is the path that a cell followed during its crawling:
Linearity = 1 (absolute straight motility)
Linearity < 1 (not straight motility)

6.6.1.4 Forward migration index

The forward migration index (FMI) is an indicator of the efficieny of cells to migrate towards a direction along an axis (X or Y). The value of this parameter is given by dividing the migration distance along the x axis (FMIx) and y axis (FMIy) with the accumulated distane (Figure 21).

Migration index for the x axis: xFMI=FMIx/aumulated distance
Migration index for the Y axis: yFMI=FMIy/aumulated distance

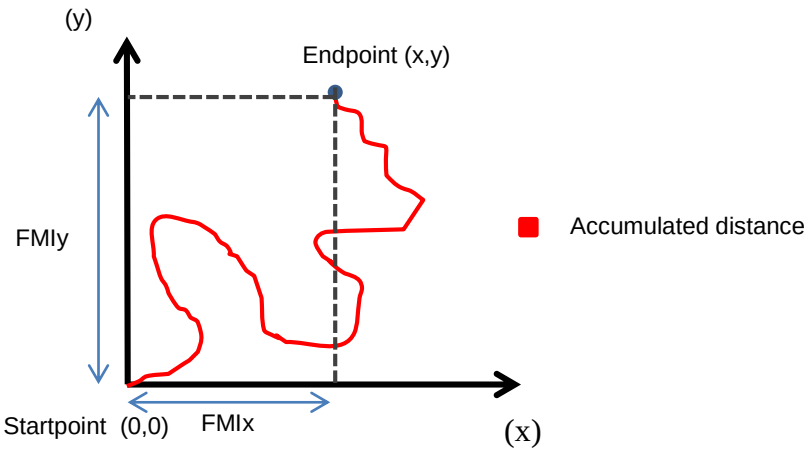

Figure 21. The FMI for the X or Y axis is calculated by dividing the distance that the cell crawled in the respective axis with its accumulated distance.

In our analysis we considered the (0,0) coordinates as a general starting point for all crawling cells independently to the actual coordinates of their crawling. In order to be able to compare the forward migration indexes in the different experiments we further considered that the blood flow was always parallel to the X axis with a right to left direction, and that the region of the injury was found along the positive area of the Y axis. This would imply that the cells that crawl upstream to the blood flow would be characterized by a positive xFMI while the cells that crawl downstream to the blood flow would be characterized by a negative xFMI. In addition a positive yFMI would be indicative of intraluminal cellular migration towards the area of the injury (implying ability for intravascular chemotaxis) while a negative yFMI would indicate intraluminal migration against the injury (implying reduced ability for intravascular chemotaxis). However, our *in vivo* experiments in the mouse ear were performed in mirovessels of different orientation and blood flow direction while the laser injury was also induced in different locations in comparison with the vessel. Thus, the analysis and comparison of the forward migration indexes in different experiments was not possible. To overcome these difficulties we have used image j software in order to reorientate all our flattened timeframe images (avi movies) and obtain a parallel to the x axis blood flow with a right to left direction prior to the cell tracking analysis. This was achieved by manually adjusting the angle of disposal of each timeframe individually (figure 22). The desired angle was counted by using the *angle tool* in image j and the correction regarding the angle was inserted in the settings of each timepoint frame in the chemotaxis tool before each analysis. This intervention allowed us not only to readjust the blood flow axis according to the x axis but also to present the laser injury along the Y axis. However, depending on the individual experiments the injury was found either along the positive side of the Y axis or along the negative side. In the cases that the injury was found in the negative area of the y axis we manually changed the + sign to – and the – sign to + in the yFMI values that we obtained from our analysis. Thus, a positive yFMI would again indicate migration towards the area of the injury albeit its physical location is in the negative area of the y axis.

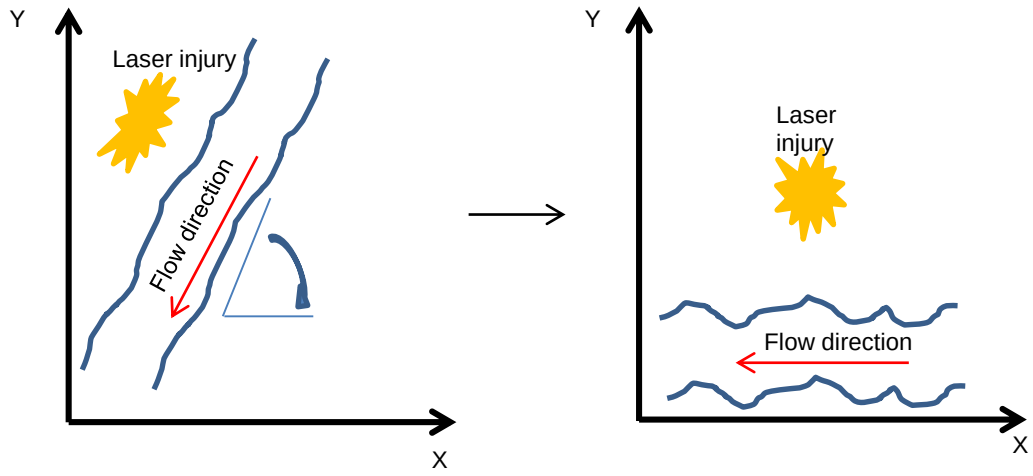

Figure 22. Schematic representation of orientation adjustment in the flattened time lapses before tracking analysis with image J. The clockwise rotation results in a parallel to the x axis blood flow and to a localization of the laser injury along the positive area of the Y axis. The orientation of the data from all our experiments was adjusted. Thus, calculation of mean FMI for the X and Y axis among one group as well as comparison of these values in different groups of experiments is possible.

6.6.2 Volocity software analysis

Our original data were exported as Tiff files from the Imspector software and were imported to the velocity software for further processing. The calibration of the imported frames was performed by dividing the X and Y dimensions (given in micrometers) with the corresponding number of pixels selected in the Imspector software. Additionally to these values, the step size between each optical scanning was edited in the settings of the velocity software for each analysis independently. Thus, the software was “informed” for the dimensions of our data in the X, Y and Z axis allowing us to perform three dimensional analysis of crawling leukocytes. As in the case of analysis with image j our analysis corresponded in information regarding minutes/frame.

6.7 Experimental protocols and experimental groups

6.7.1 *In vivo* imaging of large non atherosclerotic arteries using TPLSM

Different approaches were followed in order to investigate the potential of TPLSM for in vivo imaging of large vessels. Initially we have performed experiments in C57BL/6J mice in order to investigate the ability of TPLSM for *in vivo* stable imaging of carotid arteries free of any preparation (table 3). In a next step we have used an ECG triggering unit in order to acquire images of the carotid artery of C57Bl/6J mice always in the same phase of the heart cycle (table 3). Additionally a ventilator was used to reduce the imaging distortion due to respiratory movements. Our further experiments included in vivo imaging of carotid arteries of C57Bl/6J mice upon the contemporaneous use of our stabilizing stage, the ECG triggering unit and the ventilation device (table 3). Fifteen µl of rhodamine 6G chloride (molecular probes, Eugen Oregon, USA) were injected in the C57Bl/6J mice in order to visualize leukocytes in the circulation.

Table 3. Experimental groups assessed in the study of the potential of TPLSM for in vivo imaging of carotid arteries.

Preimaging procedure	Mice	N
no preparation	C57Bl/6J	5
ECG trigger+intubation	C57Bl/6J	7
stabilising stage+ECG trigger+intubation	C57Bl/6J	8

To analyse whether our preparation led to an acute inflammatory reaction and recruitment of neutrophils we performed experiments in C57Bl/6J and LysM^{eGFP} mice (Table 4). In the first case the anti-Ly6G 1A8 antibody (5µg, PE conjugated, BD Pharmigen) was injected in order to stain *in vivo* neutrophils.

Table 4. Experimental groups assessed in the study of preparation dependent injury to the vessel

Mice	N
C57Bl/6J	5
LysMeGFP	6

6.7.2 *In vivo* imaging of large atherosclerotic arteries using TPLSM

To test the imaging penetration of TPLSM in the presence of established atherosclerotic plaques and to further investigate the potential of *in vivo* analysis of leukocyte transmigration and motility within the atherosclerotic lesions we have performed experiments in mice of ApoE deficient background (table 5).

Table 5. Experimental groups assessed in the study of in vivo imaging of carotid arteries using TPLSM

Mice	N
ApoE-/-MHCII eGFP	4
ApoE-/-CX3CR1$^{GFP/+}$	4
ApoE-/-LysM eGFP	4

Generally in our experiments the ApoE$^{-/-}$ mice were fed with a high cholesterol diet (1,25% cholesterin, altromin) starting from the age of 4 weeks while imaging took place at the age of 18-20 weeks. The same procedure was followed for the ApoE$^{-/-}$ MHCII^{eGFP} mice which derived from crossing of the two strains (figure 23). In the case of experiments performed in bone marrow chimeras the recipient ApoE deficient mice were also fed with high cholesterol diet starting from the age of 4 weeks. The ApoE deficient mice develop reduced atherosclerotic plaques upon irradiation and transplantation of bone marrow cells from donors with no ApoE deficient background (as in the case of LysM^{eGFP} and CX3CR1$^{GFP/+}$ mice). In our experiments we performed irradiation and bone marrow transplantation when the mice were 16 weeks old (Figure 23). In that age atherosclerotic plaque formation is expected to be allready initiated. The total duration of each experiment was 1 hour during which 4 recordings of 15 minutes each were performed (figure 24).

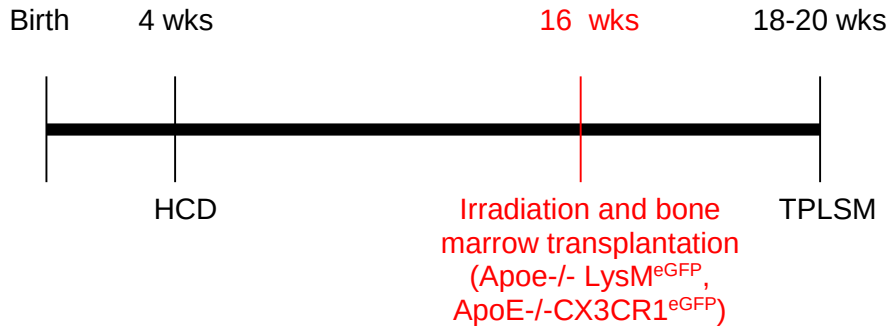

Figure 23. Time points of initiation of feeding of ApoE$^{-/-}$ mice and ApoE$^{-/-}$ chimeras with high cholesterol diet (HCD), irradiation and bone marrow transplantation in the case of ApoE$^{-/-}$ LysM^{eGFP} and ApoE$^{-/-}$ CX3CR1$^{GFP/+}$ mice and performance of in vivo imaging with TPLSM.

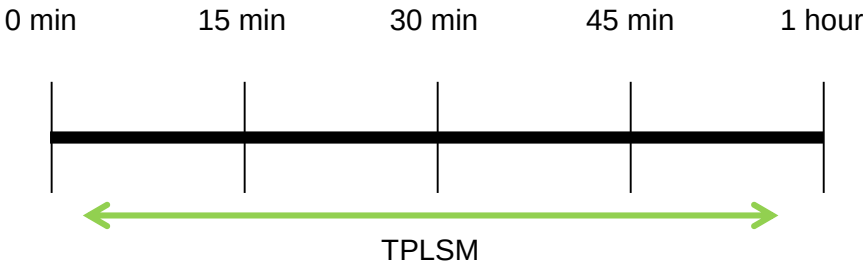

Figure 24. Experimental protocol applied in the in vivo study of cellular presence and motility within atherosclerotic plaques in the carotid arteries.

6.7.3 Identification of crawling leukocytes during steady state and atherosclerosis in carotid arteries

Next we aimed at investigating whether leukocytes are able for intravascular crawling in carotid arteries either during steady state conditions or atherosclerosis. The predominant type of leukocytes that it is expected to crawl under steady state conditions in the microvasculature are monocytes[14]. To test whether monocytes are able to crawl also in large arteries we have performed in vivo expoeriments in the carotid arteries of CX3CR1$^{GFP/+}$ mice (Table 6).

In the case of inflammation neutrophils are expected to be initially recruited in the microvasculature. Interestingly it was also shown that neutrophils are also recruited in atherosclerosis[29]. Therefore, we focused in investigating the ability of neutrophils to crawl in the presence of atherosclerotic lesions in ApoE defficient and ApoE$^{-/-}$ LysM^{eGFP} mice. In the first case neutrophils were specifically stained by injection through the tail vein of Ly6G 1a8 antibody (5 μg, PE conjugated, BD Pharmigen). During the experiments in the presence of atherosclerotic lesions we were also able to detect occasionaly neutrophils transmigration in the plaque. The total duration of each experiment was 1 hour and consisted of 4 videos with 15 minutes duration each (Figure 24). The ApoE$^{-/-}$ and ApoE$^{-/-}$LysM^{eGFP} mice were fed with high cholesterol diet from the age of 4 weeks and were imaged at the age of 18-20 weeks (Figure 25).

Table 6. Experimental groups assessed in the study of in vivo detection of leukocytes crawling in carotid arteries during steady state and atherosclerosis.

Mice	N
CX3CR1$^{GFP/+}$	6
ApoE-/-	8
ApoE-/-LysM eGFP	6

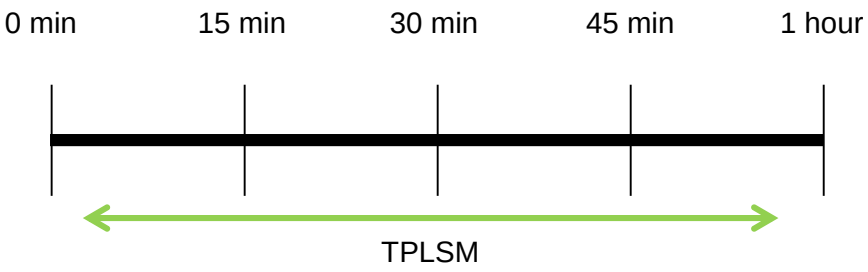

Figure 25. Experimental protocol applied in the study of in vivo imaging of carotid arteries regarding leukocytes crawling during steady state or atherosclerosis

6.7.4 Identification of crawling leukocytes during steady state in the microvasculature of the mouse ear

Our next aim was to analyse the effect of blocking of beta 2 integrins in the crawling behaviour of leukocytes during steady state in the microvasculature of the ear and

compare these results with the results obtained from carotid arteries under the same conditions. To identify the population of cells able for intraluminal crawling in post-capillary venules and arterioles we have performed experiments in LysM^{eGFP} mice (focus on neutrophils) and CX3CR1$^{GFP/+}$ mice (focus on monocytes), (Table 7).

Table 7. Experimental groups assessed in the study of the ability of leukocytes to crawl under steady state in the microvasculature of the mouse ear

Mice	N
CX3CR1$^{GFP/+}$	7
LysM eGFP	6

Six to eight vessels were imaged per mouse and the total duration of imaging of each vessel was 15 minutes. TRITC dextran (2,000,000 MW, invitrogen) was used during these experiments in order to label the plasma in red and thus define the luminal borders (Figure 26).

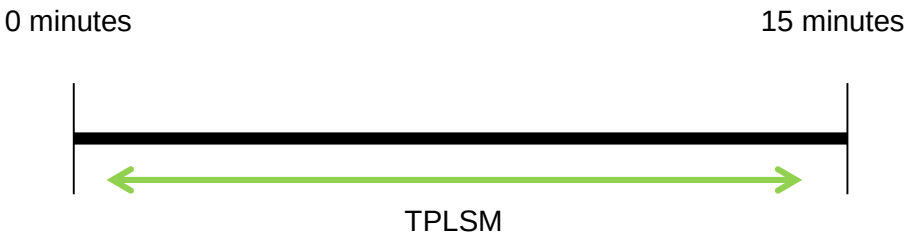

Figure 26: Experimental protocol applied in the study of the ability of leukocytes to crawl under steady state in the microvasculature of the mouse ear. 6-8 vessels were imaged per experiment. Each vessel was imaged for a period of 15 minutes.

6.7.5 Protocols for *in vivo* tracking of crawling leukocytes

The effect of blocking antibodies against beta-2 integrins during the migration cascade was analysed in the past following several approaches:

A. Transgenic knockout mice for LFA-1 or Mac-1 integrins have been used for the analysis of leukocytes crawling and transmigration to sites of inflammation[4]. However this approach could not exclude the possibility that the absence of each of these two integrins influences initial steps of the migration cascade (rolling, adhesion). Therefore, the effect detected in leukocytes crawling could be a secondary effect.

B. Blocking antibodies against LFA-1 or Mac-1 were injected prior to the in vivo imaging[57]. As in the previous case however, it could not be excluded that the effect in crawling is a secondary phenomenon.
C. An initial baseline recording was performed and the number of adhering/crawling cells were accepted to be equal to 100%. Subsequently the recording was stopped and a blocking antibody against Mac-1 or LFA-1 was injected. 20-30 minutes upon application of the antibody a secondary recording was taken place and the number of crawling cells at that time point was compared to the number of initially crawling cells[62]. However, the immediate effect of blocking of Mac-1 or LFA-1 to adhesion, crawling and transmigration of leukocytes could not be identified following this protocol. This implies that the cells analysed in the secondary recording could be a completely different population from the initially identified crawling cells. Thus, it is possible that the initially crawling cells continued crawling and eventually even transmigrated in a normal way in between the two recordings.

6.7.6 Continuous single cell tracking protocol (CSCTP)

In order to overcome the difficulties in analysis present in the previously described approaches we established a novel protocol for *in vivo* analysis of the effect of blocking of LFA-1 or Mac-1 in the crawling and transmigration process of leukocytes. Starting our experiment we identified adhering and crawling leukocytes in a baseline recording. Subsequently we injected through the tail vein catheter blocking antibodies against LFA-1 or Mac-1 as well as IgG isotype controls in a continuous way without stopping the process of recording. Following this approach we were able to identify the immediate effect of blocking of beta 2 integrins in the crawling and transmigration of leukocytes to sites of inflammation (Figure 27).

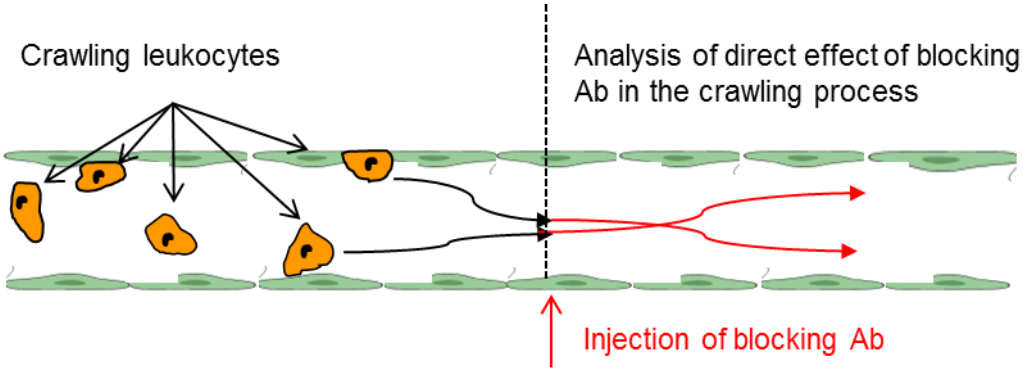

Figure 27. Continuous single cell tracking protocol (CSCTP). Blocking antibodies against Mac-1 or LFA-1 are injected during recording of crawling cells. The direct effect of blocking of beta 2 integrins in the crawling behaviour is analysed in the population of cells that are detected crawling during the injection. Cells that detach before injection or cells that adhere and crawl upon injection cannot be analysed by CSCTP. To detect the exact time point of arrival of antibodies in the area of recording, labelled antibodies were used (PE/ FITC conjugated).

6.7.7 Investigation of the effect of blocking of Mac-1 and LFA-1 in the crawling process of patrolling monocytes in microvasculature

Our results confirmed that only monocytes are able to crawl under steady state conditions in post-capillary venules and arterioles. Therefore, further experiments under these conditions were performed only in CX3CR1$^{GFP/+}$ mice. In the first set of experiments we applied the CSCTP in order to analyse the direct effect of blocking of Mac-1 and LFA-1 in the crawling process (Table 8).

Table 8. Experimental groups assessed in the study of the direct effect of blocking of Mac-1 in the crawling behaviour of patrolling monocytes in the ear microvasculature

Treatment	Mice	N
IgG2a	CX3CR1$^{GFP/+}$	13
anti LFA-1	CX3CR1$^{GFP/+}$	15
IgG2b,k	CX3CR1$^{GFP/+}$	14
anti Mac-1	CX3CR1$^{GFP/+}$	17

During our experiments we have initially detected a single patrolling monocyte crawling in a post-capillary venule or in an arteriole by the use of the epi-fluorescence camera of our microscope. Subsequently we imaged this vessel for a total period of 15 minutes. One vessel (and therefore one cell) was analysed per experiment. During our recording we injected blocking antibodies (approximately in the seventh minute of imaging) against Mac-1 (50 μg, clone M1/70, eBioscience), LFA-1(50μg, clone M17/4) or the corresponding IgG (50 μg) controls (Figure 28).

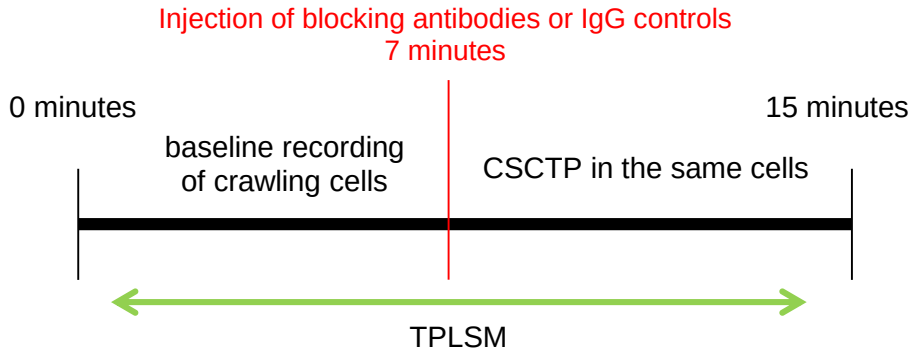

Figure 28. Experimental protocol applied in the study of the direct effect of blocking of Mac-1 in the crawling behaviour of patrolling monocytes in post-capillary venules and arterioles in the mouse ear.

LFA-1 was found to have a strong effect on adhesion and its blocking led to detachment of crawling cells. Thus, its role in the crawling of patrolling monocytes could not be analysed following this protocol. In contrast Mac-1 had a significant direct effect in the crawling behaviour but not on adhesion and therefore we focussed in further investigation only of this beta 2 integrin. Our next target was to analyse whether the direct effect of blocking of Mac-1 was long lasting. To address this question we have performed further experiments in CX3CR1$^{GFP/+}$ mice (Table 9).

Table 9. Experimental groups assessed in the study of the long-term effect of blocking of Mac-1 in the crawling behaviour of patrolling monocytes in post-capillary venules and arterioles in the mouse ear.

Treatment	Mice	N
IgG2b,k	CX3CR1$^{GFP/+}$	7
anti Mac-1	CX3CR1$^{GFP/+}$	5

The protocol that we have followed in this case included the injection of blocking antibody against Mac-1 (50μg) or the corresponding IgG2b,k(50μg) isotype control right before to the initiation of our recording. Subsequently we imaged crawling monocytes in different vessels up to 2 hours post injection in order to increase the total number of monocytes analysed per experiment. The recording of each vessel lasted for 15 minutes (Figure 29).

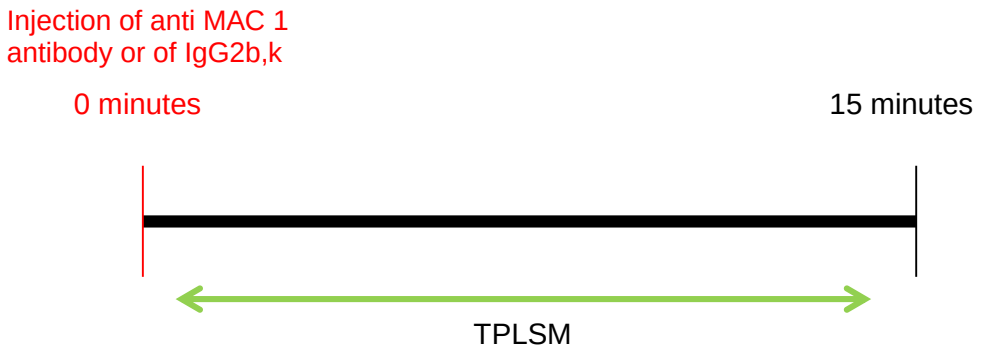

Figure 29. Experimental protocol applied in the study of the long-term effect of blocking of Mac-1 in the crawling behaviour of patrolling monocytes.

6.7.8 Investigation of the effect of blocking of Mac-1 in the crawling process of patrolling monocytes in carotid arteries

Upon investigating the effect of blocking of Mac-1 in the crawling process of patrolling monocytes in the microvasculature we focused in performing the same analysis in unstimulated carotid arteries of $CX3CR1^{GFP/+}$ mice (Table 10).

Table 10. Experimental groups assessed in the study of the effect of blocking of Mac-1 in the crawling behaviour of patrolling monocytes in carotid arteries.

Treatment	Mice	N
IgG2b,k	$CX3CR1^{GFP/+}$	6
anti Mac-1	$CX3CR1^{GFP/+}$	7

The performance of injection during our recordings had as a result a transient hemodynamic instability of the mouse which led to a loss of focus. This condition did not permit us to perform CSCTP in the case of the carotid arteries. Therefore, in this

set of experiments we injected the anti Mac-1 antibody or the corresponding IgG2b,k control (50µg each) prior to our recordings. Our region of interest in the carotid artery was the carotid bifurcation and the total duration of the recording was 1 hour (4 videos of 15 minutes each, see Figure 30).

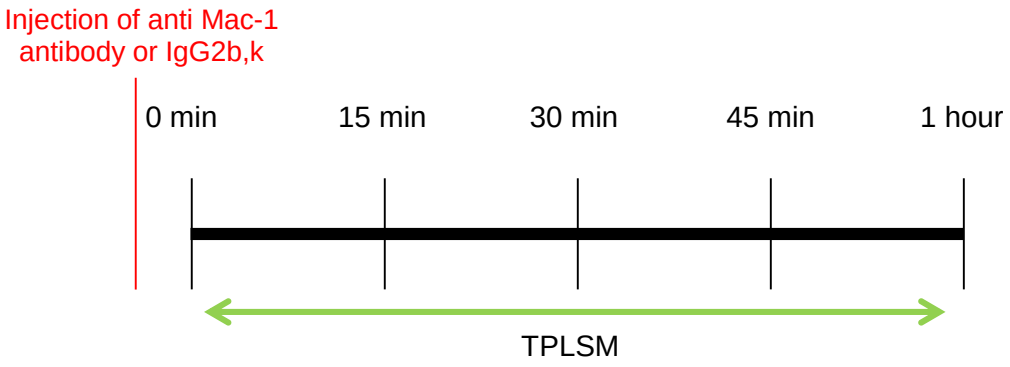

Figure 30. Experimental protocol applied in the study of the effect of blocking of Mac-1 in the crawling behaviour of patrolling monocytes in carotid arteries.

6.7.9 Effect of blocking of Mac-1 to the crawling behaviour of neutrophils upon induction of sterile inflammation in the microvasculature

In the next set of experiments we tested the effect of the induction of sterile inflamamation in neutrophil recruitment. Therefore, we have performed experiments in C57BL6/J mice (n=6) and stained neutrophils by injection of Ly6G 1A8 labelling antibody. The sterile injury was induced as described in 6.4.1.1. During our experiments we could observe that induction of sterile inflammation led to a significant rapid increase in the number of crawling and extravasated neutrophils. Next, we questioned whether Mac-1could mediate the crawling behaviour of neutronphils in this complex inflammatory microenvironment related to tissue injury. Therefore, we have performed experiments under conditions of induced acute sterile inflammation in the post capillary venules of the mouse ear of C57Bl6/J mice(Table 11). Neutrophils were labelled *in vivo* by application of the Ly6G clone 1A8 antibody. Our recordings were initiated directly upon the induction of the laser injury. Our region of interest was the post-capillary venule adjacent to the laser injury.

Table 11. Experimental groups assessed in the study of leukocyte recruitment upon induction of sterile inflammation.

Treatment	Mice	N
IgG2b,k	C57Bl/6J	5
anti Mac-1	C57Bl/6J	5

Our recordings lasted for one hour each (4 videos of 15 minutes each) during which the same vessel was imaged. During approximately the seventh minute of the first video the blocking antibody against Mac-1 or the IgG2b,k control were injected. The cells that were detected crawling during injection were analysed by CSCTP. Analysis of the crawling cells in the later time points provided us information regarding the long-term effect of blocking of Mac-1 (Figure 31).

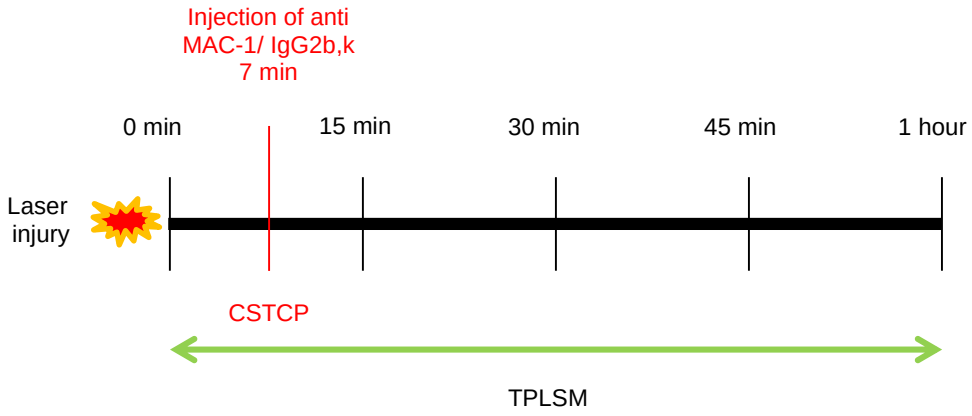

Figure 31. Experimental protocol applied in the study of the effect of blocking of Mac-1 in the crawling behaviour of neutrophils upon induction of acute sterile inflammation.

6.7.10 Effect of blocking of Mac-1 in the crawling behaviour of neutrophils in atherosclerosis

In the last part of our study we focused in analysing whether Mac-1 influenced the crawling behaviour of neutrophils also in the case of atherosclerosis in large vessels. This set of experiments was performed in the carotid arteries of 18-20 weeks old ApoE$^{-/-}$ mice (Table 12) fed with high cholesterol diet.

Table 12. Experimental groups assessed in the study of the effect of blocking of Mac-1 in the crawling of leukocytes in atherosclerosis.

Treatment	Mice	N
IgG2b,k	ApoE-/-	5
anti Mac-1	ApoE-/-	5

As in the case of imaging of carotid arteries in steady state the injection of anti Mac-1 antibody or IgG 2b,k isotype control led to loss of focus. Thus, it was not possible to perform CSCTP analysis. In this set of experiments an initial baseline recording was performed with a duration of 15 minutes. During this time period we were able to confirm the presence of crawling cells on the atherosclerotic vessel wall. Subsequently the recording was stopped and anti Mac-1 blocking antibody or IgG2b,k were injected. Shortly upon injection we continued with our recording (3 additional videos of 15 minutes each see Figure 32).

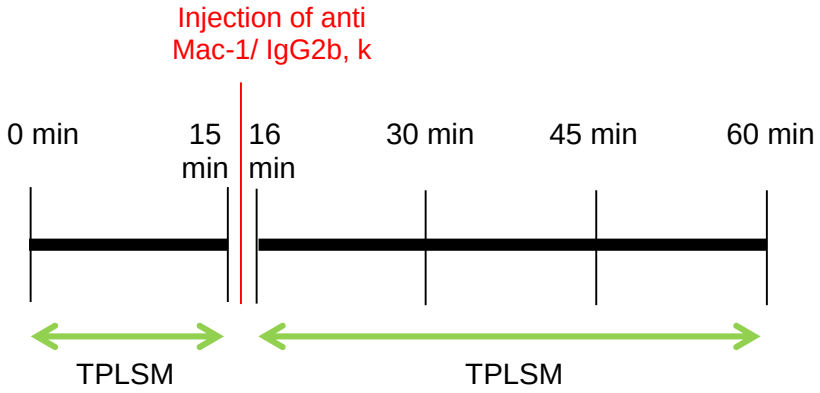

Figure 32. Experimental protocol applied in the study of the effect of blocking of Mac-1 in the crawling behaviour of patrolling monocytes in carotid arteries. A blocking antibody was injected approximately 10 minutes prior to recording. The total duration of the experiment was 1 hour (4 videos of 15 minutes each). Our imaging region of interest was the carotid bifurcation.

6.8 Statistical analysis

The statistical analysis was performed using the Sigma Plot 11.0 software (Systat, Erkrath). Results are presented as mean and SEM.Two independent groups of data were compared per analysis by the use of student´s *t*- test. Alternatively Mann-Whitney U test was applied in the cases of non normal distribution between the groups in question. In the case of comparison of data obtained from the same groups paired t-test was performed. In the case of analysis of percentages obtained from the total number of experiments (and not from each experiment indipendently) the Z statistical test was used. Statistical significance was assumed for a p-value <0.05.

7.Results

7.1 Intravital microscopy in large arteries using TPLSM

7.1.1 TPLSM in carotid arteries without the use of an ECG trigger or of the stabilising stage

As it was previously described the in vivo imaging of carotid arteries (and large vessels in general) suffers from instability and prominent loss of focus. This disadvantage significantly impairs the ability of two photon microscopy to perform stable long term *in vivo* recordings either in two dimensions (X,Y axis), three dimensions (X,Y,Z axis) and even more in 4 dimensions (X,Y,Z, spatial axis and T temporal axis, in order to obtain “3D time lapses”). To further characterize the level of imaging distortion and loss of focus induced by vessel pulsation we have performed *in vivo* real time imaging of carotid arteries of C57Bl/6J mice without the use of an electrocardiographic trigger, a ventilator or of our stabilizing stage. Initially, our only intervention was to place a free coverslip on the top of the artery which provided us an area where a few drops of buffer saline could be placed. In that way our upright water immersion objective could obtain images from the carotid artery. These experiments showed that it is still possible to differentiate the basic structures of the arterial wall (adventitia, media-intima) as well as plasma (stained by FITC or TRITC dextrans). However, they also confirmed a prominent loss of focus and instability over time since the artery was free to move in the X,Y and Z axis according to the heart and respiratory cycle of the mouse. Moreover the attempt to perform 3D time lapse recordings revealed that the slow process of imaging acquisition in addition to the fast heart rate resulted in extreme imaging artifacts during which the different optical tomographies of the carotid artery in the Z axis were presented as distinct vessels in our images (Figure 33).

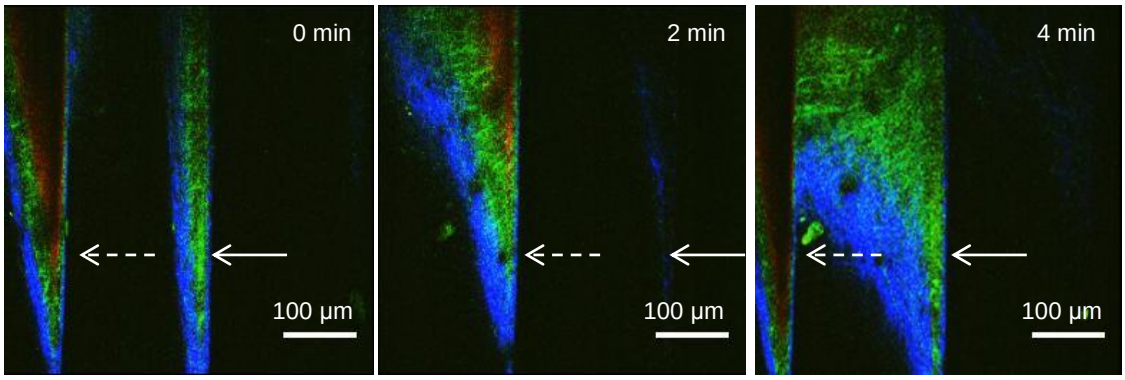

Figure 33. Freeze frame images from a flattened 3dimensional two photon time lapse recording of a carotid artery of a C57Bl/6J mouse without the use of an ECG trigger, a ventilator or of our stabilizing stage. The white arrows indicate an optical tomography of the carotid artery in a certain level of the Z axis. The dotted white arrows indicate an optical tomography of the same vessel in a deeper level of the Z axis. The basic structures of the arterial wall (media, intima, adventitia) can still be differentiated however our images suffer from motion artifacts and continuous loss of focus. Adventitia is presented in blue (due to SHG), media and intima in green (due to auto-fluorescence) and plasma in red, (due to injection of TRITC dextran).

7.1.2 TPLSM in carotid arteries with the use of ECG trigger in ventilated mice

In order to overcome the prominent imaging distortion and loss of focus we have intubated (as described in 6.4.2.1) C57Bl/6J mice (n= 7) and additionally connected them to an ECG triggering unit before imaging. The rhythmical and smooth respiration rate due to ventilation greatly reduced the out of frame loss of focus in our 2-dimensional time lapses (X,Y spatial axis, T temporal axis). Furthermore the use of the ECG trigger was also very efficient in reducing the in frame loss of focus. A further important benefit of the application of the ECG trigger was that the different optical tomographies of the artery were imaged during the same phase of the heart cycle. Therefore, the different levels of the vessels along the Z axis were imaged in the same spatial area. This allowed us to perform stable 3-dimensional scans (X,Y,Z axis) and furthermore relatively stable 3-dimensional scan time lapses (X,Y,Z and T axis). However, although the out of frame as well as the in frame loss of focus were greatly reduced and in some cases it was possible to perform relatively long term stable in vivo imaging (approximately for 4-5 minutes), eventually loss of focus occurred in a time dependent manner (figure 34). This loss of focus did not affect only the Z axis but also the X and Y axis.

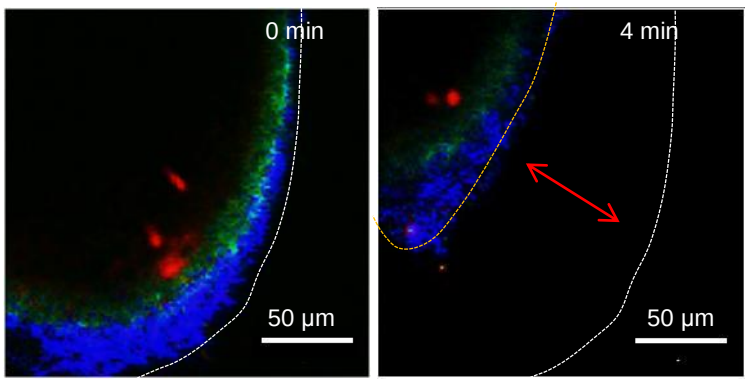

Figure 34. Freeze frame images from a flattened 3 dimensional time lapse recording in the carotid artery of a C57Bl/6J mouse. The ECG triggered acquisition of images significantly increased the quality and stability of our recordings. However, a time dependent shift in the X and Y axis was observed. Adventitia is presented in blue (due to SHG), media – intima in green (due to auto-fluorescence) and neutrophils in red (due to injection of PE conjugated Ly6G 1A8 antibody). The white dotted line represents the border of the vessel in the initial time point of our imaging. The yellow dotted line represents the border of the vessel in a later time point. The red double edged arrow indicates the shift of the vessel in the space over time.

7.1.3 TPLSM in carotid arteries with the simultaneous use of ventilation, ECG trigger and stabilizing stage

In order to avoid all the previously described difficulties of the *in vivo* imaging of large vessels we have used a stabilizing stage in addition to the ECG trigger unit and performed *in vivo* imaging of the carotid arteries of ventilated C57Bl/6J mice (n=8). The contact of a cover slip (glued on the bottom of our circular stage as described in 6.3.2.3) with the artery absorbs the imaging artifacts due to pulsation of the heart and of the vessels reducing in that way the in frame loss of focus in the vertical axis. Additionally, the gentle placement of a thin plastic sheet under the artery provides a stable and isolated microenvironment to the vessel from the surrounding tissue which reduces the out of frame loss of focus. In that way we were able to significantly increase the mean time of stable imaging from 4,3 minutes with the use of only the ECG trigger unit in ventilated mice, to 14,14 minutes with the simultaneous use of our stabilizing stage, the ECG trigger unit and ventilation (figure 35).

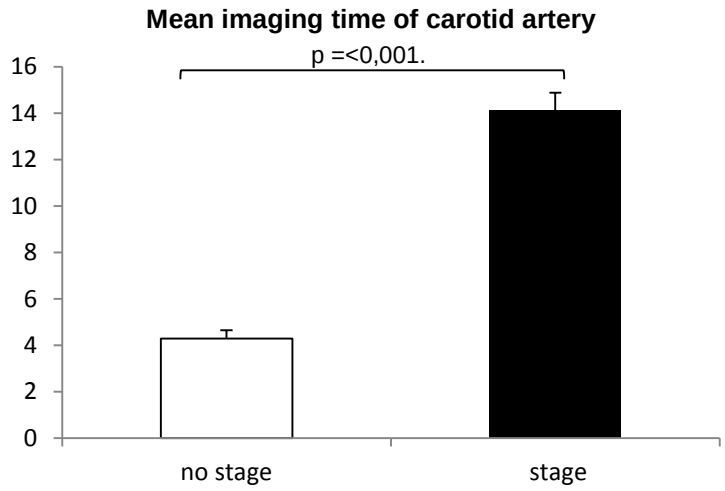

Figure 35. Comparison of mean times of stable imaging of carotid arteries of C57Bl/6J mice without the use of the stabilizing stage (only ECG trigger and intubation were used) and with the use of the stabilizing stage (in addition to the use of the ECG trigger and the intubation). The use of the stabilizing stage significantly increased the mean time of stable imaging ($p< 0,001$, n= 7-8 mice per group).

Furthermore, experiments performed with *in vivo* injection of rhodamine 6G (which stains in a non specific way all subsets of leukocytes) confirmed that there is no cessation in the blood flow due to the placement of the stage (Figure 36).

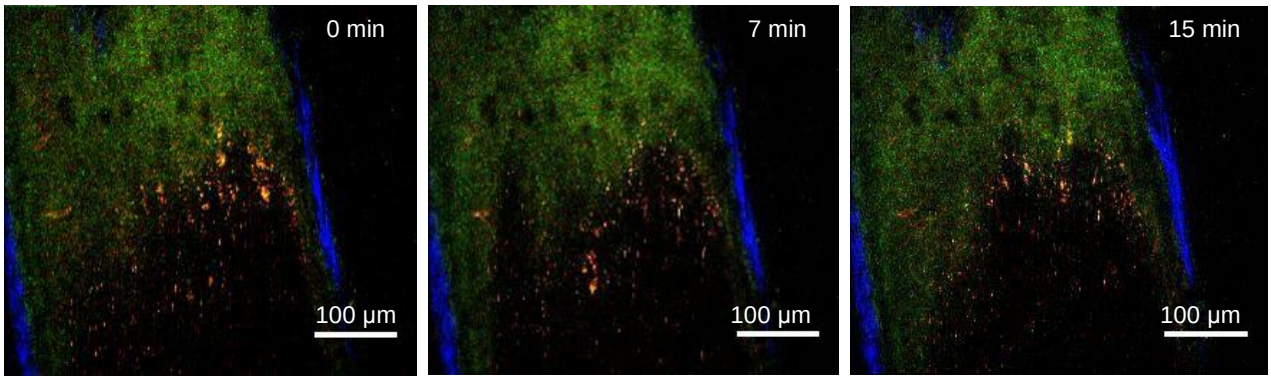

Figure 36. Freeze frame images taken from 3 dimensional time lapse recordings in the common carotid artery of a C57Bl/6J mouse. The use of the stabilizing stage in addition to the ECG-trigger and intubation of the mouse significantly increased the mean time of stable imaging. Presence of circulating leukocytes confirm that there is no cessation in the blood flow due to the placement of the stage. The adventitia is presented in blue (due to SHG), media and intima in green (due to auto-fluorescence), and leukocytes in orange (due to injection of rhodamine 6G).

7.1.3.1 Considerations regarding the use of the stabilizing stage

Concerning the establishment of this surgical model we took into account the following considerations:

- Maintenance of normal heart rhythm
- Induction of minimal injury to the vessel during the surgical preparation
- Maintenance of normal flow conditions

7.1.3.1.1 Maintenance of normal heart rhythm

The contact of the cover glass glued on the bottom of our circular stage with the carotid bifurcation could potentially lead to a stimulation of the carotid sinus and this eventually could lead to hemodynamic effects such as decreased heart rate, lowered cardiac output and decreased venous return as described in 6.4.2.4. In order to test whether the contact of the stage with the carotid bifurcation influences the hemodynamic condition of the mice we tested the heart rate before and after the application of our stabilizing stage. This approach would provide us with information about possible changes in the heart and vascular function of the mice (Figure 37 A). However, our analysis showed that there is no significant difference in the heart rate of the mice before and after the application of the stage (Figure 37 B).

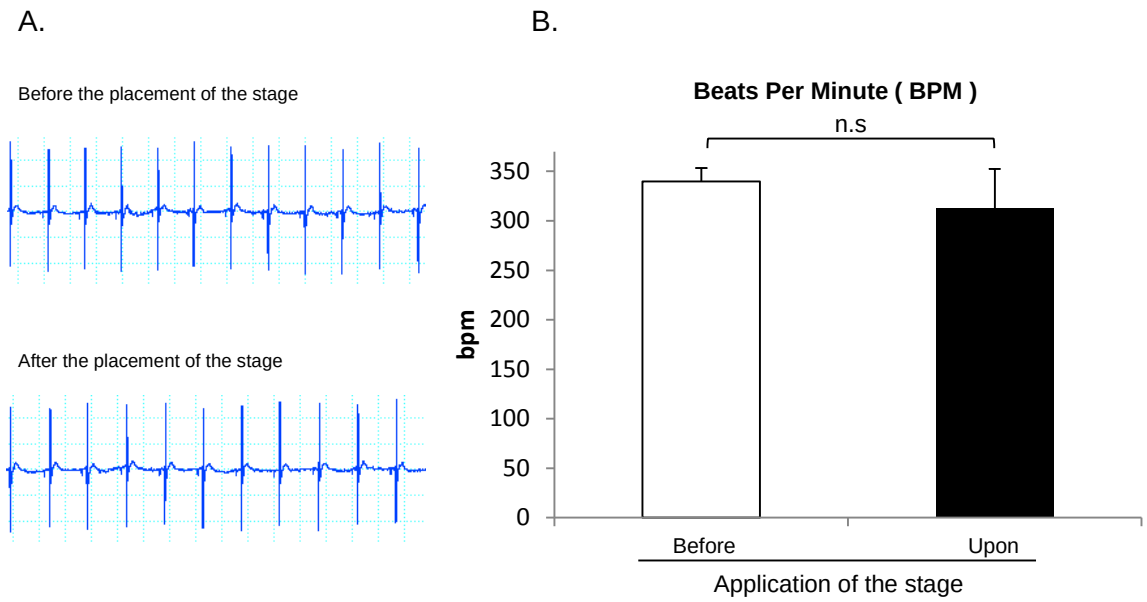

Figure 37. Effect of placement of the stabilising stage in the cardiac rhythm. **A.** Electrocardiographic test before and after the placement of the stage (in both cases the bpm were approximately equal to 300). **B.** There is no significant difference (p=0,544, n=7 mice) in the beats per minute of the mice before and upon the placement of our stabilizing stage.

7.1.3.1.2 Vessel injury induced via surgical preparation.

Neutrophils are the subset of leukocytes that is initially recruited in cases of acute inflammation including sterile inflammation and tissue injury. However, during steady state neutrophils are generally thought to be present in the blood stream and do not adhere on the endothelium or transmigrate in the tissue[1]. These observations were confirmed by experiments that we performed in the microvasculature of the ear during steady state (see 7.2.1). Therefore, a massive recruitment of neutrophils in the carotid arteries upon surgery would be indicative of inflammation caused by our surgical preparation. To further analyse whether the surgical preparation of the carotid artery provoked tissue injury and subsequently a relevant neutrophil recruitment we have performed experiments in C57Bl/6J mice in which neutrophils were labelled *in vivo* by injection of PE labelled Ly6G 1A8 antibody and also in LysM^{eGFP} mice in which the most of the cells expressing GFP are neutrophils[131]. Our intravital imaging was focused on *in vivo* imaging in two distinct parts of the carotid arteries: the common carotid artery (in the vicinity to the carotid bifurcation) and the area distal to the carotid bifurcation (external – internal carotid arteries). The total

duration of each experiment was 1 hour. Typically the preferable area for interactions of neutrophils with the endothelium was the region of the bifurcation and the external/ internal carotid artery. In the case of the common carotid artery we did not observe interactions of neutrophils with the endothelium either in the C57Bl/6J or the LysM^{eGFP} mice (Figure 38). In the carotid bifurcation and the internal and external carotid arteries we could observe occasionally transient adhesion of neutrophils in 40% of the experiments performed in C57Bl/6J mice and in 50% of the experiments performed in the LysM^{eGFP} mice (n=5-6 per group).

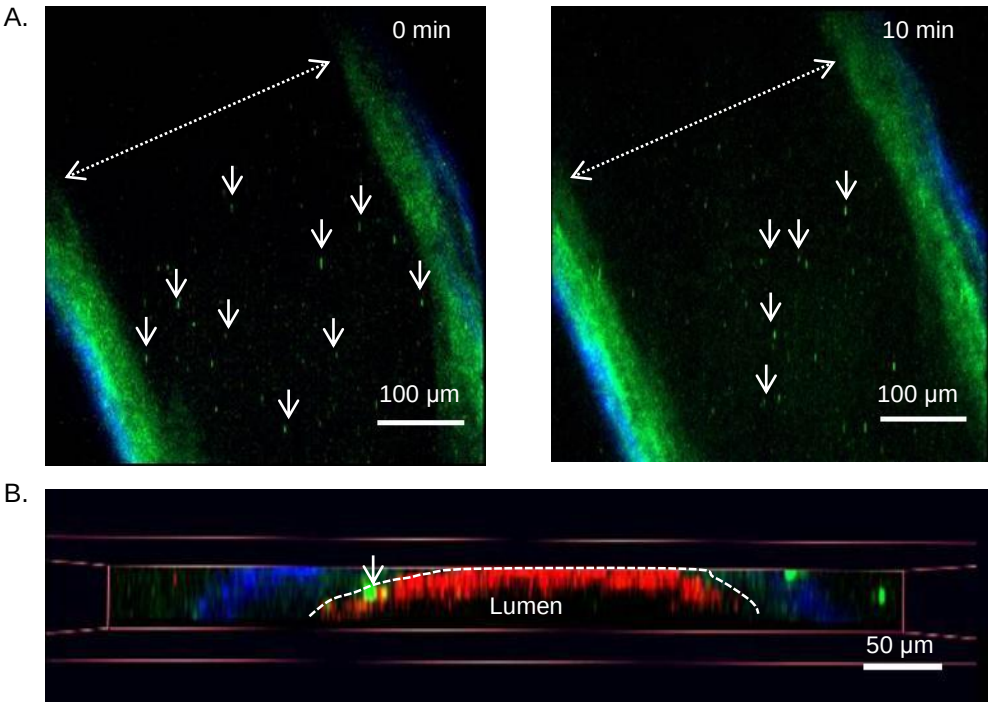

Figure 38. Freeze images from time lapse recordings in carotid arteries of LysM^{eGFP} mice. Effect of surgical preparation. **A.** In vivo imaging in the common carotid artery of LysM^{eGFP} mice (XY projection). Typically neutrophils did not adhere on the arterial endothelium in that area. **B.** In vivo imaging in the external carotid artery of LysM^{eGFP} mice (XZ projection). More interactions of neutrophils with the endothelium were detected in this area. Adventitia is presented in blue (due to SHG), media and intima in green (due to auto-fluorescence), neutrophils in green (due to GFP expression) and plasma in red (due to application of TRITC dextran).

7.1.3.1.3 Maintenance of physiological flow conditions

The areas of bifurcations are favourable for atherosclerotic plaque formation due to the disturbed oscillatory blood flow conditions in these regions[138,139]. Three dimensional reconstructions of carotid arteries from our experiments (Figure 39) demonstrate, as expected, that the internal and external carotid arteries are localized anatomically in a deeper level in the Z vertical axis in comparison to the common carotid artery and the carotid bifurcation.This differentiation of the level where the different parts of the carotid artery are found could lead in disturbances in the blood flow conditions upon preparation since the placement of a plastic sheet slightly elevates the artery in the area proximal and distal to the carotid bifurcation.

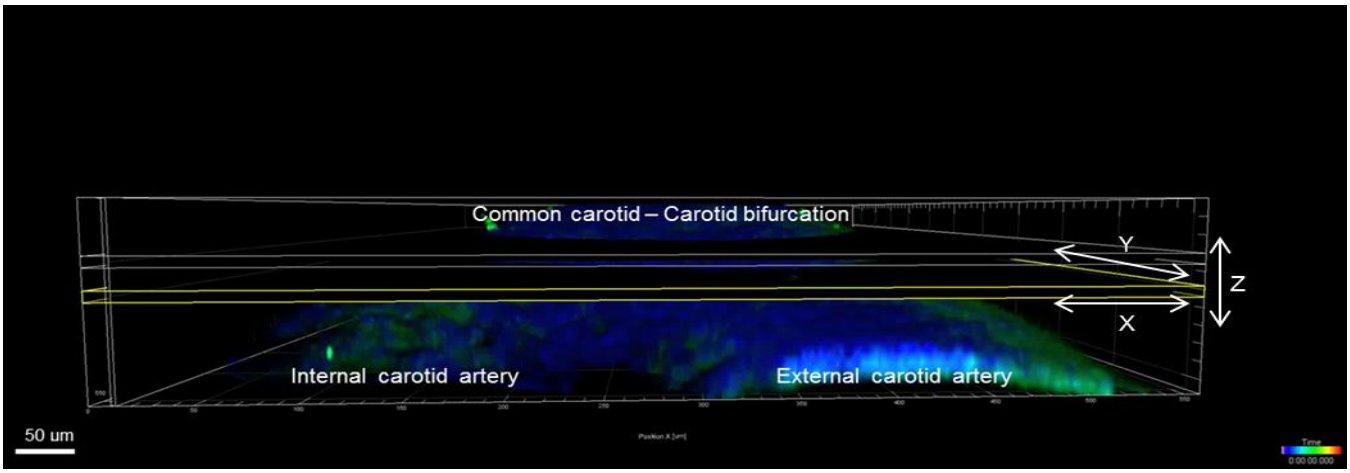

Figure 39. 3-dimensional reconstruction of different parts of the carotid artery (X,Z projection). Part of the common carotid artery, the carotid bifurcation, the internal and external carotid arteries are visible. The internal and external carotid arteries are located deeper in the tissue in comparison to the common carotid artery and the bifurcation. The adventitia is presented in blue (due to SHG) and parts of the media in green (due to auto-fluorescence).

In order to investigate the flow conditions in the different areas of the carotid artery we have injected fluorescent beads and performed in vivo imaging with the use of the CCD camera of our microscope in the carotid arteries of C57Bl/6J mice. This allowes us to perform very fast acquisition of images and thus enabled us to track cells and fluorescent beads following the blood flow in arterioles and venules. In the case of

carotid arteries we could detect a very fast laminar blood flow in the areas of the common and internal carotid during both cardiac systole and diastole. However, flow conditions could not be quantified since the beads were following the fast flow of the blood and thus were visualized as lines and not as distinct particles (Figure 40).Therefore, it was not possible to track them in sequential time frames in order to calculate the flow velocity and furthermore the shear stress within the vessel. We could still however observe that in contrast to the common carotid artery the flow was mainly oscillatory in the area of the external carotid artery (Figure 40). In that case, the beads were presented like lines only during systole (Figure 40A). However due to oscillation during diastole their velocity was reduced and thus they where presented with a spherical shape (Figure 40B) .

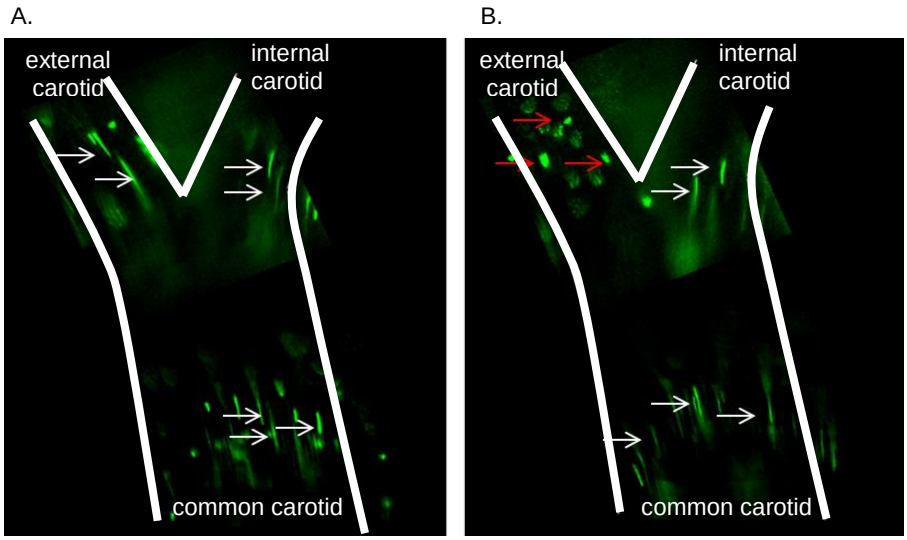

Figure 40. IVM performed by the use of a CCD camera in different parts of the carotid artery (common, external and internal carotid artery) upon injection of FITC labelled beads in C57Bl/6J mice (n=6). The white arrows indicate fluorescent beads (presented as green lines) following a fast laminar flow during systole and diastole in the common carotid and internal arteries. The red arrows indicate beads (presented with a green spherical shape), following oscillatory flow patterns in the external carotid artery during diastole.

7.1.3.2 Applications of new stage for in vivo imaging and quantitative analysis of leukocyte migration in large vessels using TPLSM

The following sections will describe how we applied our newly established model of TPLSM imaging to the visualization of leukocyte trafficking in three distinct scenarios:

- In vivo detection of leukocytes intraluminal crawling
- In vivo detection of leukocytes transmigration in the atherosclerotic plaque
- Analysis of motility of emigrated leukocytes within the atherosclerotic plaque

7.1.3.2.1 In vivo imaging of leukocyte intraluminal crawling

Although leukocyte intraluminal crawling was described to take place in post-capillary venules and arterioles, there is still no data in the literature showing crawling phenomenon in large arteries. Therefore, we have focused our interest to investigate whether this post-adhesion event can be detected in large vessels under either steady state or chronic inflammatory conditions (such as atherosclerosis). Under steady state conditions our main interest was to analyse whether non inflammatory patrolling monocytes could also crawl in large non inflamed arteries (as already described in the case of microvasculature[14]). In order to address this question we have performed experiments in the carotid arteries of CX3CR1$^{GFP/+}$ mice (n=5). During these experiments we confirmed that GFP positive cells were able to crawl also on the endothelium of carotid arteries in the area of the carotid bifurcation (Figure 41).

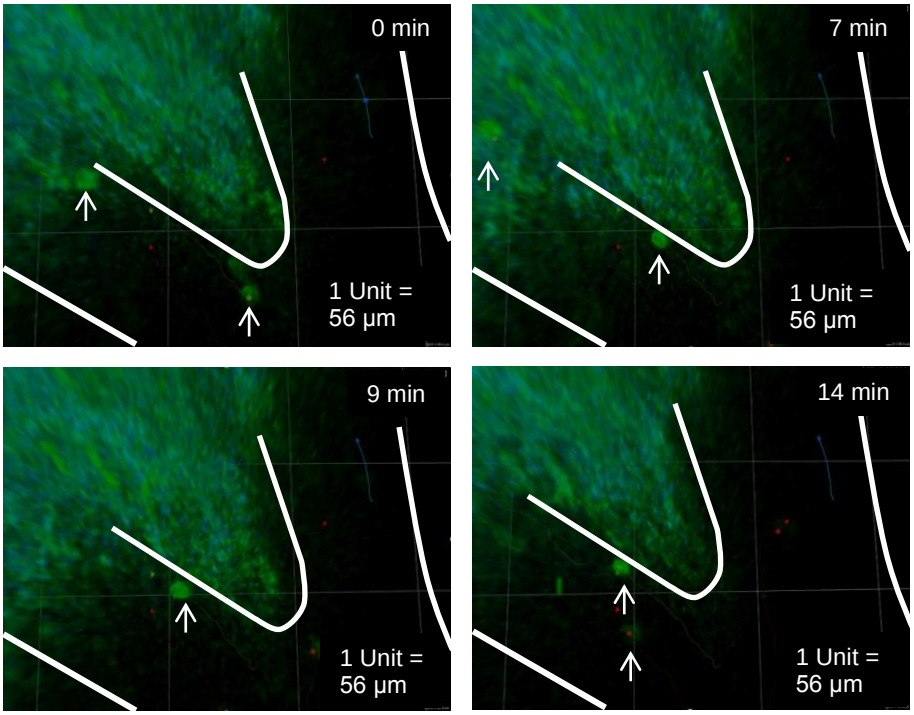

Figure 41. Freeze frame images from 3D time-lapse recording of the carotid artery of a CX3CR1$^{GFP/+}$ mouse. Single monocytes are able to adhere and crawl along the arterial endothelium in steady state conditions. The white arrows indicate crawling monocytes in different time points. Intima is presented in green (due to auto-fluorescence) and monocytes also in green (due to GFP expression).

We next aimed to verify whether this population of GFP+ cells are non classical (patrolling) monocytes or classical (inflammatory) monocytes. Although patrolling monocytes are characterized by high expression of CX3CR1 (thus high GFP expression in the CX3CR1$^{GFP/+}$ mice) and inflammatory monocytes by low expression of CX3CR1 (thus low GFP expression in the CX3CR1$^{GFP/+}$ mice), the *in vivo* distinction based only on this differentiation can be very demanding and not objective. In order to overcome this difficulty we have injected the labelling PE conjugated anti GR1 antibody, which is specific for neutrophils and inflammatory monocytes, intravenously in CX3CR1$^{GFP/+}$ mice (n=4). Following this approach the patrolling monocytes could be characterized by high expression of CX3CR1 (and therefore also of GFP) and by no expression of GR1. In that way they were identified as a population of green cells. On the other hand the inflammatory monocytes were characterized by low expression of CX3CR1 (and therefore of GFP) but were GR1

positive. Thus, they were identified as a population of cells that expresses both green and red fluorescence. In addition we could also differentiate neutrophils as CX3CR1 (GFP) negative but GR1 positive cells (identified as red cells, see Figure 42).

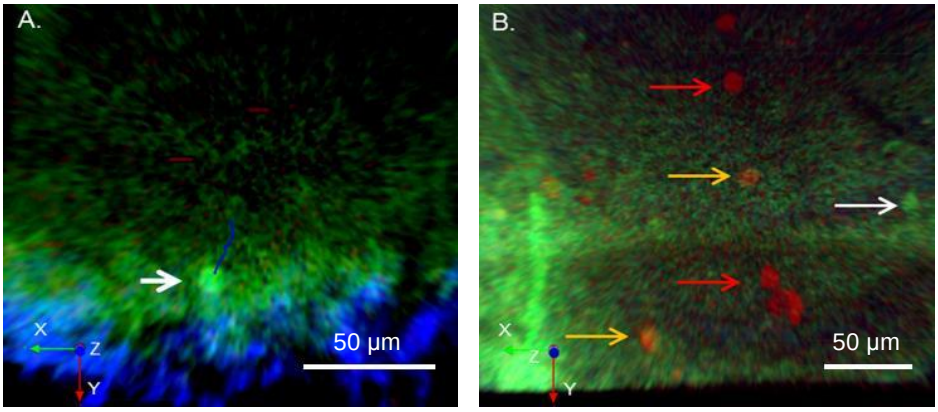

Figure 42. Identification of different subsets of leukocytes interacting with the endothelium of carotid arteries upon injection of the anti GR1 antibody (PE conjugated) **A.** The white arrow indicates a CX3CR1^{high}GR1- patrolling monocyte. The blue line indicates its crawling path. No inflammatory monocytes or neutrophils are detected in that case. **B.** The white arrow indicates CX3CR1highGR1- patrolling monocyte, yellow arrows indicate CX3CR1^{low}GR1+ inflammatory monocytes. Red arrows indicate CX3CR1-GR1+ neutrophils. Adventitia is presented in blue (SHG) and Media – intima in green (auto-fluorescence).

Following this approach we could identify that the majority of cells interacting with the endothelium in the carotid artery under steady state conditions were patrolling monocytes (74.2 %) while 7.1% and 16.7% were inflammatory monocytes and neutrophils respectively. Additionally in this set of experiments we observed patrolling monocytes crawling in 100% of the carotid arteries imaged. In contrast interactions of inflammatory monocytes and neutrophils with the endothelium were detected in 50% of our experiments. The comparison among the different subset of monocytes revealed that the percentage of crawling non inflammatory (patrolling) monocytes is significantly higher in comparison with the inflammatory subset (Figure 43).

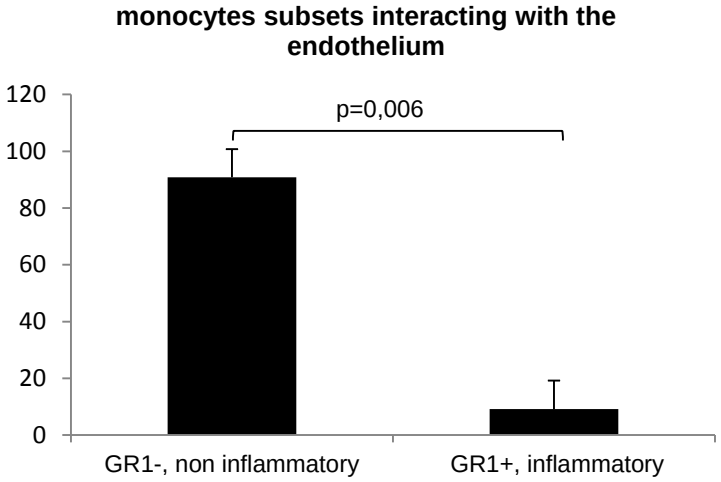

Figure 43. Percentages of non inflammatory (patrolling) and inflammatory monocytes among the total population of monocytes interacting with the endothelium of the carotid bifurcation in steady state. (n=4 experiments,30 cells).The percentage of non inflammatory monocytes is significantly higher from the percentage of the inflammatory subset (p=0,006)

In the case of atherosclerosis we have focused in detecting neutrophils adhering and crawling on atherosclerotic plaques or in areas adjacent to them (plaque shoulders). Therefore, we have performed experiments in $ApoE^{-/-}$ mice (n=8) (during which we injected PE conjugated Ly6G 1A8 antibody in order to label neutrophils) and in $ApoE^{-/-}$ $LysM^{GFP/+}$ (n=6) chimeras (which contained GFP+ neutrophils). In both cases we could detect adhesion and crawling of neutrophils on the inflamed endothelium (Figure 44).

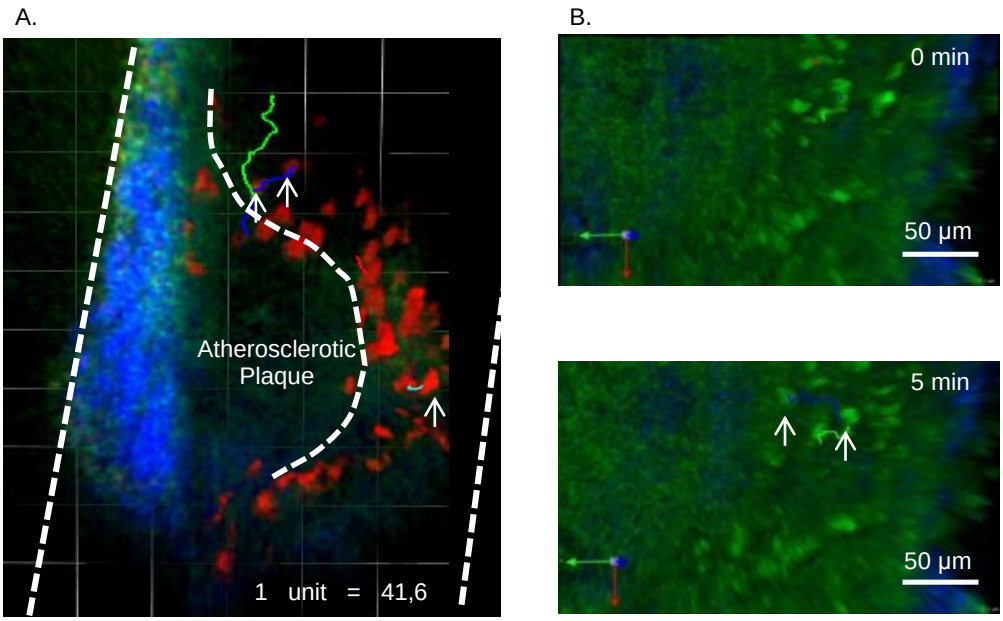

Figure 44. Neutrophil crawling in atherosclerosis. **A.** Neutrophils crawling around the area of an atherosclerotic plaque in the carotid artery of an ApoE$^{-/-}$ mouse. Arrows indicate neutrophils and coloured lines indicate neutrophils crawling paths. Adventitia is presented in blue (due to SHG), media- intima in green (due to auto-fluorescence) and neutrophils in red (due to injection of Ly6G 1A8 PE conjugated antibody). **B.** GFP+ neutrophils crawling in areas close to atherosclerotic plaque (plaque shoulders) in the carotid artery of an ApoE$^{-/-}$ LysM^{eGFP} mouse.

7.1.3.2.2 *In vivo* imaging of leukocyte migration into atherosclerotic plaques

After having detected leukocytes crawling in carotid arteries during steady state and atherosclerosis we have further tested whether our model could be used in order to visualize the next step of leukocytes migration cascade in large atherosclerotic arteries which is transmigration. In order to detect leukocyte emigration in real time into the atherosclerotic wall we have performed experiments in ApoE$^{-/-}$ mice and labelled *in vivo* neutrophils with the Ly6G 1A8 antibody (PE conjugated). In addition, we have performed experiments also in ApoE$^{-/-}$LysM^{eGFP} chimeras. In both cases we could rarely detect leukocytes luminal transmigration into the plaque (figure 45). Interestingly, in the case of ApoE$^{-/-}$LysM^{eGFP} mice we also observed neutrophils transmigration in the atherosclerotic plaque through the adventitial side of the vessel wall (figure 46).

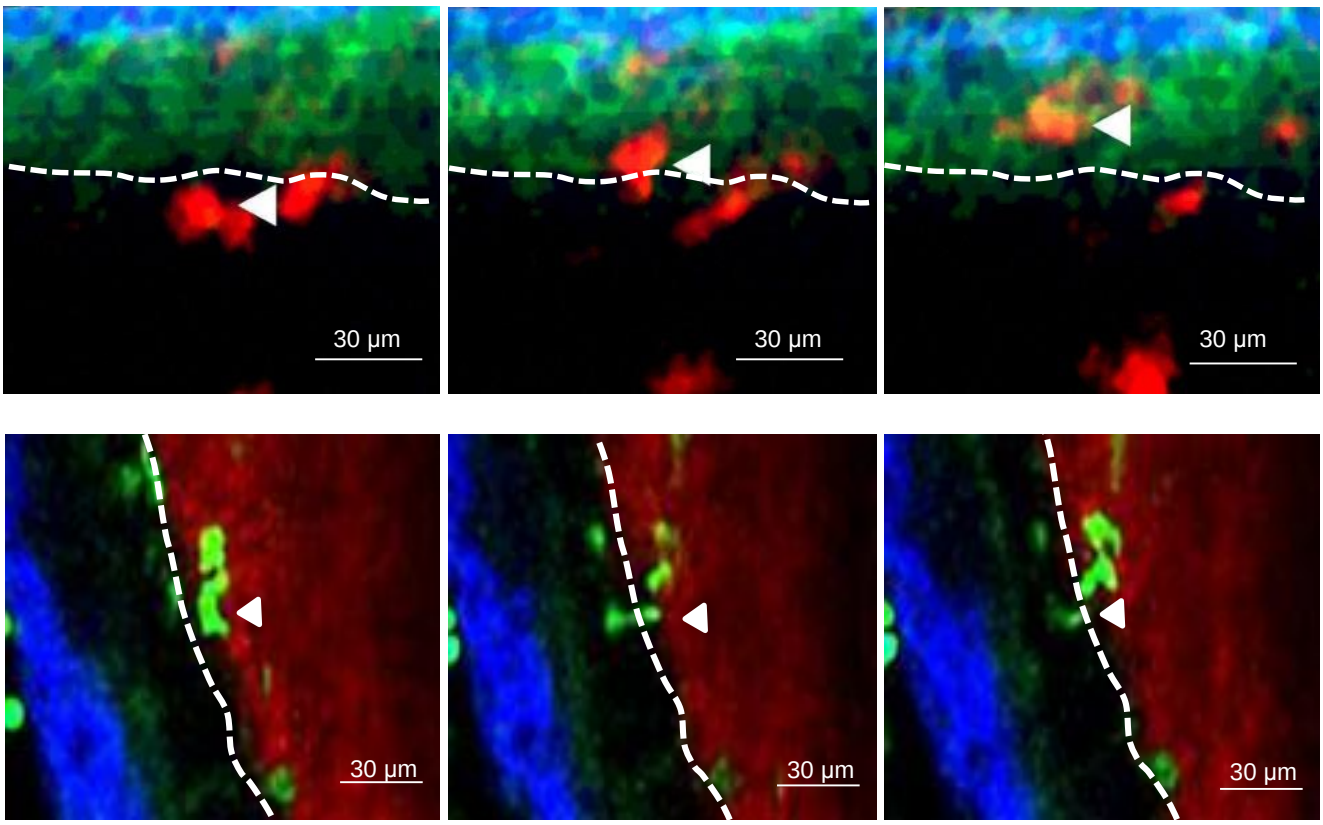

Figure 45. Freeze frame images from 3-dimensional time lapse recordings during which luminal neutrophil migration into atherosclerotic plaques occurred. **A.** Neutrophil luminal transmigration in the shoulder of an atherosclerotic plaque of an ApoE$^{-/-}$ mouse (YZ projection). Neutrophils are presented in red (due to labelling with PE conjugated Ly6G 1A8 antibody). **B.** GFP + neutrophil (presented in green) luminal transmigration in the shoulder of an atherosclerotic plaque of an ApoE$^{-/-}$LysM^{eGFP} mouse. Adventitia is presented in blue (due to SHG), media – intima in green (due to auto-fluorescence) and plasma in red due to injection of TRITC dextran.

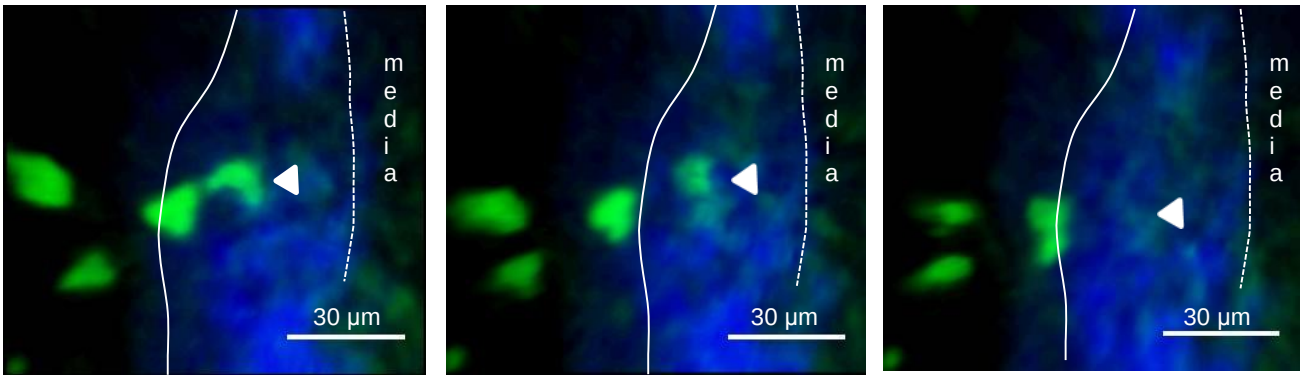

Figure 46. GFP+ neutrophil transmigrating in an atherosclerotic plaque through adventitia. The arrow indicates the migrating neutrophil. The dotted lines indicate the border between adventitia and media. The continuous line indicates the external border of the arterial wall.

7.1.3.2.3 *In vivo* imaging of leukocyte presence and motility within atherosclerotic plaques

To test which kind of leukocytes are recruited and can be imaged within the atherosclerotic plaque we have performed experiments in ApoE$^{-/-}$CX3CR1$^{GFP/+}$ mice (n=4), ApoE$^{-/-}$MHCII^{eGFP} mice (n=4) and ApoE$^{-/-}$LysM^{eGFP} mice (n=4). CX3CR1$^{GFP/+}$ monocytes were detected within the plaque close to the adventitial area of the artery. We were further able to detect MHCII GFP + antigen presenting cells (dendritic cells, macrophages) as well as LysM GFP + cells (neutrophils) within the atherosclerotic plaques (Figure 47).

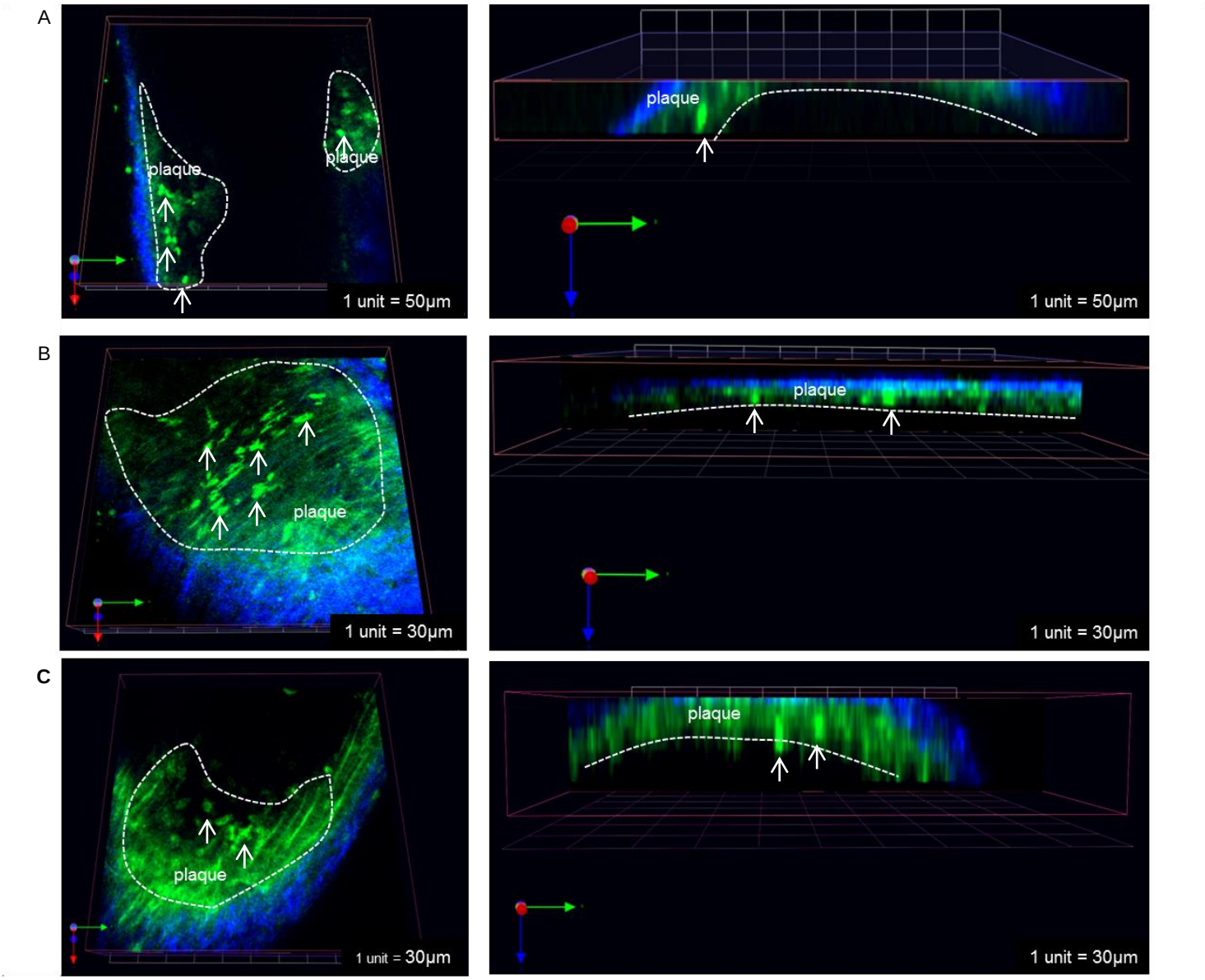

Figure 47. Different types of leukocytes located within the arterial wall in the area of atherosclerotic plaque formation. **A.** LysM GFP + neutrophils indicated by arrows. **B.** CX3CR1 GFP+ cells indicated by arrows. **C.** MHCII eGFP + cells indicated by arrows. left pictures : XY perspective, right pictures: XZ perspective.

Furthermore neutrophils were detected migrating within the atherosclerotic plaque in all three axis (X,Y,Z) with a mean velocity of 6,4 µm/ minute (Figure 48A,B).

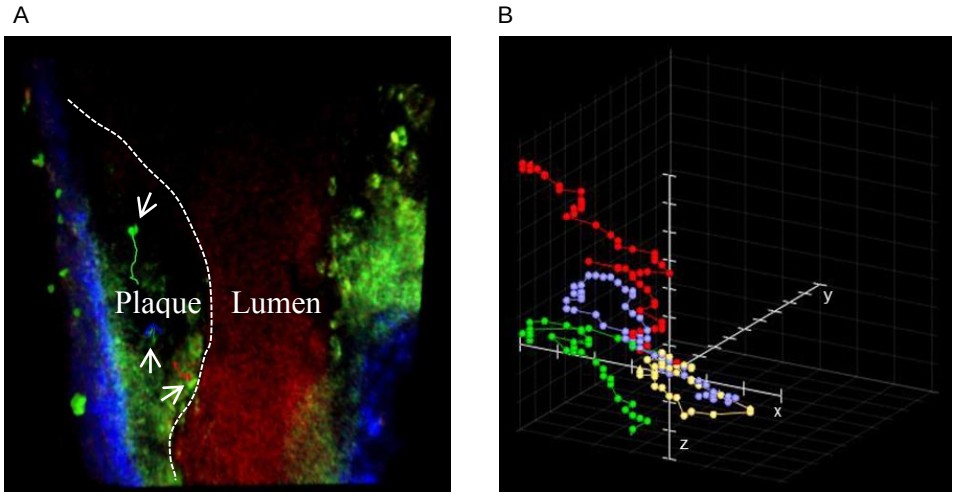

Figure 48. Freeze frame images from flattened 3 dimensional time lapse recordings in the carotid artery of an ApoE$^{-/-}$LysM^{eGFP} mouse. **A.** Neutrophil intraplaque migration within an atherosclerotic plaque (XY projection). The arrows indicate the location of the neutrophils and the coloured lines their path. Adventitia is presented in blue (due to SHG) and media – intima in green (auto-fluorescence).**B.** Tracking paths of neutrophils in 3 dimensions (X, Y, Z axis).

In total, our results indicate that the use of our newly established method for *in vivo* imaging of large arteries by TPLSM provides for the first time the possibility to perform *in vivo* analysis of dynamic cellular processes in large vessels. Leukocyte crawling (either under steady state conditions or inflammation), transmigration and interstitial migration that were so far studied only in the microvasculature can now be detected and analysed also in the macrovasculature.

7.2 Analysis of leukocyte crawling in microvasculature and macrovasculature during steady state conditions and inflammation

Dynamic cellular processes such as crawling were so far analysed in real time only in the case of post capillary venules and arterioles. The beta-2 integrins LFA-1 and Mac-1 are thought to mainly mediate the process of leukocyte crawling in small vessels. However, the direct effect of blocking of LFA-1 or Mac-1 in the crawling behaviour of leukocytes under inflammatory or steady state conditions in the microvasculature is still poorly analysed. In the next part of our experiments we focus

in the process of crawling and investigate the direct and long term effect of blocking of LFA-1 and mainly Mac-1 in leukocyte crawling in the microvasculature during steady state and inflammation. Additionally, we apply our newly established model in order to investigate whether Mac-1 is also implicated in leukocyte crawling in large arteries during steady state and atherosclerosis. Furthermore, we aim to investigate whether its role on leukocyte crawling is comparable in large arteries and microvasculature.

7.2.1 Subsets of leukocytes crawling in micro and macrovasculature under steady state

In this part of our project we investigated the role of beta 2 integrins in the crawling process of leukocytes during steady state. Our first aim was to test which kind of leukocytes are able to adhere and crawl under these conditions in the small vessels of the skin of the mouse ear. Patrolling monocytes are the main subset of leukocytes that are expected to crawl in the microvasculature under steady state conditions[14].
However, the potential of neutrophils for adhesion and crawling in the absence of inflammation was not fully investigated so far. To directly examine the ability of neutrophils to crawl along the non stimulated endothelium of arterioles and venules we have performed experiments in the ear of LysM^{eGFP} mice. In these experiments we could detect only very transient interactions of single GFP+ neutrophils with the endothelium. These occurred downstream to the blood flow imitating a process of passive E- selectin dependent slow rolling rather than active crawling (Figure 49). For these reasons we did not take into consideration this phenomenon as crawling and we did not perform further analysis in this field.

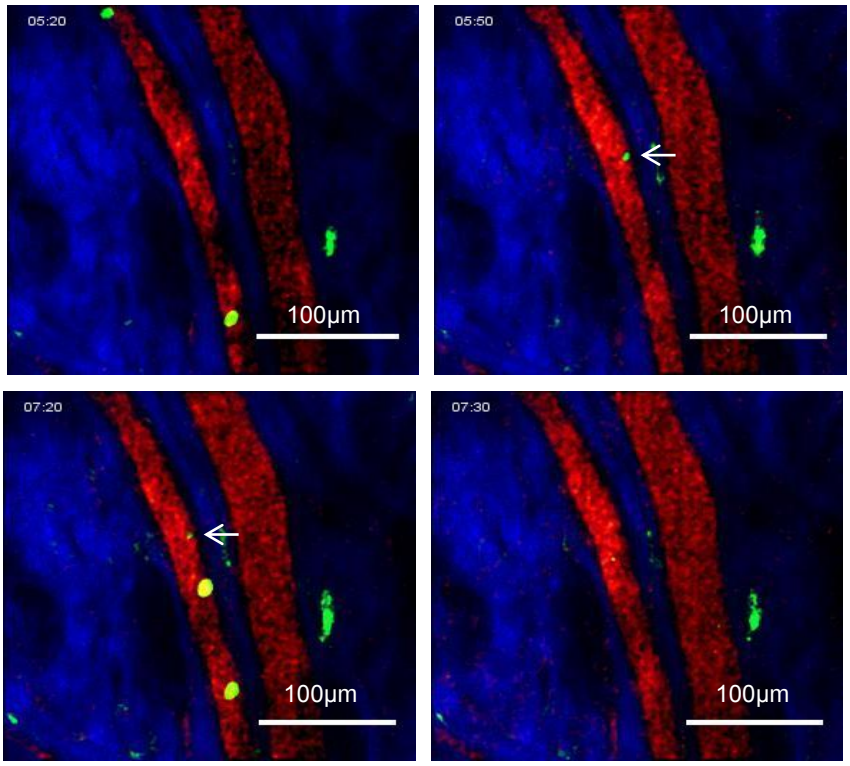

Figure 49. Freeze frame images from flattened 3 dimensional time lapse recordings in a post-capillary venule of the ear of a LysM^{eGFP} mouse under steady state conditions. The blue line indicates the crawling path of the neutrophil. The interaction of the cell with the endothelium is very transient and therefore the neutrophil is detected with difficulty. The interstitial area is presented in blue (due to SHG) and the plasma in red (via application of TRITC dextran).

In a next step we tested the ability of monocytes to crawl under steady state conditions in the postcapillary venules and arterioles of the skin of the mouse ear. Therefore, we have performed *in vivo* imaging in the ear of CX3CR1$^{GFP/+}$ mice. As expected single patrolling monocytes were detected crawling for long distances along the endothelium during steady state (Figure 50).

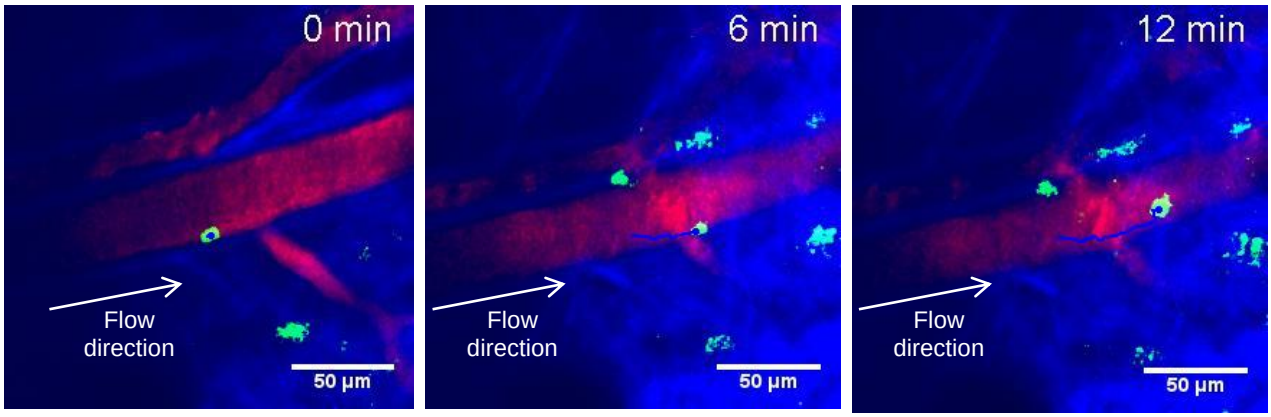

Figure 50. Freeze frame images from flattened 3 dimensional time lapse recordings in a post-capillary venule of the ear of a CX3CR1$^{GFP/+}$ mouse under steady state conditions. The arrow indicates the crawling monocyte and the blue line its track. The interstitial area is presented in blue (due to SHG), the plasma in red (due to application of TRITC dextran) and the monocyte in green (due to GFP expression).

In the case of large arteries, as previously shown (7.1.3.2.1), the application of our innovative model allowed us to confirm the ability of leukocytes to crawl on the endothelium also of carotid arteries during steady state. Furthermore we could observe that the majority of crawling cells in CX3CR1$^{GFP/+}$ mice were patrolling and not inflammatory monocytes.

7.2.2 Comparison of crawling behaviour of patrolling monocytes in micro and macrovasculature

In the next part of the project, we aimed to analyse the crawling behaviour of patrolling monocytes in the carotid artery and compare it with their crawling behaviour in the microvasculature of the ear. We have therefore analysed the following crawling parameters: velocity, distance and direction. Patrolling monocytes crawled with a mean velocity of 8,64µm/min in the ear microvasculature (post-capillary venules/ arterioles) while in the carotid arteries their mean velocity was 7,06 µm/min (Figure 51A). There was no statistically important difference between these two values (p= 0.150) and therefore the crawling velocity of the patrolling monocytes was considered to be comparable in small vessels and large arteries. As in the case of crawling velocity, the mean crawling distance in the arteries (79,6 µm) was comparable with

the mean crawling distance in the microvasculature (76,4 µm) (p= 0.824, see Figure 51B). Regarding crawling direction, in both cases of small vessels and carotid arteries, we did not detect significant differences between the percentages of cells crawling upstream/ perpendicular and downstream to the flow (Figure 51C).

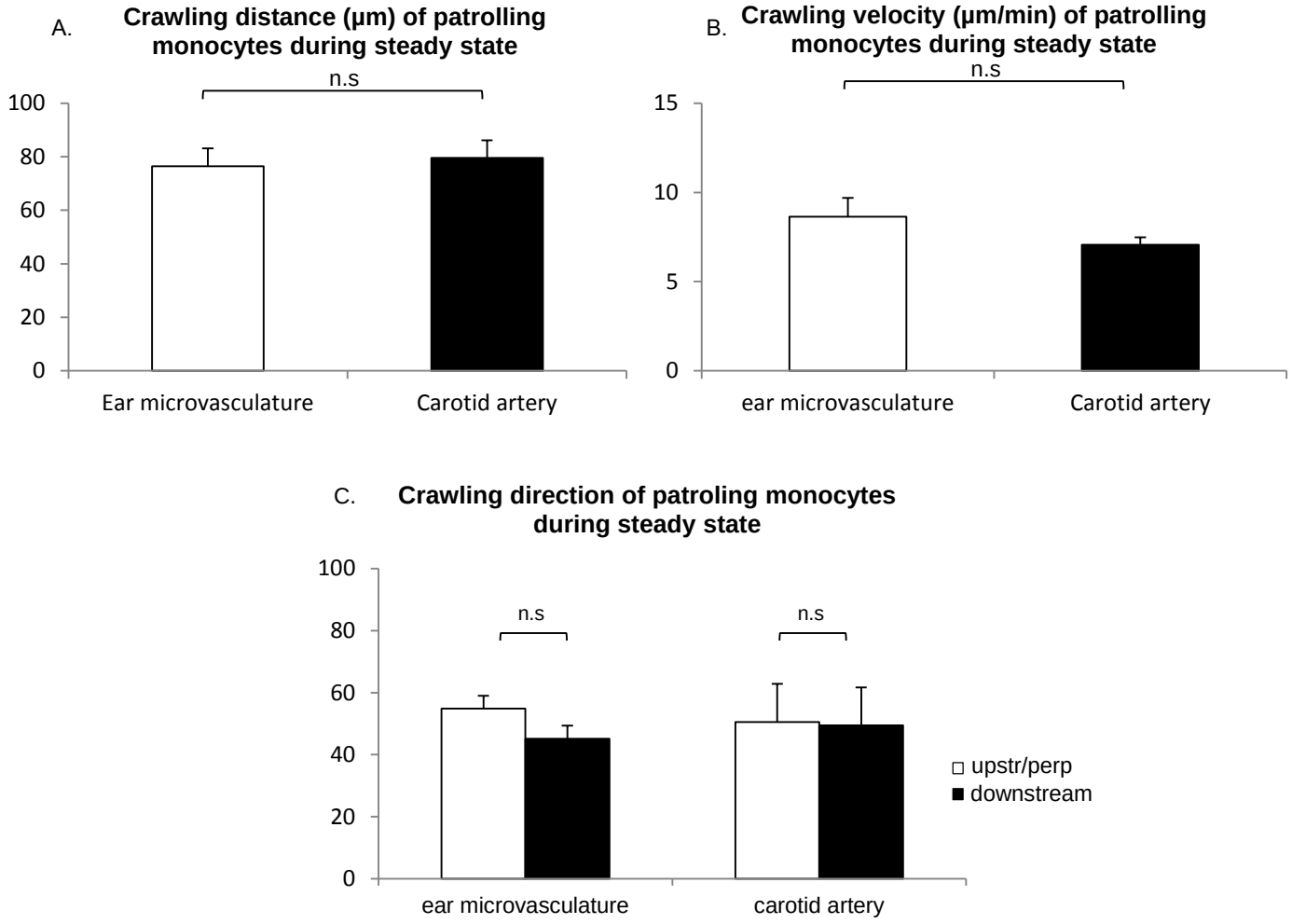

Figure 51. Comparison of the crawling characteristics of monocytes in the microvasculature (post-capillary venules and arterioles n= 7 mice, 49 cells) and macrovasculature (carotid arteries n= 6 mice, 33 cells) of CX3CR1$^{GFP/+}$ mice. **A.** Comparison of crawling velocity (µm/ min) of patrolling monocytes in ear microvasculature and in carotid arteries. No significant differences were detected between the two groups (p= 0.150). **B.** Comparison of crawling distance (µm) of patrolling monocytes in ear microvasculature and in carotid arteries. No significant differences were detected between the two groups (p= 0.824). **C.** Comparison of crawling direction of patrolling monocytes in ear microvasculature and in carotid arteries. No significant differences were detected between percentages of upstream/ perpendicularly crawling and downstream crawling cells either in small vessels (p= 0.901) or carotid arteries (p=0.706).

7.2.3 Effect of blocking of beta-2 integrins LFA-1 and Mac-1 in crawling of patrolling monocytes

7.2.3.1 Direct effect of blocking of antibodies against of LFA-1 and Mac-1 in the crawling of patrolling monocytes in microvasculature (CSCTP analysis)

In this group of experiments we aimed to analyse the role of beta-2 integrins LFA-1 and Mac-1 in the crawling behaviour of patrolling monocytes under steady-state conditions in the microvasculature of the mouse ear. Therefore, we tested the direct effect of blocking of beta-2 integrins on adhesion, crawling direction and crawling velocity of monocytes in CX3CR1$^{GFP/+}$ mice.

7.2.3.1.1 Direct effect in adhesion, crawling direction and crawling velocity

Upon application of blocking antibody against LFA-1 the 88.88% of the total population of cells analysed by CSCTP (regardles their initial crawling direction) detached. In contrast blocking of Mac-1 led to detachment of a significantly lower percentage of cells (5.88% see Figure 52A and 53). On the other hand upon injection of anti LFA-1 13.33% of the total population of cells changed crawling direction. However, a significantly higher percentage of cells changed crawling direction in the experiments were Mac-1 was blocked 52.94% (figure 52B and 53). These data indicate that Mac-1 mainly regulates the crawling direction of patroling monocytes while LFA-1 plays a crucial role on their adhesion.

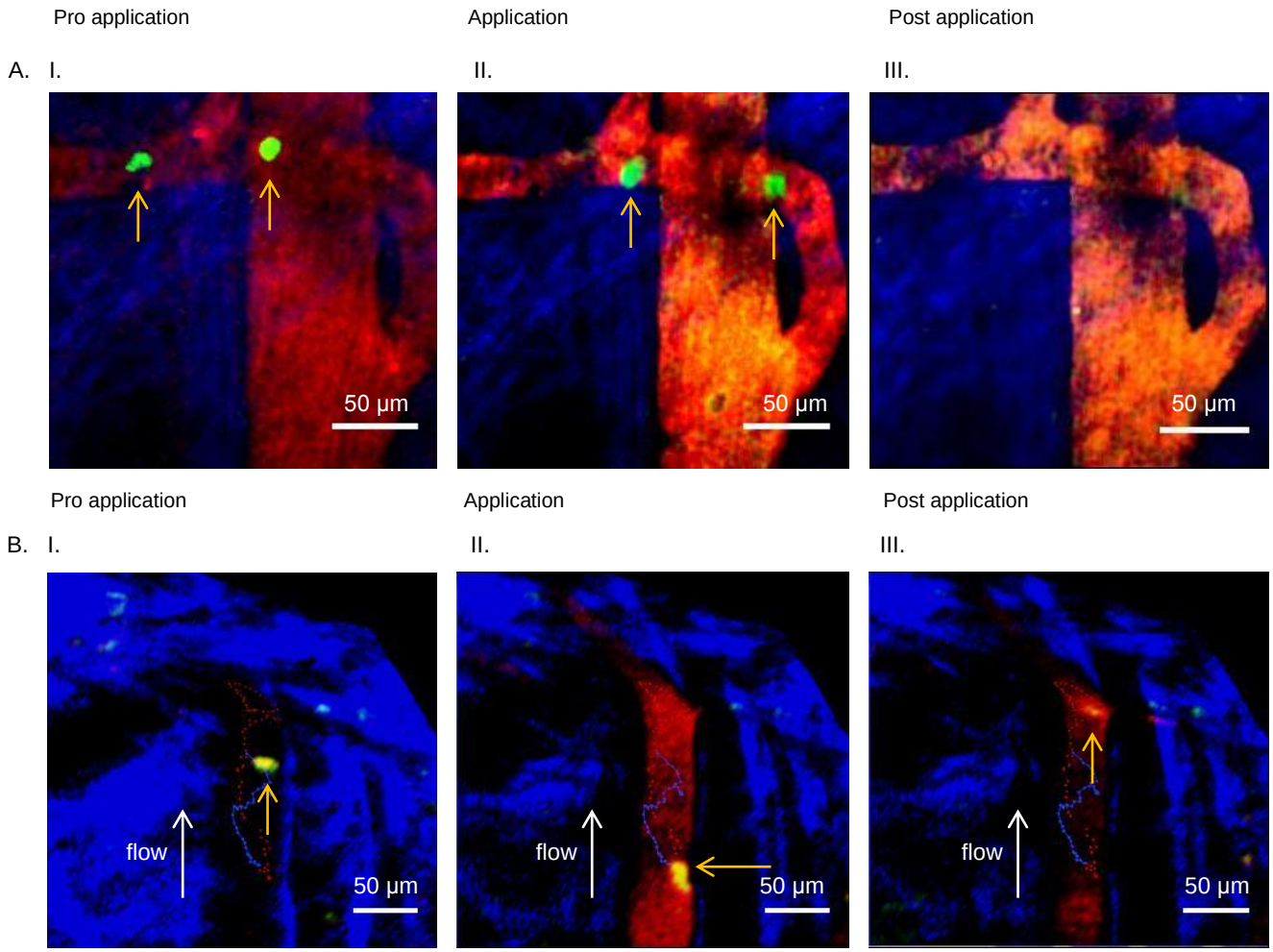

Figure 52. Freeze frame images from experiments regarding the direct effect of blocking of beta-2 integrins in the crawling behaviour of patrolling monocytes in CX3CR1$^{GFP/+}$ mice. **A.** Effect of anti LFA-1 blocking antibody on adhesion of patrolling monocytes I. Patrolling monocytes crawling in steady state. II. application of anti LFA-1 blocking antibody during recording of crawling monocytes III. Detachment of cells shortly after injection of anti LFA-1. Monocytes are presented in green (due to GFP expression), and plasma in red (due to injection of TRITC-dextran). Anti LFA-1 antibody was FITC conjugated and therefore plasma appeared yellowish upon injection. **B.** Effect of anti Mac-1 blocking antibody on crawling of patrolling monocytes I. A patrolling monocyte is shown crawling upstream during steady state. II. Application of anti-Mac-1blocking antibody during recording of the crawling monocyte. III. Change in crawling direction shortly after injection of anti Mac-1. The interstitial area is presented in blue (due to SHG), the monocyte in green (due to GFP expression), and anti Mac-1 in red (PE conjugated).

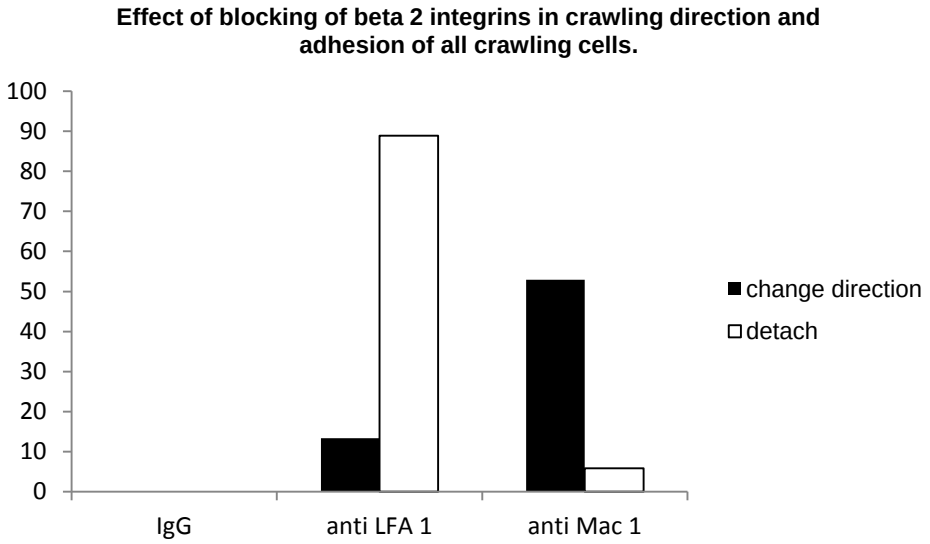

Figure 53. Direct effect of injection of anti LFA-1 (n=15 mice,15 cells) and anti Mac-1 (n=17 mice, 17 cells) blocking antibodies on adhesion and crawling direction in the total population (both upstream/ perpendicularly or downstream crawling) of patrolling monocytes. A significantly higher percentage of cells changed crawling direction upon injection of anti Mac-1 in comparison to injection of anti LFA-1(p=0,041). In contrast, a significantly higher percentage of cells detached upon injection of anti LFA-1 in comparison with injection of anti Mac-1 (P <0,001). Injection of either IgG2A or IgG2b,k isotype controls did not influence adhesion or crawling. Therefore, the results from these two groups are presented as "IgG" in the graph. One vessel and one cell was analysed per experiment. Our statistical analysis regarded the total population of crawling monocytes from all experiments and therefore SEM could not be calculated. In order to compare the percentages from the different groups of experiments, Z statistical test was applied.

Additionally, our analysis showed that the change in crawling direction of monocytes upon blocking of Mac-1 regarded mainly the upstream/perpendicularly crawling cells. In this context we found that injection of anti Mac-1 blocking antibody led to a change of direction (from upstream to downstream) of 72.73% of the upstream/ perpendicularly crawling monocytes. In contrast, a significantly lower percentage of downstream crawling cells changed crawling direction to upstream (9.09%, p<0,001, see Figure 54). Therefore, we assumed that Mac-1 is a key regulator of the upstream crawling of patrolling monocytes. Injection of IgG2b,k isotype control antibody did not influence the direction neither of the upstream nor of the downstream crawling population of monocytes.

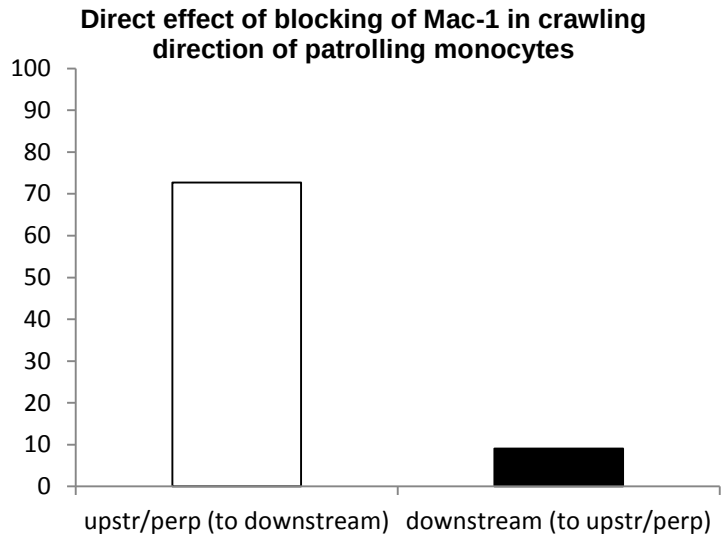

Figure 54. Direct effect of injection of anti Mac-1 blocking antibody on the crawling direction of patrolling monocytes (n=17 mice, 17 cells). The cells are grouped according to their baseline (prior to injection) crawling direction. Blocking of Mac-1 resulted in a change of the crawling direction of 72,73% of upstream/perpendicularly crawling cells. In contrast a significantly lower percentage of the downstream crawling population (9,09%), changed crawling direction ($p<0,001$). Our statistical analysis regarded the total population of crawling monocytes (one cell was analysed per experiment) from all our experiments and therefore SEM could not be calculated. In order to compare percentages in the two different groups of cells Z statistical test was applied.

These data indicate that LFA-1 plays a crucial role in patrolling monocytes adhesion on the endothelium while Mac-1 regulates the upstream crawling of these cells. The role of LFA-1 in the crawling process could not be analysed since blocking of this beta-2 integrin leads to detachment of the patrolling monocytes. Thus, in the next set of experiments we have focused in analysing the effect of blocking of only Mac-1 in the crawling behaviour of patrolling monocytes under steady state.

In a next step we analysed the direct effect of blocking of Mac-1 in the crawling velocity of the patrolling monocytes that crawled before, during and after the injection in a continuous way (the analysis was performed by application of the CSCTP). The velocity of crawling cells at the baseline before application of IgG2b,k isotype control or of anti Mac-1 antibody was 9.56 μm/min and 10.53 μm/min respectively and no difference was detected between these values ($p=0.297$). Directly upon application of

IgG2b,k or of anti Mac-1 the velocities of patrolling monocytes were counted as 9.44 µm/min and 9.28 µm/min, respectively. Again in that case no statistical deference was detected between the two groups (p=0.890). Therefore we have assumed that blocking of Mac-1 does not significantly influence the crawling velocity of the patrolling monocytes in the microvasculature under steady state conditions (Figure 55A).

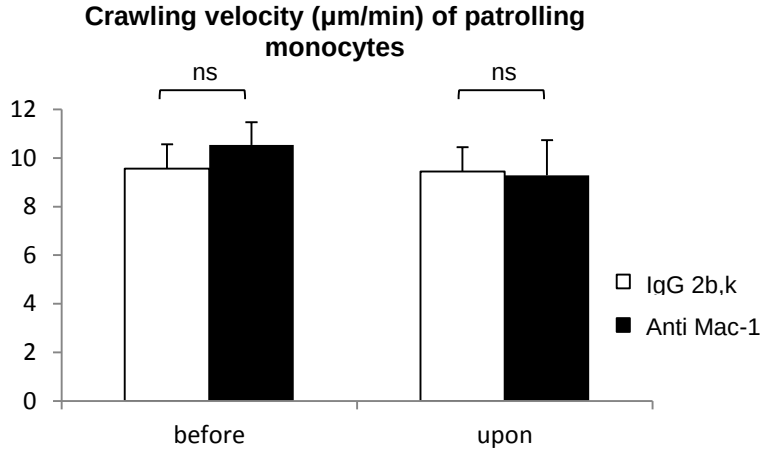

Figure 55. Direct effect of injection of anti Mac-1in the crawling characteristics of patrolling monocytes analysed by CSCTP (n=15-17 mice, 15-17 cells per group). Comparison of the direct effect of injection of IgG2b,k and anti Mac-1in the crawling velocity of patrolling monocytes analysed by CSCTP. No important differences were observed between the two groups before (p=0,297) and after injections (p=0,890).

In summary these results show that Mac-1 is a key player in the upstream/ perpendicular to the blood flow crawling of monocytes however it does not influence dynamic aspects of monocyte crawling such as velocity.

7.2.3.2 Long term effect of blocking of Mac-1 integrin in patrolling monocytes in the microvasculature

In order to further investigate the role of Mac-1 in the crawling behaviour of patrolling monocytes we have performed further experiments in CX3CR1$^{GFP/+}$ mice and imaged in later time points. Since detection of single patrolling monocytes in the skin of the mouse ear can often be a long-lasting procedure we have increased the duration of our experiments to 120 minutes (upon systemic injection of blocking antibody). In that

way we could analyse more vessels and thus more cells per experiment in comparison with the CSCTP during which we focused in the analysis of only one vessel and therefore usually one cell per experiment. This approach allowed us to obtain information on whether the direct effect of blocking of Mac-1 on the crawling behaviour of patrolling monocytes (detected by CSCTP analysis) has a long lasting character. Our analysis was performed in two groups of experiments: in the first group anti Mac-1 antibody was injected and in the second IgG2b,k isotype control antibody prior to the initiation of our recordings. The crawling parameters that were analysed included crawling direction, velocity, linearity and distance. Baseline recordings as well as continuous single cell tracking protocol were not performed in this set of experiments.

7.2.3.2.1 Long term effect of anti Mac-1 antibody on crawling direction of monocytes

Patrolling monocytes presented an almost equal ability for upstream/perpendicular or downstream crawling upon IgG2b,k injection. On the other hand in the experiments where Mac-1 was blocked the majority of the patrolling monocytes crawled downstream to the blood flow while only a smaller percentage of monocytes crawled upstream/ perpendicular to the blood flow, see Figure 56)

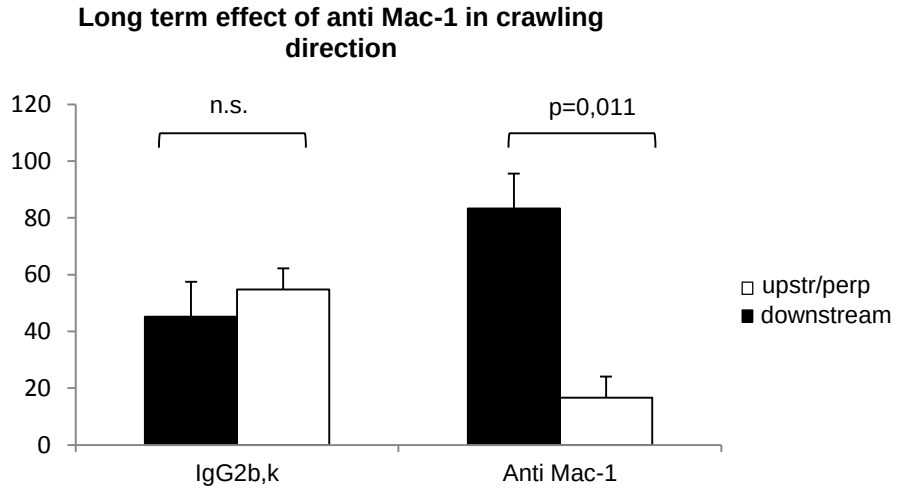

Figure 56. Comparison of the long term effect of injection of IgG2b,k and of anti Mac-1 antibody (n=5-7 per group, 25-49 cells) in the crawling direction of patrolling monocytes analysed by CSCTP. Upon injection of anti Mac-1 the minority of monocytes crawled upstream or perpendicularly to the blood flow (83,34% downstream, 16,64% upstream/perpendicular, p= 0,011). Upon injection of IgG2b,k isotype equal percentages of monocytes crawled upstream/perpendicularly to the blood flow (54,82% upstream/ perpendicular and 45,18% downstream, p= 0,706).

7.2.3.2.2 Long term effect of anti Mac-1 antibody on crawling velocity, distance and linearity of patrolling monocytes

In the case of crawling velocity we did not detect significant differences between the groups of experiments performed upon application of anti Mac-1 blocking antibody and IgG2b,k control (Figure 57A). As in the case of velocity also in the case of crawling distance we could not detect statistically important differences between the two groups of experiments (Figure 57B). Finally, to further analyse the effect of blocking of Mac-1 in the crawling process we have quantified the linearity of crawling monocytes but again in that case we could not detect significant differences between application of anti Mac-1 blocking antibody and application of IgG2b,k (Figure 57C).

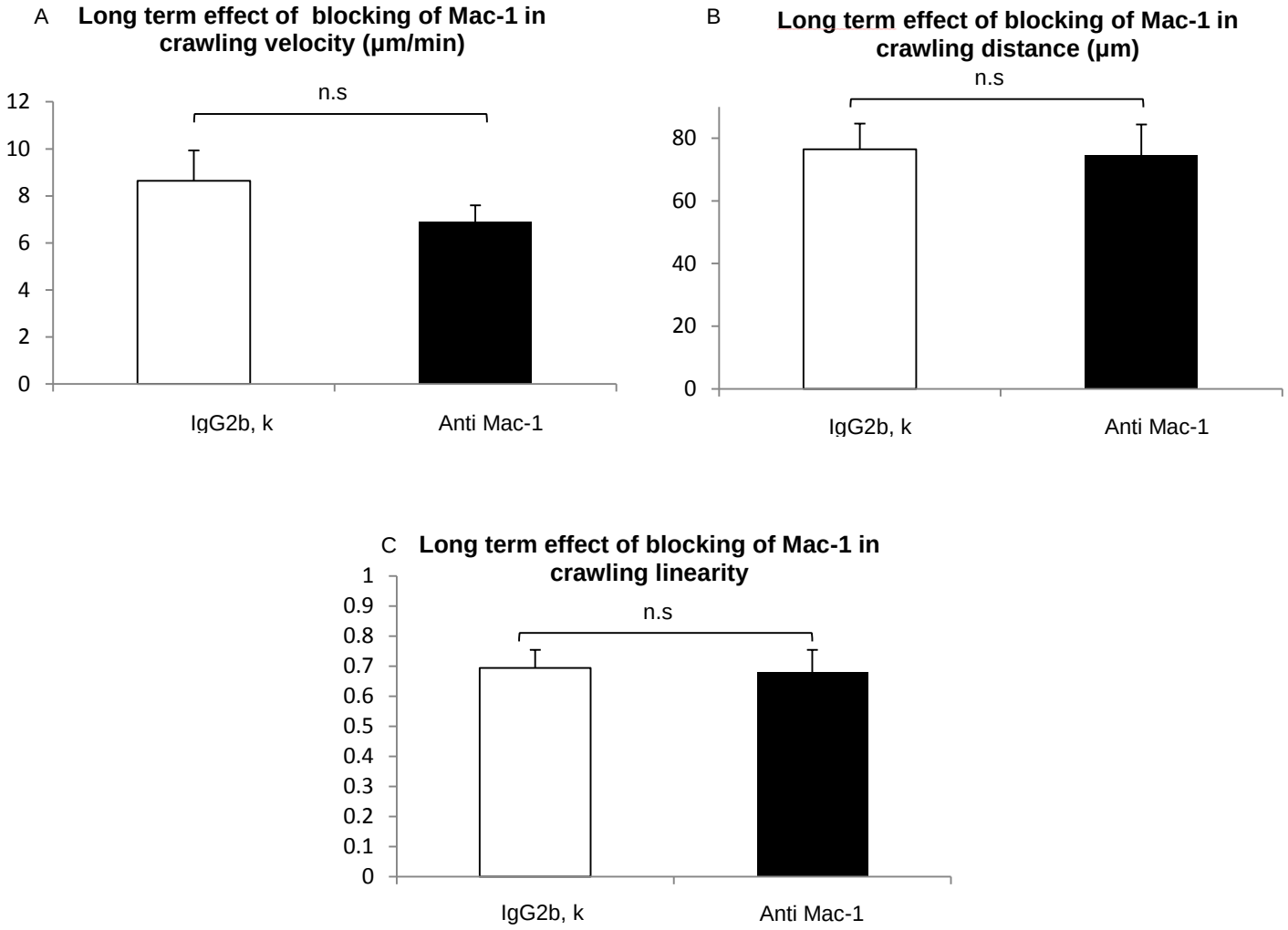

Figure 57. Comparison of crawling characteristics of patrolling monocytes upon injection of IgG2b,k and anti Mac-1 antibody. (n=5-7 mice, 25-49 cells per group) A. Comparison of the mean crawling velocities of patrolling monocytes. No significant difference was detected between the two groups (p=0,220). B. Comparison of crawling distance of patrolling monocytes. No significant difference was detected between the two groups (p=0,348). C. Comparison of crawling linearity of patrolling monocytes. No significant difference was detected between the two groups (p=0,943).

These results indicate that the direct effect of blocking of anti Mac-1 antibody in the crawling direction of the upstream/perpendicularly crawling monocytes is long lasting since it can be detected also in later time points. In that case the majority of the cells crawl downstream to the blood flow. However we did not detect any differences in the crawling parameters (velocity, distance and linearity) between our groups in later time points.

7.2.3.3 Long term effect of blocking of Mac-1 integrin on crawling of patrolling monocytes in carotid arteries (comparison with microvasculature)

Our next goal was to analyse whether (like in the microvasculature), Mac-1 is also involved in the regulation of crawling of monocytes in the macrovasculature under steady state conditions. For that reason we have further performed *in vivo* imaging in the carotid arteries (area of carotid bifurcation) of CX3CR1$^{GFP/+}$ mice. In this set of experiments we have focused in the general analysis of the long term effect of blocking of Mac-1 in the crawling process of patrolling monocytes and aimed to compare it with the effect of anti Mac-1antibody injection in the crawling of monocytes in the microvasculature. We have therefore divided our experiments in two groups: In the first we have injected IgG2b,k and in the second anti Mac-1 blocking antibody prior to imaging. In contrast to the microvasculature, the total duration of each of our experiments in carotid arteries was 1 hour. In that case we imaged in the same area of the artery in a continuous way and a relatively high number of cells could be analysed within this time period. Similarly to the previous set of the experiments, we focused in analysing the most important aspects of crawling behaviour of monocytes during steady state. These include the crawling direction, velocity, distance and linearity.

7.2.3.3.1 Long term effect of anti Mac-1 antibody on crawling direction in carotid arteries

As it was previously shown (7.2.3.2) Mac-1 participates in the process of crawling of patrolling monocytes in post-capillary venules and arterioles by regulating their upstream crawling. In the experiments performed in the carotid arteries of CX3CR1$^{GFP/+}$ mice there was an equal percentage of cells crawling upstream/ perpendicular to the blood flow and of cells crawling downstream in the case of application of IgG2b,k isotype (figure 58). In contrast, (as also in the microvasculature see 7.2.3.2) upon injection of anti Mac-1 antibody there was a significant increase in the percentage of the downstream crawling cells (76,78%) in comparison with the percentage of upstream/ perpendicular crawling (23,22%, see figure 58).

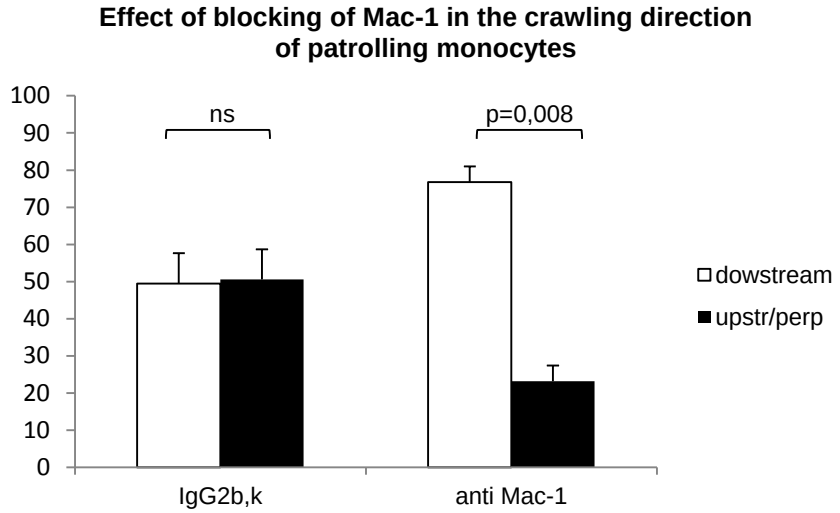

Figure 58. Comparison of crawling direction of patrolling monocytes upon injection of IgG2b,k and anti Mac-1 antibody in large arteries(n=6-7 mice per group, 33-35 cells per group). Upon injection of IgG2b,k an equal percentage of cells crawled upstream/ perpendicular (50,54%) and downstream (49,46%) to the blood flow. No significant difference was detected between these proportions (p=0,087). In contrast blocking of Mac-1 resulted in a significant increase of the percentage of downstream crawling monocytes (76,78%) in comparison to the upstream crawling cells (23,22%, p=0,008).

Therefore it can be assumed that, as in the case of small vessels, Mac-1 regulates the upstream crawling of patrolling monocytes also in the large arteries.

7.2.3.3.2 Long-term effect of anti Mac-1 antibody in crawling velocity, distance and linearity in carotid arteries

The next parameters that were analysed regarding the effect of blocking of Mac-1 in monocytes crawling in carotid arteries, were crawling velocity, distance and linearity. Injection of anti Mac-1 antibody had no long term effect in the crawling velocity of patrolling monocytes in the microvasculature. However, in the case of carotid arteries it led to a significant increase of the crawling velocity in comparison with the control experiments (figure 59A). On the other hand blocking of Mac-1 had no significant effect in the crawling distance in comparison with the control experiments neither in the case of microvasculature (p= 0,348) nor in the case of carotid arteries (p= 0,947 see figure 59B). Finally although we did not observe any significant differentiation

upon blocking of Mac-1 in the crawling linearity of monocytes in the microvasculature there was a significant increase in the value of this crawling parameter in the carotid arteries in comparison with the control experiments (p= 0,002 , Figure 59C).

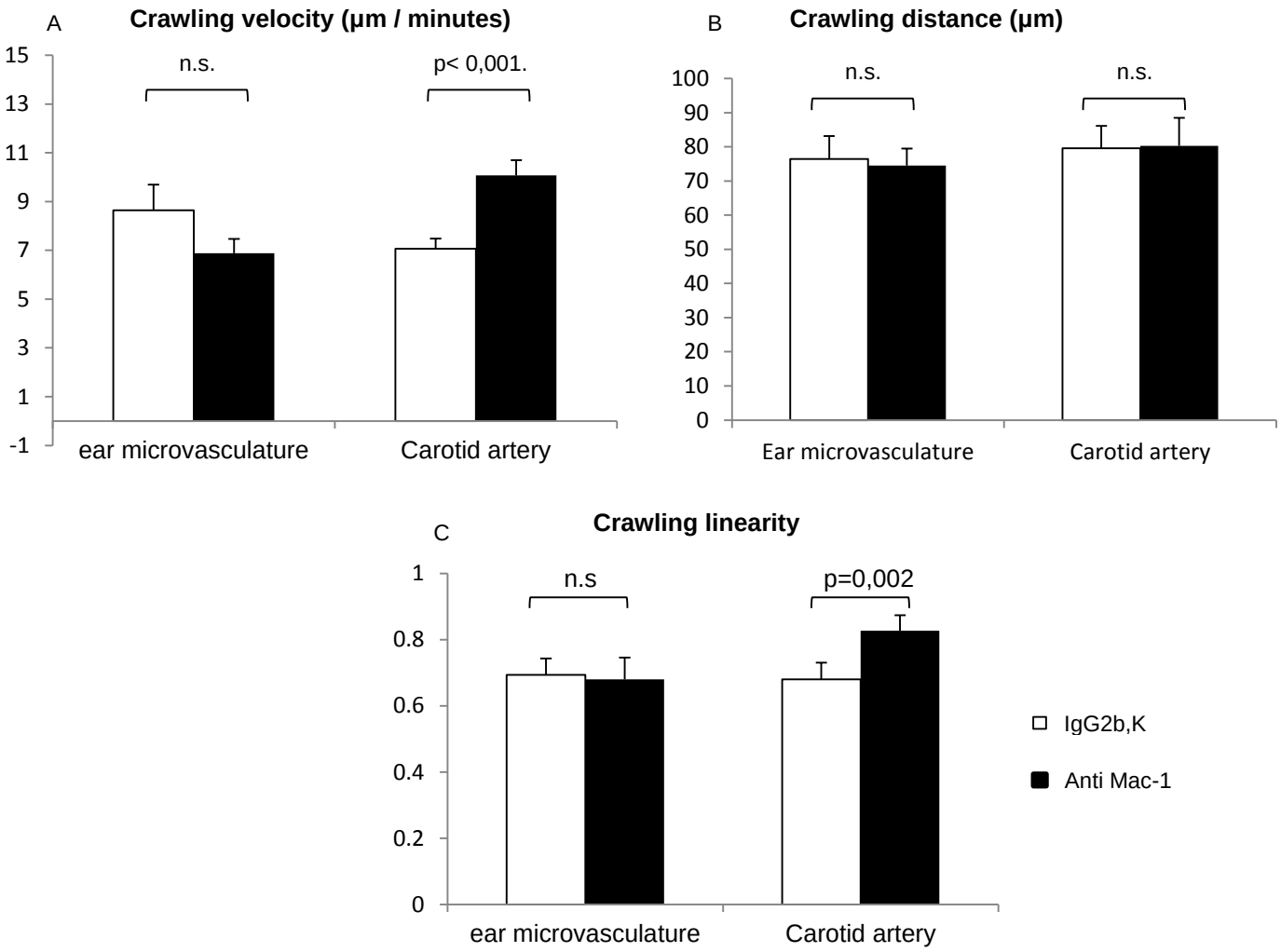

Figure 59. Comparison of crawling characteristics of patrolling monocytes in microvasculature and carotid arteries upon injection of IgG2k,b and anti Mac-1 antibody (n=6-7 per group). **A.** Comparison of the mean crawling velocity of patrolling monocytes. In contrast to the case of small vessels where we did not detect differences in the crawling velocity upon injection of IgG2b,k or anti Mac-1 (p=0,220), the crawling velocity of patrolling monocytes in carotid arteries was significantly higher upon injection of anti Mac-1 in comparison with the control experiments (p<0,001). **B.** Comparison of the mean crawling distance of patrolling monocytes. No significant difference was detected in the crawling distances of patrolling monocytes upon injection of anti Mac-1 antibody in both small vessels (p=0,348) and carotid arteries (p=0,947) in comparison with the control experiments. **C.** Comparison of the mean crawling linearity of patrolling monocytes. In contrast to the case of small vessels where no difference was detected upon injection of IgG2b,k or anti Mac-1 (p=0,943), the crawling linearity of patrolling monocytes in carotid arteries was significantly higher upon anti Mac-1 injection in comparison with the control experiments (p=0,02).

These data indicate that while blocking of Mac-1 does not affect crawling characteristics such as velocity, distance and linearity in the small vessels, in large arteries it leads to an increase in the crawling velocity and linearity of patrolling monocytes. This could imply a different contribution of Mac-1 in the crawling of monocytes in these two different parts of the vascular tree.

7.3. Leukocytes crawling in micro and macrovasculature under conditions of inflammation

After having analysed the effect of blocking of Mac-1 in the crawling behaviour of patrolling monocytes under steady state conditions in the microvasculature as well as in the macrovasculature we have focused in analysing the role of Mac-1 also in leukocytes crawling under inflammatory conditions. The predominant type of cells that are initially recruited in inflammatory reactions in small vessels are neutrophils while this kind of cells is also recruited in the inflamed wall of large arteries in atherosclerosis[29]. Therefore, we have focused in investigating the role of Mac-1 in neutrophils crawling in the mouse microvasculature under conditions of acute sterile inflammation and compare it with its role in neutrophils crawling in large inflamed carotid arteries (in the case of atherosclerosis).

7.3.1 Neutrophils crawling in microvasculature under acute sterile inflammatory conditions

In order to investigate the effect of blocking antibodies against the beta-2 integrin Mac-1 in the crawling characteristics of neutrophils under acute inflammatory conditions we have performed experiments in the microvasculature of the mouse ear of C57Bl/6J mice upon induction of sterile injury (as described in 6.4.1.1). As shown in the figure 61, an induction of necrosis in the interstitium via laser ablation in the perivenular region (50-75 µm from the postcapillary venules) led to a rapid significant increase in the number of adhering and crawling neutrophils in comparison to steady state as well as in the number of extravasated cells.

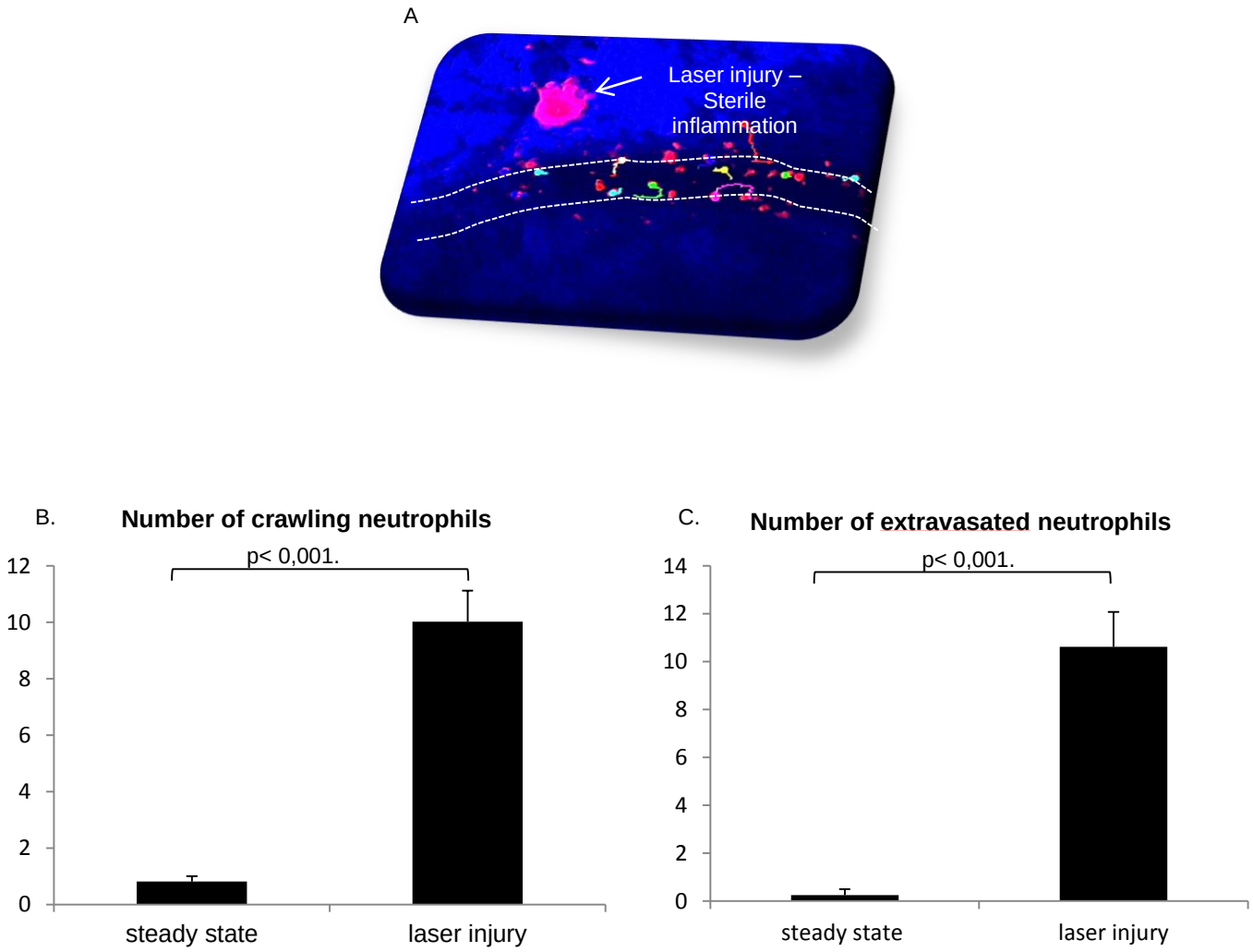

Figure 60. Effect of laser injury on neutrophil recruitment. **A.** Laser induced injury in the vicinity of a post-capillary venule of a C57Bl/6J mouse. The area of necrosis is highly auto-fluorescent without the need of further labelling. The dotted lines indicate the borders of the vessel while coloured continuous lines indicate the paths of the migrating neutrophils. Interstitial area is presented in blue (due to SHG) and neutrophils in red via labelling with PE-conjugated anti-Ly6G-1A8 antibody (n=6 mice/vessels per group, $p<0.01$). **B.** Induction of sterile inflammation leads to a significant increase in the count of crawling neutrophils. **C.** Induction of sterile inflammation leads to a significant increase to the count of extravasated neutrophils (n=6 mice/vessels per group, $p<0.01$).

As described in 7.2.1, under steady-state conditions neutrophils adhere to the endothelium in a very transient and passive way, whereas the vast majority of them follow a downstream direction to the blood flow. However, within 60 minutes upon induction of sterile inflammation in the ear, the pattern of crawling direction of

neutrophils is inversed since the majority of them crawl upstream/ perpendicular to the flow in an active way and less crawl downstream to the blood flow in a more passive way (figure 61A). Interestingly, the neutrophils that crawl upstream/ perpendicularly to the blood flow transmigrate in higher percentages in comparison to the downstream crawling population (Figure 61B).

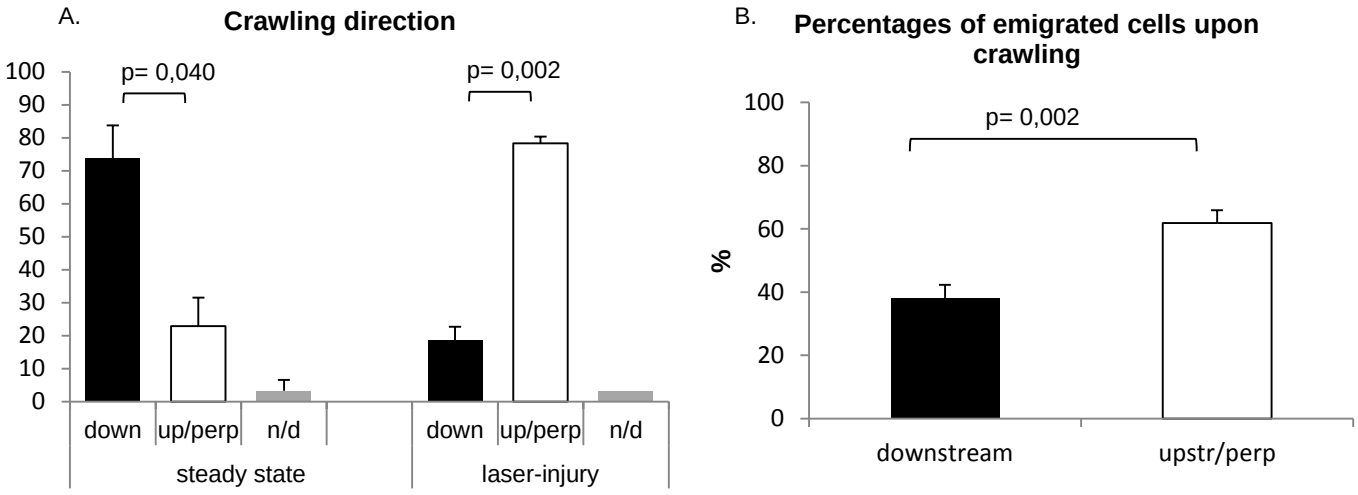

Figure 61. Crawling direction of neutrophils in the microvasculature of C57Bl6/J mice in steady-state and upon acute sterile inflammation in the mouse skin (n=6). **A.** Neutrophils (labelled by injection of fluorescent Ly6G 1A8 antibody) crawl mainly downstream in steady state. In contrast, in sterile inflammation the majority of cells crawl upstream or perpendicular to the blood flow. **B.** Percentages of transmigrating cells grouped according to their crawling direction in different time points of recording (the total duration is one hour). The upstream/perpendicularly crawling neutrophils transmigrate in higher percentages in comparison to the downstream crawling cells.

7.3.1.1 Effect of blocking of Mac-1 in the crawling of neutrophils in acute sterile inflammation

Next we aimed to evaluate whether Mac-1 plays a role in the crawling behaviour of neutrophils in the microvasculature of the ear under acute sterile inflammatory conditions. As in the case of steady state we focused in analysing both the direct and long term effect of blocking of Mac-1 in the crawling process. To achieve this, two analysis protocols were used per experiment (as discussed in 6.7.9). Following the first protocol we analysed the direct effect of blocking of Mac-1 in the crawling of neutrophils by application of the CSCTP analysis. Following the second protocol,

analysis was performed in later time points (within 60 minutes upon the induction of the laser injury) in order to investigate the long term effect of blocking of Mac-1 on neutrophil crawling. These experiments were performed in the microvasculature of the ear of C57Bl/6J mice and neutrophils were labelled *in vivo* with injection of PE conjugated Ly6G 1A8 antibody. Injection of the anti Mac-1 blocking antibody or the IgG2b,k isotype control antibody in the mice was performed approximately during the 7th minute of recording (Figure 62).

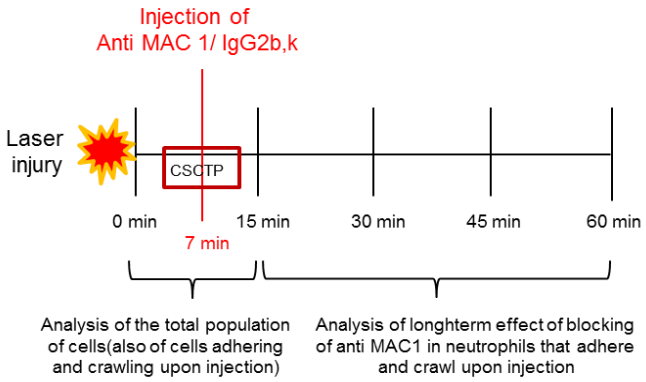

Figure 62. Experimental protocol followed in the experiments regarding the effect of injection of anti Mac-1 or IgG2b,k in the crawling behaviour of neutrophils under conditions of acute sterile inflammation. CSCTP as well as long term analysis were performed in the same experiment. Detailed information is provided in 6.7.9.

7.3.1.1.1 Direct effect of blocking of Mac-1 in the crawling direction of neutrophils in acute sterile inflammation in the microvasculature of the mouse ear.

Our CSCTP analysis showed that application of IgG2b,k isotype control antibody did not influence the crawling direction of neutrophils since they continued crawling in the same direction (regardless this was upstream/perpendicular or downstream) for several minutes upon injection (figure 63A). On the other hand injection of anti Mac-1 blocking antibody led occasionally to a change in crawling direction of the initially (prior to injection) upstream/ perpendicularly crawling neutrophils (Figure 63B).

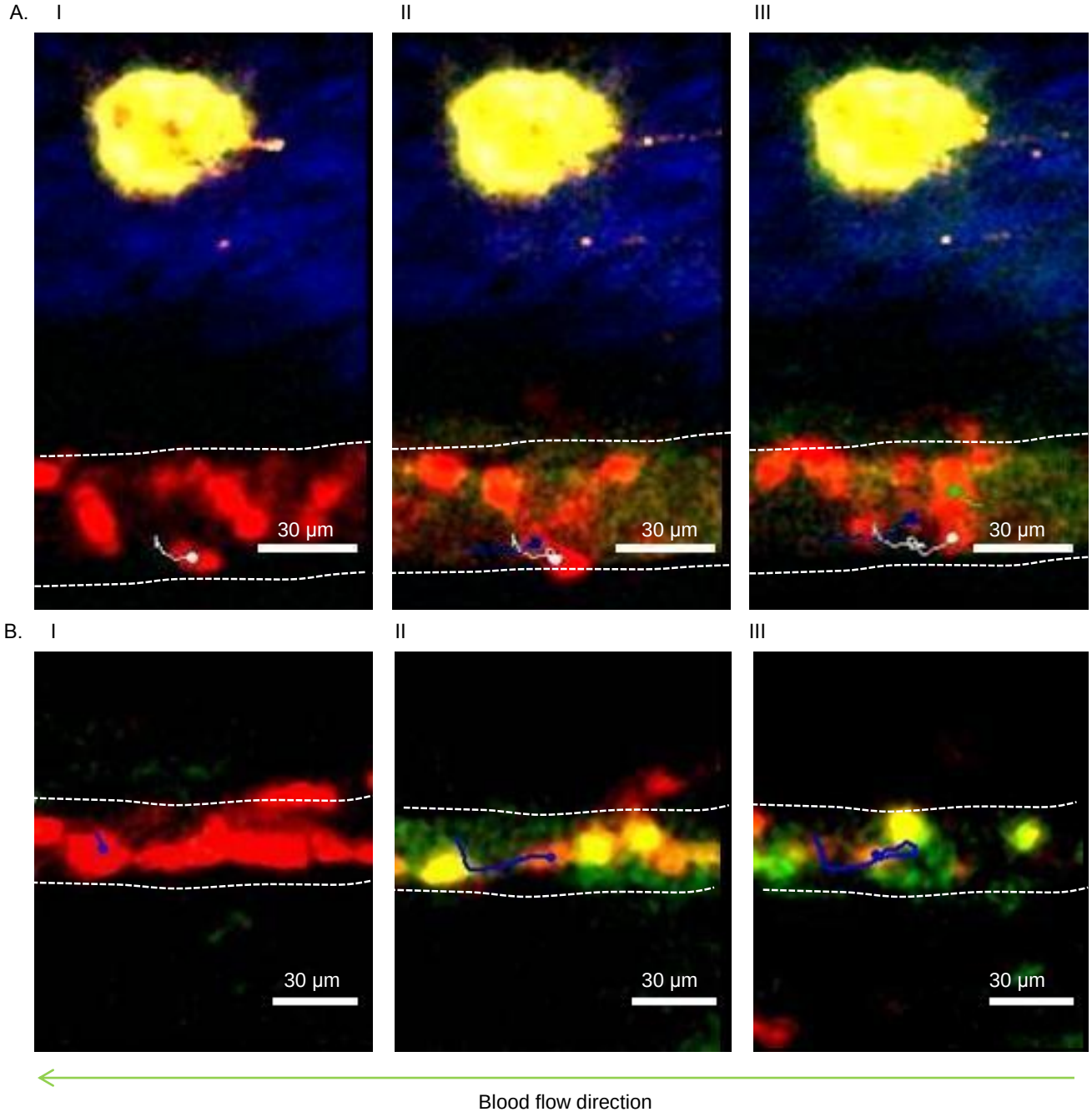

Figure 63. Direct effect of injection of IgG2b,k and anti Mac-1 in the crawling direction of upstream crawling neutrophils (analysis performed by application of CSCTP). **A i.** Neutrophil detected crawling upstream to the blood flow prior to the injection of IgG2b,k. **A ii.** Injection of IgG2b,k (FITC conjugated). **A iii.** The neutrophil continues crawling upstream upon injection. The white line indicates its crawling path. **B i.** Neutrophil detected crawling upstream to the blood flow prior to the injection of anti Mac-1 blocking antibody. **B ii.** Injection of anti Mac-1(FITC conjugated). **B iii.** The imaged neutrophil changes its crawling direction from upstream to downstream. The blue line indicates its crawling path. Sterile injury (yellow spot) in the first line of images is presented via auto-fluorescence signal (not shown in the second line of images). Neutrophils are presented in red via labelling with PE-conjugated anti Ly6G 1A8 antibody. The blood vessels are presented in green after injection of green FITC-conjugated blocking anti Mac-1 or IgG2b,k .

Our quantitative CSCTP analysis showed that only 23.3% of the cells that crawled upstream/perpendicular to the flow at the baseline (prior to the injection) changed their crawling direction to downstream upon injection of anti Mac-1 antibody (Figure 63). Additionally there was no change detected in the crawling direction of the downstream crawling neutrophils upon injection of anti Mac-1 antibody. The injection of IgG2b,k isotype control antibody had no direct effect in the crawling direction of neutrophils. We have furthermore observed that blocking of Mac-1 resulted in a direct detachment of 29.9% of the upstream/perpendicularly crawling neutrophils while injection of IgG2b,k isotype led in detachment of 27.08% of the upstream/perpendicularly crawling cells. There was no significant statistical difference regarding detachment between the two groups (p= 0.195 see figure 64).

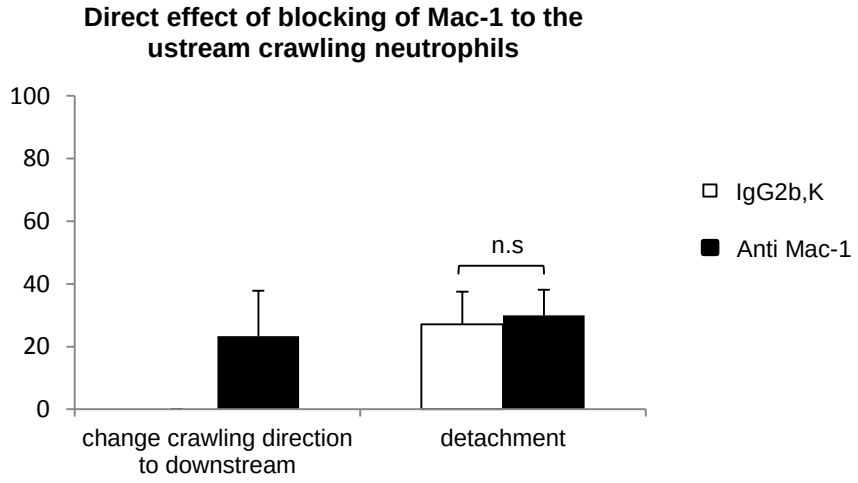

Figure 64. Percentages of upstream/ perpendicularly crawling neutrophils that changed direction or detached upon injection of anti Mac-1 blocking antibody or IgG2b,k isotype control in the microvasculature of C57Bl/6J mice. (n=5 mice, 15 to 20 cells per group). 23.3% of the upstream crawling neutrophils changed crawling direction upon injection of anti Mac-1 antibody while IgG2b,k had no effect in the crawling direction. 27.08% and 29.9% of the upstream/perpendicularly crawling cells detached upon injection of IgG2b,k or anti Mac-1 respectively but there was no significant difference between these two groups (p=0.195).

These results suggested that blocking of Mac-1 did not have any significant direct effect in the adhesion and crawling of neutrophils in the onset of the immune response under conditions of acute sterile inflammation.

7.3.1.1.2 Direct effect of blocking of Mac-1 in neutrophil crawling characteristics in acute sterile inflammation in the microvasculature of the mouse ear.

To better investigate any possible direct effect of blocking of Mac-1 in the crawling behaviour of neutrophils we have further analysed the following crawling parameters: forward migration index in X and Y axis, crawling velocity and crawling distance. Our analysis concerned the comparison of the crawling characteristics before and after the injection of anti Mac-1 blocking antibody or IgG2b,k isotype and was performed by application of CSCTP.
Upon quantifying the percentages of the upstream/perpendicularly or downstream crawling neutrophils upon induction of sterile inflammation we focused in analysing how Mac-1 influences their efficiency to crawl along one direction/axis. Hence, we have analysed the forward migration index of the crawling cells along the X and Y spatial axis. As described in 6.6.1.4 the xFMI provides indication regarding the efficiency of the cells to crawl upstream or downstream to the blood flow while the yFMI provides indication of the efficiency of the cells to crawl intravascularly towards or against the area of the injury.

Our analysis regarding the yFMI showed that there is no difference between the control group and the group treated with anti Mac-1 antibody at the baseline before injections (p=0.482).The yFMI upon blocking of Mac-1 was still comparable to the yFMI upon injection of IgG2b,k in the cells that were analysed by CSCTP (p=0.6, see figure 65A). The positive values of yFMI in all cases indicate a higher efficiency of neutrophils to crawl intravascularly towards the area of injury.

We next focused to analyse whether blocking of Mac-1 influenced the ability and efficiency of neutrophils for upstream or downstream crawling. As expected there was no significant difference (p=0.183) in the xFMI before injection of anti Mac-1 or IgG2b,k. In these measurements we observed that neutrophils were more efficient for upstream crawling (as this was indicated by the positive value of the xFMI). Furthermore blocking of Mac-1 did not have any significant direct effect in the xFMI of the cells in comparison with the control experiments (p=0.316 see figure 65B). Still in

the time point right upon the injection of IgG2b,k or anti Mac-1 the cells were more efficient for upstream crawling as this was expressed by a positive value for xFMI. Our further analysis showed that, as expected, there was no difference in the crawling velocities of neutrophils at the baseline between our groups (p=0.147). In addition blocking of Mac-1 did not have any significant direct effect in the velocity of the crawling neutrophils that were analysed by CSCTP in comparison with our control experiments (p = 0.659, see figure 65C). This was also true for the case of mean crawling distance since we again we did not detect any significant difference between the two groups before and after injections of anti Mac-1 blocking antibody and IgG2b,k isotype control antibody (p_{before}=0.686, p_{after}=0.289 see figure 65D).

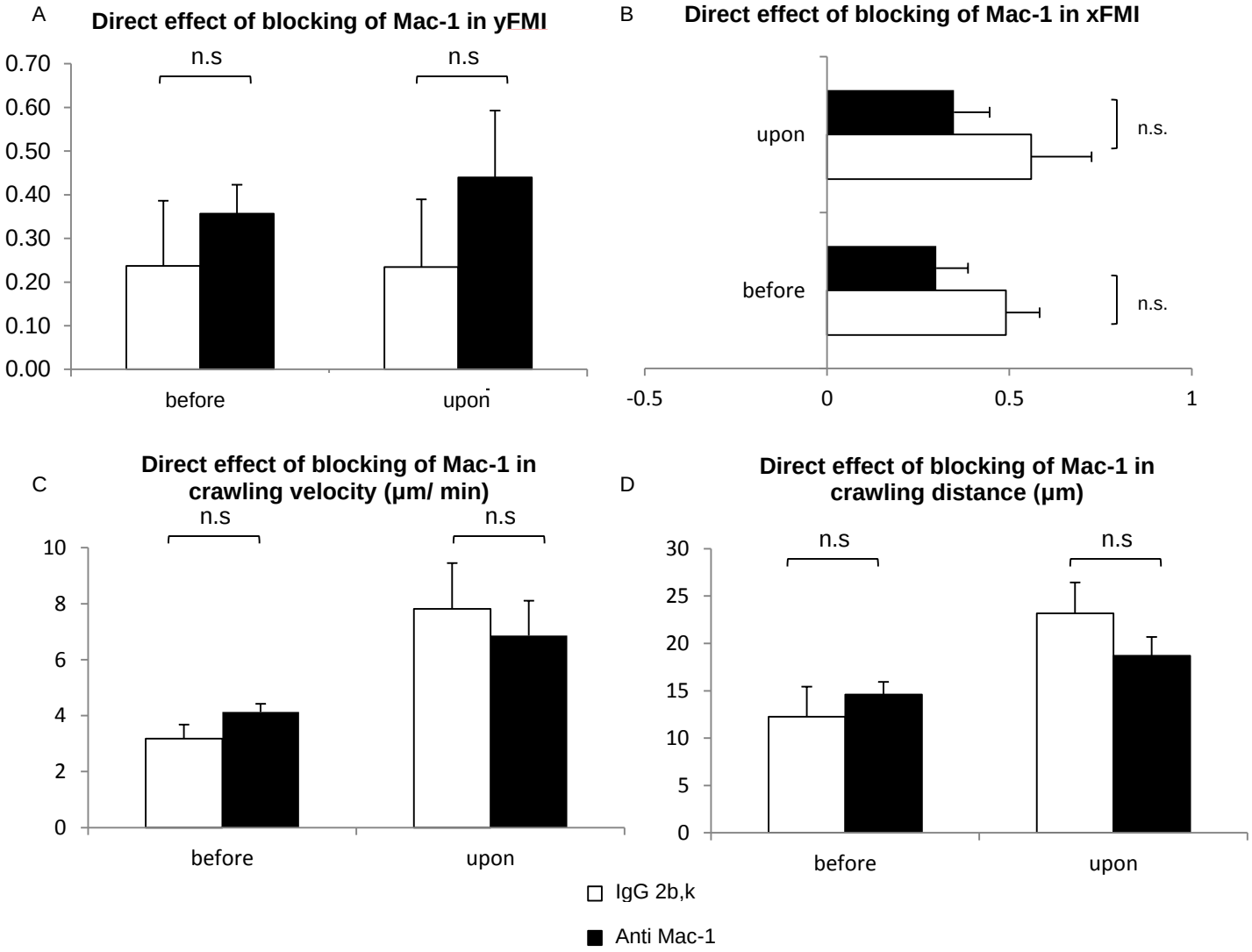

Figure 65. Analysis of the direct effect of blocking of Mac-1 in the crawling characteristics of neutrophils in acute sterile inflammation in C57Bl/6J mice (n=5 per group). **A.** Blocking of Mac-1 did not have any significant direct effect in the yFMI of crawling neutrophils (p=0.6). **B.** Blocking of Mac-1 did not have any significant direct effect in the xFMI of crawling neutrophils (p=0.316). **C.** Blocking of Mac-1 did not have any significant direct effect in the mean crawling velocity of neutrophils (p=0.147). **D.** Blocking of Mac-1 did not have any significant direct effect in the mean crawling distance of neutrophils (p=0.289).

These results indicate that blocking of Mac-1 does not have any direct effect in the crawling behaviour of neutrophils (as this is described by crawling direction, efficiency of crawling along the X or Y axis, crawling velocity and crawling distance) in the onset of the immune reaction related to sterile inflammation.

7.3.1.1.3 Long term analysis of the role of Mac-1 for neutrophil crawling in the model of acute sterile inflammation in the mouse skin

To further investigate whether blocking of Mac-1 had a later effect on neutrophil crawling direction we have analysed the percentages of upstream/perpendicular and downstream crawling neutrophils in different time periods (within one hour) after the induction of the laser ablation. In the control group, there was constantly a significantly higher percentage of cells crawling upstream/perpendicularly to the blood flow in all time points (Figure 66). Upon treatment with anti Mac-1 blocking antibody we could detect a significantly higher percentage of cells crawling upstream/ perpendicularly to the blood flow in comparison with the population of cells that crawled downstream in the first (0-15 minutes) and last time period (45-60 minutes). In contrast, in the second (15-30 minutes) and third (30-45 minutes) time period the percentages of upstream/perpendicularly crawling cells were almost equal with the percentages of the downstream crawling cells and no statistical difference (p_{15-30}=0,695, p_{30-45}=0,716) was detected between these two populations of neutrophils.

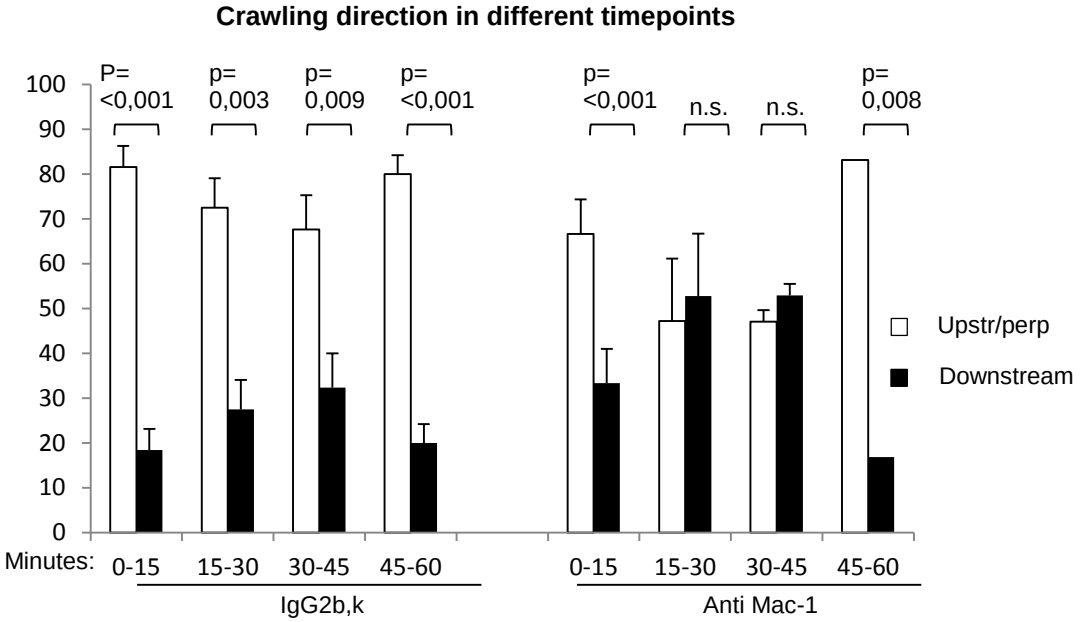

Figure 66. Crawling direction of neutrophils in acute sterile inflammation in different time periods upon injection of IgG2b,k or anti Mac-1 antibody (n=5 mice per group, 30-40 cells per group per time period). The majority of neutrophils crawl upstream/ perpendicular to the blood flow in both groups of experiments in all time points except from the second (15-30 minutes) and third time period (30-45 minutes) in the case of blocking of Mac1 beta-2 integrin.

These data indicate that although blocking of Mac-1 had no direct effect in the crawling direction of neutrophils (as analysed by CSCTP) it had a later transient effect in the two time periods following the injection (15-30 and 30-45 minutes). While in these time periods the majority of neutrophils in the control group crawled upstream or perpendicularly to the blood flow, in the case of blocking of Mac-1 the percentage of upstream/ perpendicularly crawling cells was equal to the percentage of downstream crawling cells.

7.3.1.1.4 Long term effect of blocking of Mac-1 in the crawling parameters of neutrophils

As it was previously described (7.3.1.1.1) there was no direct effect of blocking of Mac-1 in the efficiency of neutrophils to crawl along the X (xFMI) and Y (yFMI) axis. Our next aim was to investigate whether these parameters were influenced in later

time points upon administration of anti Mac-1 antibody. Our analysis concerning the yFMI showed that in the first time period (0-15 minutes) of our recording (during which the blocking antibody against Mac-1 or IgG2b,k was injected) neutrophils generally were efficient in crawling intravascularly towards the area of the injury and there was no difference between the two groups of experiments (p=0,469 , figure 67A). Upon injection of anti Mac-1 antibody we observed in the second (15-30 minutes) and third (30-45 minutes) time period of recording, a tendency of neutrophils to be more efficient for crawling against the site of the injury (expressed by negative values for the yFMI). In contrast, the mean yFMI in the control group was positive (although we detected big variations among our experiments) for the same time periods indicating the ability of cells to crawl intravascularly towards the injury. However, we did not detect statistically important differences between these two groups (p_{15-30} = 0,686, p_{30-45} = 0,362, see figure 67). Finally in the last time period (45 -60 minutes) the yFMI of the cells in the treated group was close to 0. However, again no statistical difference was detected with our control experiments in which the yFMI had still a positive value (p= 0,303, figure 67A).

We next focused in analysing the long term effect of blocking of Mac-1 in the xFMI. In the first time period (0-15 minutes during which injection took place) we could observe a modest reduction in the xFMI of the total population of crawling neutrophils upon application of anti Mac-1 in comparison with the control experiments. However this tendency did not reach a statistically important difference (p= 0,151, Figure 67B). In the second time period (15-30 min) of our recording the neutrophils presented a significantly higher efficiency for downstream crawling upon blocking of Mac-1 (expressed by a negative value for the xFMI) in comparison with the control group where the cells were still more efficient for upstream crawling (p=0,038). In the third time period (30-45 minutes) there was still a tendency of the cells in the treated with anti Mac-1 group to be more effective for downstream crawling, however we did not detect important statistical differences with our control group (p= 0,149). Finally in the last time period of our experiments (45-60 minutes) the xFMI of neutrophils upon blocking of Mac-1 was once again positive and similar to the xFMI of the control group (p= 0,486) revealing that the cells regained their ability and efficiency for upstream crawling (figure 67B).

These data suggest that blocking of Mac-1 does not significantly influence the efficiency of neutrophils to crawl towards the area of the injury, it transiently influences however their efficiency for upstream crawling for a period of 15 minutes (from the 15th to the 30th minute of recording). Injections of anti Mac-1 or IgG2b,k took place approximately in the 7th minute of recording.

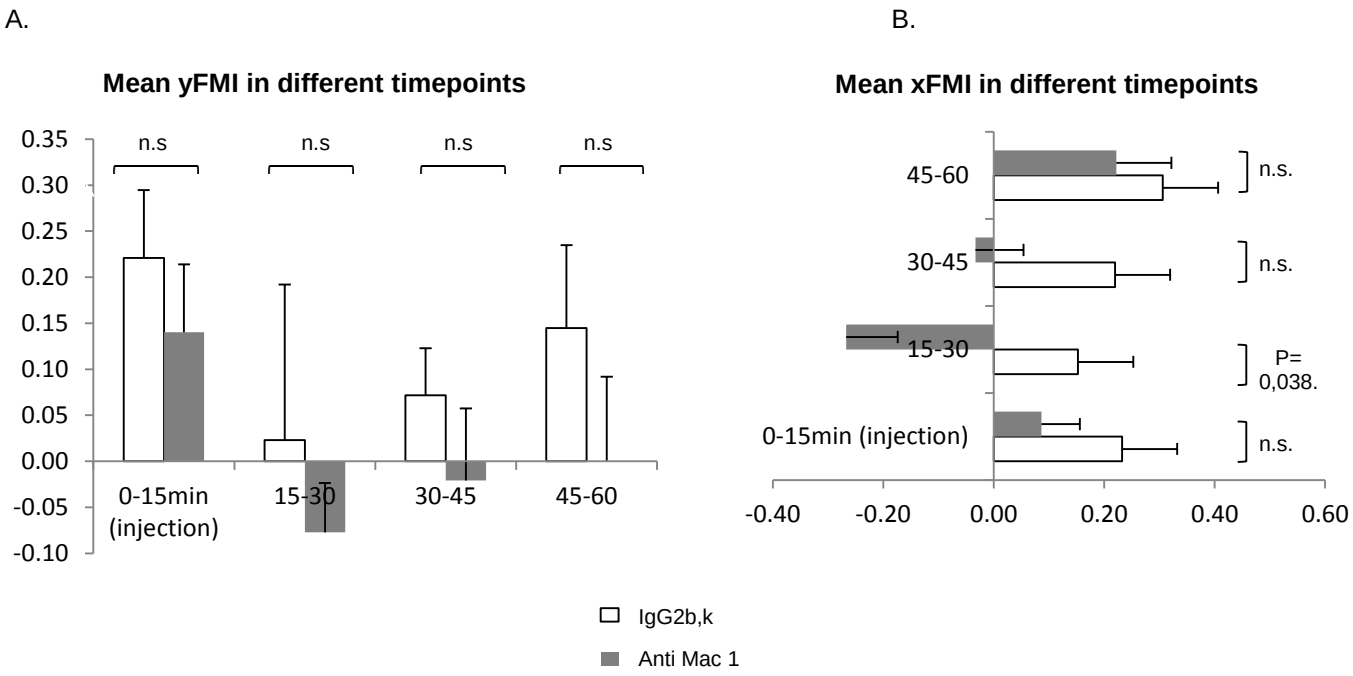

Figure 67. Analysis of the long-term effect of blocking of Mac-1 integrin in the crawling characteristics of neutrophils in acute sterile inflammation (n=5 mice per group). **A.** General effect of blocking of Mac-1 in the yFMI of the total population of crawling cells in different time points. No differences were detected with our control experiments (p_{0-15}=0,469, p_{15-30}=0,686, p_{30-45}=0,362, p_{45-60}=0,303). **B.** General effect of blocking of Mac-1 in the xFMI of the total population of crawling cells in different time periods. The xFMI of the crawling neutrophils was significantly reduced in the second time period (15-30 minutes) of recording in comparison with our control group. No significant differences were detected in the rest time periods (p_{0-15}=0,151, p_{15-30}=0,038, p_{30-45}=0,140, p_{45-60}=0,486).

To further characterize the long-term effect of blocking of Mac-1 in the crawling behaviour of neutrophils under conditions of acute sterile inflammation we have performed analysis of their crawling velocity, distance and, linearity.

Our statistical analysis showed that upon injection of anti Mac-1 antibody there was a significant increase (p=0,035) in the velocity of neutrophils in the second time period (15 - 30 minutes) of our recording in comparison to the control experiments. In the

next time periods there was a moderate tendency of the cells to crawl faster in the case of treatment with anti Mac- 1 antibody. However, we did not detect a significant difference in the crawling velocity between the treated and the control group (figure 68A).

In the analysis we performed regarding crawling distance, we detected a significant increase upon injection of anti Mac-1 antibody in the second time period (15 - 30 minutes) of our recordings in comparison with our control experiments at the same time period. Although there was a moderate tendency of increased crawling distance also in the third time period in the treated group this was not expressed as a statistically important difference in comparison with the control group (p=0,763, see figure 68B).

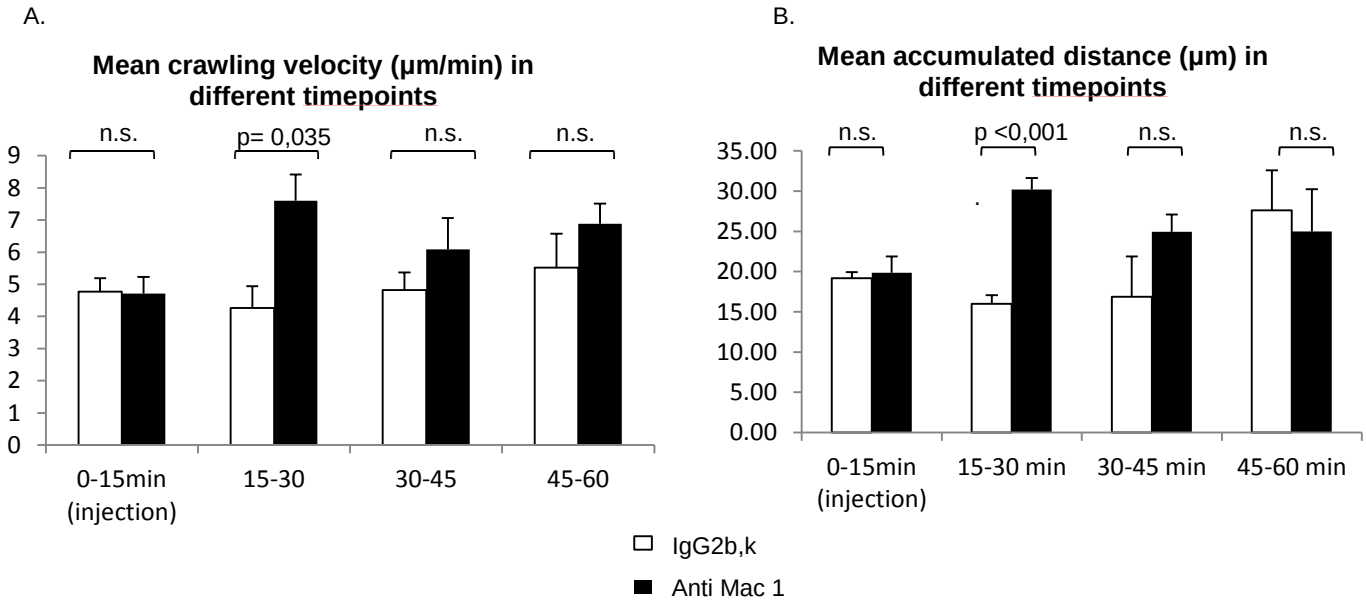

Figure 68. A. General effect of blocking of Mac-1 in the crawling velocity of the total population of neutrophils in different time periods (n=5 mice per group). Neutrophils crawled with a significantly higher velocity in the second time period of recording while this parameter was unaffected in the rest time periods (p_{0-15}=0,759, p_{15-30}=0,038, p_{30-45}=0,366, p_{45-60}=0,371) **B.** General effect of blocking of Mac-1 in the crawling distance of the total population of crawling neutrophils in different time periods (n=5 mice per group). As in the case of velocity the crawling distance of the total population of neutrophils was significantly increased in the second time period while it was unaffected in the rest time periods (p_{0-15}=0,731, p_{15-30}<0,001, p_{30-45}=0,486, p_{45-60}=0,763). Injection of IgG2b,k or of anti Mac-1 blocking antibody took place during the first time period approximately to the seventh minute.

Finally in order to fully describe the long term effect of blocking of Mac-1 in the crawling behaviour of neutrophils we have also analysed the linearity of crawling in different time points. In that case we did not detect any differences in the ability of neutrophils to follow a linear crawling path upon injection either of anti Mac-1 or of IgG2b,k isotype control antibody during the different time periods of our recordings (Figure 69).

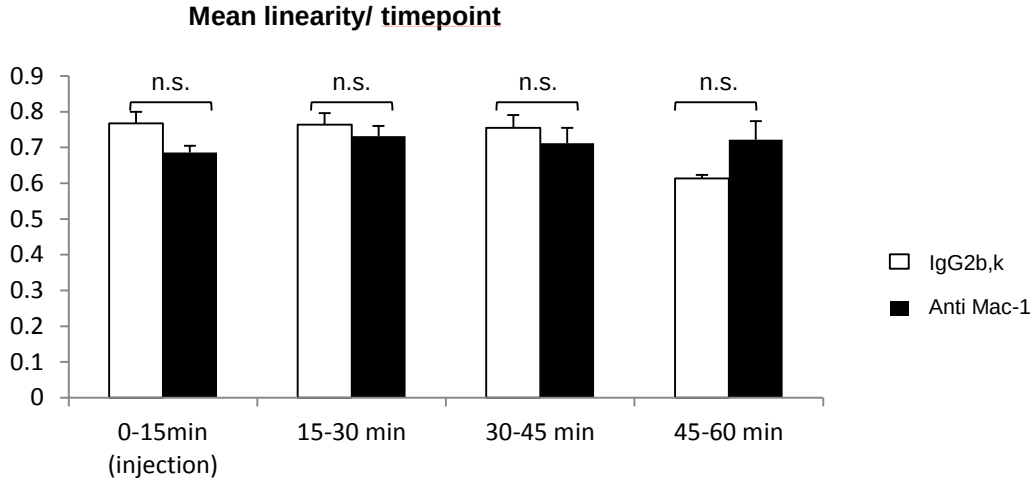

Figure 69. Analysis of the crawling linearity of neutrophils in different time periods. Blocking of Mac-1 did not influence the ability of neutrophils to follow linear crawling paths in comparison with injection of IgG2b,k. (p_{0-15}=0,087, p_{15-30}=0,547, p_{30-45}=0,532, p_{45-60}=0,343)

These data show that upon blocking of Mac-1 integrin there is a significant increase in the crawling velocity and distance of neutrophils in the second time period of our recording (during the 15th – 30th minute, while injection took place at approximately the 7th minute of recording). Interestingly in the same time period there was a significant decrease in the efficiency of neutrophils for upstream crawling (as this was studied by analysis of the xFMI).Therefore, we can assume that blocking of Mac-1 influences in a very transient way (for a period of 15 minutes) the crawling parameters of neutrophils.

7.3.1.2 In vivo imaging and quantitative analysis of neutrophil crawling in the model of mouse atherosclerosis

In this part of the project we focused on the analysis of neutrophils crawling in large arteries in the presence of an atherosclerotic plaque. First, we analysed whether intravascular crawling of neutrophils, like in the inflamed microvasculature, is occurring during neutrophils migration cascade into the atherosclerotic lesions. Second, we aimed in investigating the effect of blocking of beta2 integrin Mac-1 for neutrophils crawling in atherosclerosis and provide a comparison with the case of acute sterile inflammation in the microvasculature. Using our model for stable long-term *in vivo* imaging of large arteries we were able to observe for the first time crawling of neutrophils on the atherosclerotic plaque of ApoE$^{-/-}$ mice and to perform quantitative analysis of its basic characteristics. We found that in contrast to the case of sterile inflammation in the microvasculature (where there was a significantly higher proportion of neutrophils crawling upstream or perpendicularly to the blood flow), in the case of atherosclerosis in the carotid arteries the percentage of cells that crawled upstream/ perpendicular was comparable to the percentage of cells that crawled downstream to the blood flow direction (p=0,661 see figure 70).

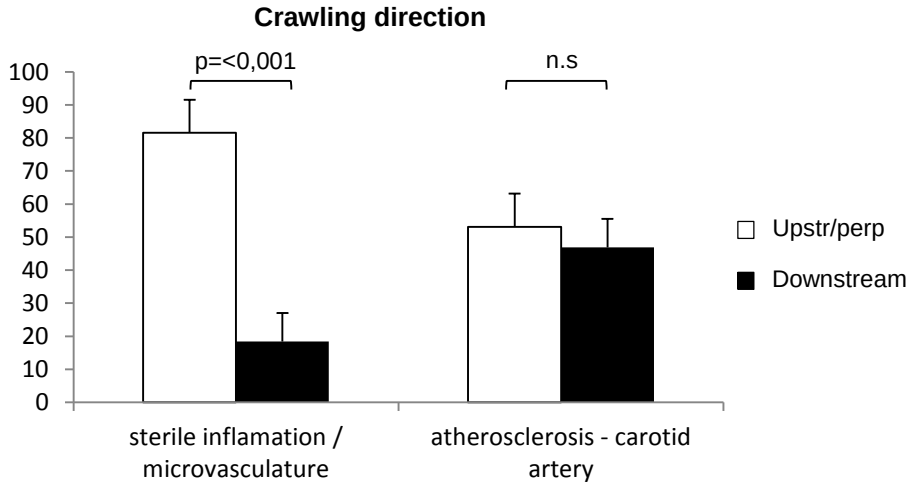

Figure 70. Crawling direction of neutrophils in post-capillary venules (acute sterile inflammation= 5 mice, 40 cells) and carotid arteries (atherosclerosis, n= 5 mice, 45 cells). In the case of the post-capillary venules there is a significant higher percentage of neutrophils crawling upstream/perpendicular to the blood flow (p=0,001) while in the case of carotid

arteries similar percentages of neutrophils crawl upstream/perpendicular and downstream to the blood flow (p=0,061).

Next, we focused in analysing the crawling velocity and distance in atherosclerotic arteries of ApoE$^{-/-}$ mice. Our results showed that the mean crawling velocity of neutrophils at the baseline recording was significantly higher (p= 0,019) in comparison with the crawling velocity of neutrophils in the microvasculature (Figure 71A). As it matters the crawling distance in the case of atherosclerosis neutrophils crawl for a mean distance of 29,96 μm while in the case of sterile inflammation neutrophils crawl for a distance of 20,15 μm. Our statistical analysis showed again that the mean crawling distance in carotid arteries is significantly higher (p=0,013) in comparison with the small vessels (figure 71B).

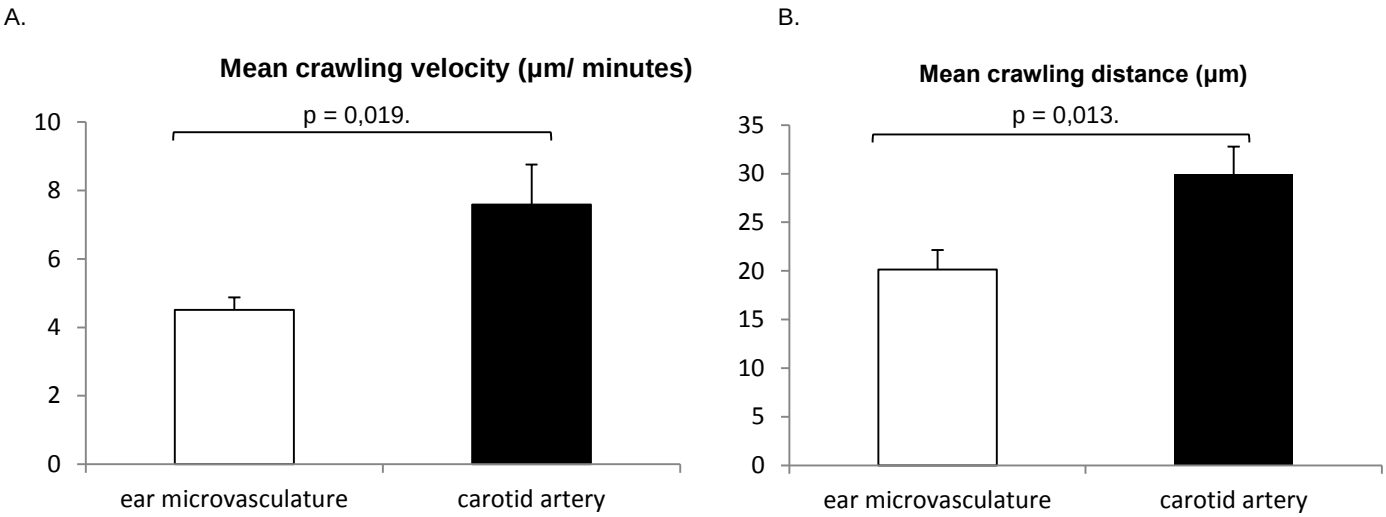

Figure 71. Comparison of crawling characteristics of neutrophils in the microvasculature and carotid arteries under conditions of acute sterile inflammation and atherosclerosis respectively. **A.** Comparison of crawling velocity in the microvasculature of C57Bl/6J mice with that in carotid arteries of ApoE$^{-/-}$ mice (n=5 mice per group). Neutrophils crawled with a significantly higher velocity in carotid arteries in comparison with the microvasculature (p=0,019). **B.** Comparison of crawling distance in microvasculature and carotid arteries. Neutrophils crawled for a significantly higher distance in carotid arteries in comparison with the microvasculature (p=0,013).

Furthermore we have also analysed the crawling linearity of neutrophils in atherosclerotic vessels. In result, the crawling linearity of neutrophils in the atherosclerotic carotid arteries was statistically comparable to the crawling linearity of neutrophils in postcapillary venules upon induction of sterile inflammation (figure 72)

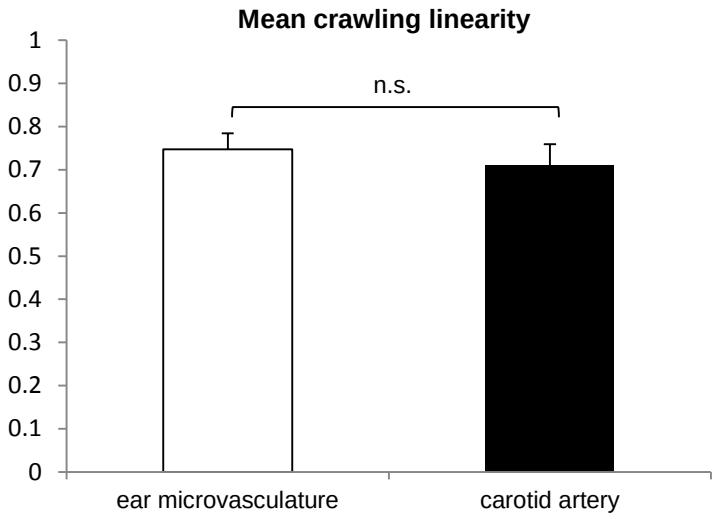

Figure 72. Comparison of crawling linearity in microvasculature and carotid arteries. No statistical differences were detected (n=5 mice per group, p= 0,570)

7.3.1.2.1 Role of Mac1 in neutrophil crawling in atherosclerosis

Our next focus was to investigate in real time whether Mac-1 integrin mediates the crawling process of neutrophils in large atherosclerotic arteries. In this set of experiments our goal was to follow the same experimental protocol regarding the time points of injection of IgG2b,k and anti Mac-1 antibody as in the case of the analysis regarding sterile inflammation in the microvasculature. Our initial experiments however, revealed an unexpected loss of focus shortly after injection which did not allow us to perform stable imaging in a continuous way (Figure 73A). In the same context, we could also observe in some cases disturbed electro-cardiographic patterns expressed by supraventricular arrhythmias (figure 73B). Therefore, CSCTP analysis could not be performed in the case of atherosclerosis.

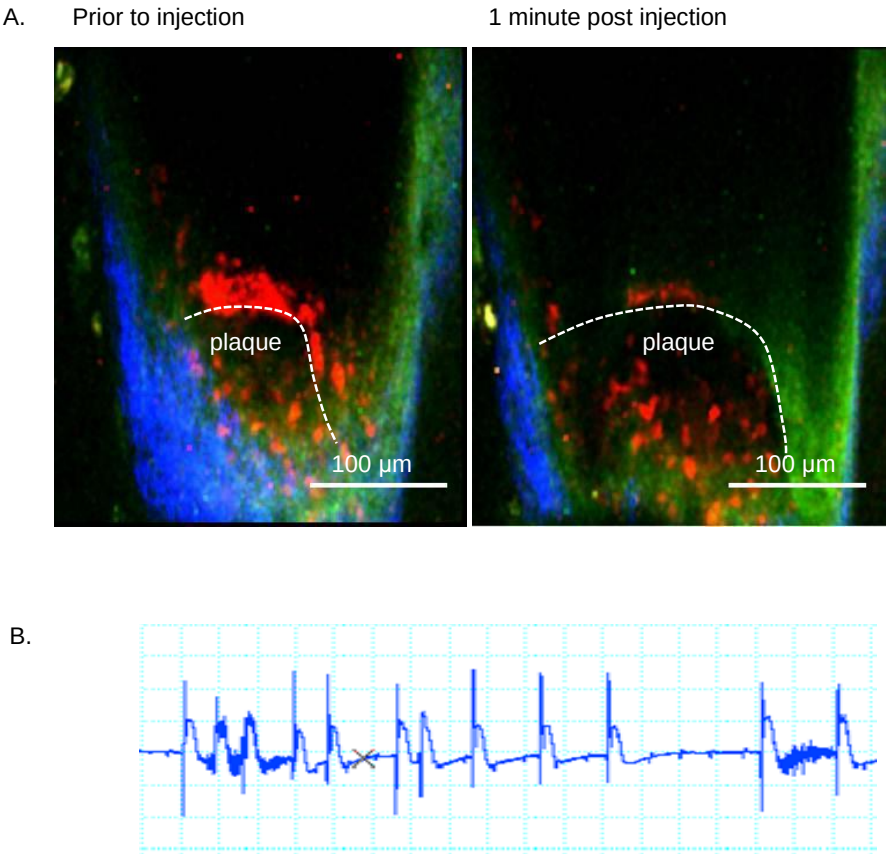

Figure 73. A. In vivo injection of anti Mac-1 antibody during imaging of neutrophils adhering and crawling on an atherosclerotic plaque. Loss of focus is occurring shortly after injection. Thus, CSCTP cannot be performed in that case. **B.** Altered electrocardiographic pattern of mice upon injection.

In order to circumvent these limitations we have initially performed baseline recordings in the presence of atherosclerotic plaques, subsequently we stopped our imaging and injected the IgG2b,k isotype or anti Mac-1 antibody and finally we performed further in vivo recordings up to 30 minutes upon the injection which corresponded in the time period where the strongest effect of blocking of Mac-1 was observed in the small vessels in the case of sterile inflammation. Therefore, we were able to compare our results from the atherosclerotic arteries with our data from the microvasculature. The results from the two time periods upon blocking of Mac-1 in the case of atherosclerosis were combined and analysed together. In the next part of

our project we first questioned whether blocking of Mac- 1 affected the crawling direction of neutrophils. The percenatge of upstream crawling cells at the baseline recording in the control group was 52,8% while the percentage of downstream crawling cells was 47,2%. However, there was no statistical difference between these two values (p=0,599). Upon application of IgG2b,k 51,4% of the cells crawled upstream and 49,6% crawled downstream to the bloof flow (no statistical difference was detected, p=0,854). In the experiments where anti Mac-1 was injected, the proportion of the upstream crawling cells at the baseline recording was 51,2% while the proportion of the downstream crawling cells was 48,8% (no statistical difference was observed between these two values, p=0,785). Upon injection of anti Mac-1 54,9% of the crawling neurtrophils followed an upstream direction while a comparable percentage of cells (45, 1%) crawled downstream to the blood flow (p= 0,340, figure 74).

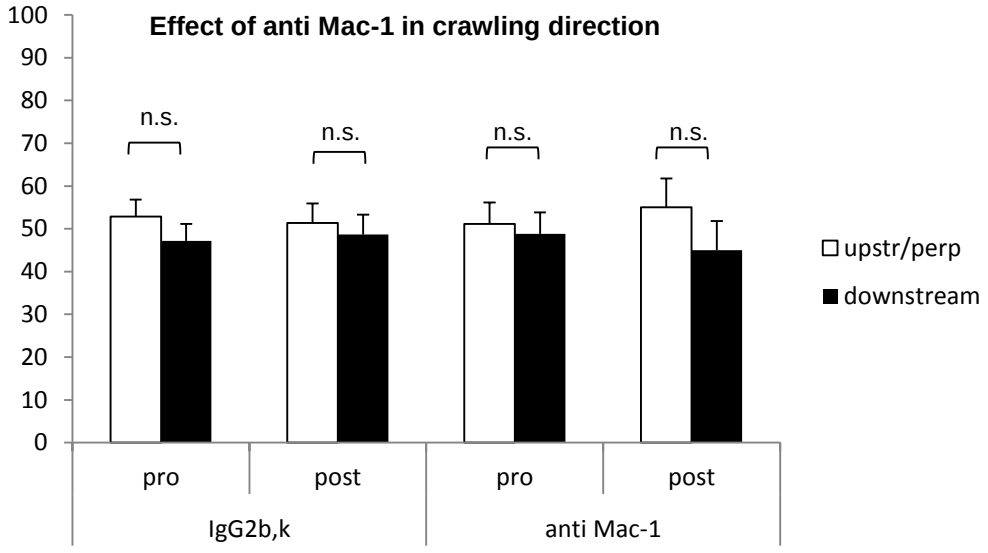

Figure 74. Comparison of crawling direction before and after injection of IgG2b,k isotype control and anti Mac-1 blocking antibody (n=5 mice per group). Blocking of Mac-1 did not have any effect in the crawling direction of neutrophils in atherosclerotic plaques.

We have furthermore analysed the effect of blocking of Mac-1 to the crawling velocity of neutrophils in atherosclerotic carotid arteries. The mean crawling velocity of neutrophils at the baseline before injection of anti Mac-1 and of the IgG2b,k

isotype control antibody were comparable (p=0,914). Interestingly upon injection there was no difference in neutrophils crawling velocity between the treated with anti Mac-1 group and the control group (p=0,717, figure 75A). Additionaly we have quantified the crawling distance of neutrophils before and after injections of IgG2b,k and anti Mac-1antibody. Before application of IgG2b,k and anti Mac-1 the mean crawling distance was 28,69 μm and 39,16 μm respectively. However, there was no statistically important difference between these two values (p= 0,984). After the injection of IgG or anti Mac-1 the crawling distances were 24,88μm and 38,95 μm respectively. Again in that case there was no important statistical difference between the control experiemtns and the experiements where Mac-1 was blocked (p=0,610 figure 75B).

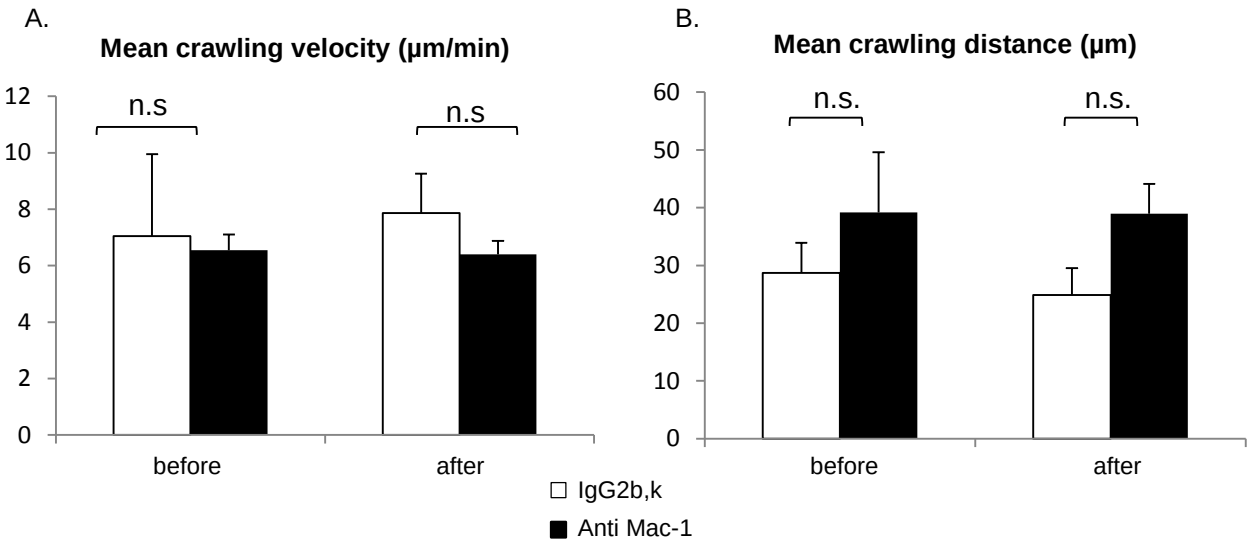

Figure 75. Comparison of crawling characteristics before and after injection of IgG2b,k isotype control and anti Mac-1 blocking antibody (n=5 mice per group) in atherosclerosis **A.** No difference was detected as expected in the baseline before injection of IgG2b,k or anti Mac-1 (p=0,914). Furthermore blocking of Mac-1 did not have any effect in the crawling velocity of neutrophils in comparison to injection of IgG2b,k (0,717). **B.** Comparison of crawling distance before and after injection of IgG2b,k isotype control and anti Mac-1blocking antibody. As in the case of crawling velocity no difference was detected in the baseline before injection of IgG2b,k or anti Mac-1 (p=0,984). Again in that case blocking of Mac-1 did not have any effect in the crawling distance of neutrophils in comparison to injection of IgG2b,k (0,610).

Finally, we have analysed the crawling linearity to test whether Mac-1 influenced the ability of neutrophils to follow linear crawling paths in the arteries. As in the previous case we could not detect differences between the control group and the experiments where Mac-1 integrin was blocked. In the baseline the linearity was equal to 0,73 in the experiemnts were IgG2b,k was later injected while in the experiments where anti Mac-1 was injected it was equal to 0,74 (p=0,887). After IgG2b,k injection the mean crawling linearity was equal to 0,86 while upon anti Mac-1 antibody injection equal to 0,72 . No important statistical difference was detected between these two groups (p= 0,789, figure 76)

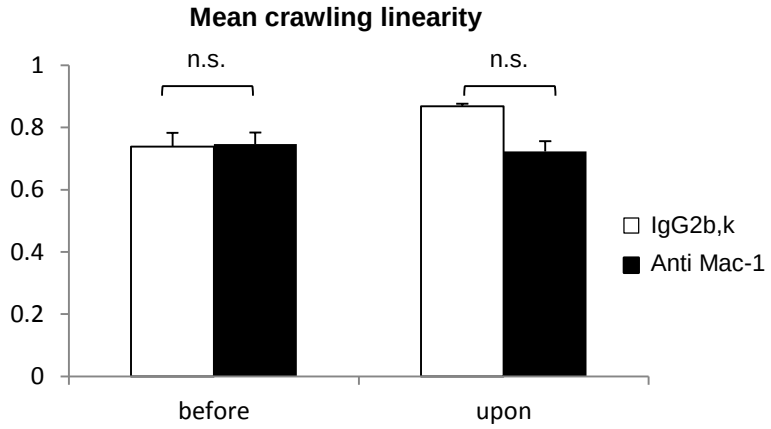

Figure 76. Comparison of crawling linearity before and after injection of IgG2b,k isotype control and anti Mac-1 blocking antibody (n=5 mice per group). No difference was detected in the baseline before injection of IgG2b,k or anti Mac-1 (p=0,887). As in the cases of velocity and distance blocking of Mac-1 did not have any effect in the crawling linearity of neutrophils in comparison the control group (p=0,789).

Our results demonstrate for the first time that neutrophil crawling takes place apart from acute inflammatory conditions in post-capillary venules, also in the case of large arteries in the presence of atherosclerotic plaques. In contrast to the micro-vasculature, where a significant majority of cells crawl upstream/perpendicularly to the blood flow during sterile inflammation, in the case of atherosclerosis in carotid arteries the percentages of cells crawling upstream/perpendicular to the blood flow are similar to the percentages of cells crawling downstream to the blood flow. Furthermore we show that in the presence of established atherosclerotic plaques Mac-1 is dispensable for neutrophils crawling on the endothelium since it does not

influence any of the crawling parameters (direction, velocity, distance, linearity) of the crawling neutrophils.

8. Discussion

8.1 Experimental animals

This study was based on experiments performed in mice. Characteristics such as rapid breeding, availability of genetically modified mice, low costs for animal care, wide range of labelling or blocking antibodies and extended immunological characterization are considered to be decisively important advantages for the use of these animals. Additionally, a plethora of already described surgical mouse models in the literature allows us to perform standardized intravital experiments. Furthermore, the ease in handling of mice gives us the possibility to establish new models for further intravital experiments in organs that so far could not be analysed in other animal species *in vivo*. In the same context the small size of the mice is an extra advantage especially in the case of the use of TPLSM since penetration depth of this technique (though greater than that of other intravital techniques) is still limited. In our study we have used the following mouse lines: C57BL/6J, LysM^{eGFP}, CX3CR1$^{GFP/+}$, ApoE$^{-/-}$, ApoE $^{-/-}$ LysM^{eGFP}, ApoE$^{-/-}$ CX3CR1$^{GFP/+}$, and ApoE$^{-/-}$ MHCII^{eGFP}.

The C57Bl/6J mice are the most commonly used inbred strain and they do not express any kind of fluorescence in their tissues or cellular compartment. However, the advance in labelling antibodies technology permits us to in vivo stain different types of leukocytes. Thus, we can perform intravital microscopy in these mice using microscopic setups that are based in emission of fluorescence, such as TPLSM. The C57Bl/6J strain was used in our experiments in order to investigate the effect of blocking of Mac-1 integrin in crawling of neutrophils stained by the Ly6G 1A8 antibody under inflammatory conditions.

Furthermore, depending on the needs of our experiments we have used the transgenic LysM^{eGFP} mice, which express green fluorescent protein on mainly on their neutrophils[131]. These mice were previously used in experiments in the microvasculature and carotid arteries in order to better visualize these kind of cells[93,135].

The CX3CR1^{eGFP} line expresses green fluorescent protein in the cells that express the CX3CR1 receptor, which are mainly monocytes (both classical and non classical), and in a small proportion of dendritic cells[130]. Therefore, they are ideal for *in vivo* imaging of monocytes in both cases of microvasculature or large arteries either during steady state or inflammation. A further advantage of this strain is that the non inflammatory monocytes express GFP in low levels while the inflammatory subsets in high. Therefore, theoretically, it is possible to distinguish these two subpopulations of monocytes although the differentiation depending only on fluorescence intensity can be demanding.

The ApoE$^{-/-}$ line consists of hypercholesterolemic mice that develop gradually atherosclerotic plaques in several parts of their arterial tree. This process is enhanced by feeding of these mice with a diet rich in cholesterol. The ApoE$^{-/-}$ mice have been widely used in the research regarding atherosclerosis since the plaques that they develop resemble the ones in humans as it concerns their different phases of development and location[128]. As it was previously described an inflammatory reaction could be detected *in vivo* in atherosclerosis prone regions such as carotid bifurcation and external carotid artery in ApoE$^{-/-}$ mice, already after 4 weeks of feeding with high cholesterol diet[29] .This was expressed as leukocytes adhesion on the endothelium and resembled a very early cellular recruitment in the process of atherogenesis. In this time point however, there was no established plaque formation detected. To investigate the recruitment of neutrophils in already established atherosclerotic plaques we have performed experiments in the carotid arteries of ApoE$^{-/-}$ mice at the age of 18-20 weeks upon feeding with high cholesterol diet for longer periods of time (14-16 weeks) during which an atherosclerotic lesion could develop[128].

8.2 Two-photon microscopy: general advantages and disadvantages

Two photon microscopy has some great advantages in comparison with other types of fluorescence microscopy such as conventional fluorescence microscopy and confocal microscopy. These regard reduced phototoxicity and bleaching, great imaging depth and enhanced signal to noise ratio[148]. In addition, 3D scan time lapse

recordings are possible, allowing for analysis in 4 dimensions (XYZ spatial axis and T temporal axis)[148]. These characteristics render this technique the most adequate tool for *in vivo* analysis of dynamic cellular processes in living tissue. However, the process of imaging acquisition is relatively slow since it is based in a point per point scanning process on the tissue. Therefore, fast processes such as rolling cannot be analysed using TPLSM. In addition in the case of non stable organs (such as pulsating carotid arteries) the slow process of scanning results in imaging distortion and continuous loss of focus[118].

8.3 Imaging models

8.3.1 Mouse ear model

In order to perform experiments regarding leukocytes crawling in the microvasculature in steady state or in acute inflammation, imaging of intact stable vessels is required. Commonly used models for in vivo imaging of post-capillary venules or arterioles are the mouse cremaster muscle and mesenteric model[4,63,151].
The mouse cremaster muscle and mesentry have several characteristics that were proved to be of high importance for in vivo imaging.
Some of these are the almost two dimensional vessel structure, the typical pattern of expression of cell adhesion molecules and the high vessel density. However, the relatively high level of leukocytes rolling upon surgical preparation implies that these are mildly inflammatory models[151]. The mouse ear model shares the same advantages with the cremaster muscle and the mesentery model (such as two dimensional vessel structure, normal expression of adhesion molecules and high vessel density). However, it is based in a less invasive preparation rendering it a non-inflammatory model ideal for analysis of leukocytes behaviour during inflammatory reactions but also during steady state.

8.3.2 Carotid artery model

The *in vivo* imaging of large arteries and even more the application of two photon microscopy gained a lot of attention over the last years[93,114,118,142]. *In vivo* imaging of

large arteries was expected to give answers in questions regarding the dynamic behaviour of leukocytes during their recruitment in areas of atherosclerotic plaque formation[92,113,117,141]. These included a deeper insight in the mechanistic processes that regulate the migration cascade of leukocytes in atherosclerosis. So far only initial steps (rolling and adhesion) were analysed by the use of conventional intravital techniques[114,117]. Although this approach was very successful in the analysis of this kind of processes it did not succeed in providing us further information regarding the important steps of crawling and transmigration in atherosclerotic lesions.

Interestingly leukocytes are found both in the internal (intimal) and external (adventitial) side of the atherosclerotic plaque[13]. The available *in vivo* information regarding leukocytes luminal or adventitial (through micro-vessels that develop in that area which are named vasa vasorum) recruitment is mainly based in detection of firm cellular adhesion and not in direct analysis of cells transmigration[117]. Even more the presence and motility of leukocytes within established plaques could so far be analysed only by means of ex vivo imaging[152]. These difficulties are attributed to limitations of the microscopy techniques themselves (limited resolution, limited imaging penetration depth) but also to limitations of the available surgical models for preparation of the large arteries which did not focus initially in stability of the vessels. The technical limitations of the conventional intravital microscopy could be circumvented by the use of two photon laser scanning microscopy. As already discussed (8.2) this advanced technology allows for in vivo imaging in relatively high depth without destruction of the tissue due to phototoxicity. The first studies of large arteries by TPLSM revealed the great advantages of this technique since they provided with information regarding the structure of the vessel wall (blue signal was always obtained from the adventitial part of the artery while green from the medial and intimal area without the need to stain these structures). However, the significant loss of focus attributed to the pulsation due to the heart cycle but also to the normal respiratory movement of the mice, limited the *in vivo* application of TPLSM for imaging of large vessels. Previous studies based on surgical models provided long-term stability however, they failed to preserve normal flow conditions[124]. Further approaches relied on triggered imaging by electrocardiographic and ventilation devices. This approach greatly succeeded in increasing imaging quality and in preventing for short time periods the loss of focus. However, long term analysis still

suffered from image distortion and loss of focus while three dimensional imaging was thought to aggravate this condition. Therefore, one of our initial goals was to establish a novel model which would allow us to overcome all these problems and perform stable long-term imaging with the use of two photon laser scanning microscopy.

8.4 Discussion of the results

8.5 Establishment of novel model for in vivo imaging of large arteries

Our initial attempts to visualize carotid arteries of C57Bl/6J mice by the use of two photon microscopy without the aid of any special surgical preparation or of triggered imaging encountered a prominent instability and loss of focus during our experiments. Although the basic structures of the arterial wall could be still visualized, the distortion in the image due to in frame (due to pulsation) and out of frame (due to respiration) loss of focus did not permit us for further investigation and analysis of any kind of cellular processes. To overcome these limitations we have applied the already established method of triggered imaging acquisition according to the heart cycle of the mouse[118]. As it was described in the literature, the triggered imaging of vessels according to their cardiac and respiratory cycle with the use of two photon microscopy, significantly increases the quality of imaging and decreases the loss of focus due to pulsation and respiratory movements[93,118]. In our experiments we have connected the anaesthetized intubated mice to an ECG device that analysed the electrical activity of the heart throughout the experiment. Through this device our microscope was triggered to acquire images always in the same phase of the heart cycle (during cardiac systole). This approach significantly reduced the image distortion and loss of focus. The ventilation of the mice led to smooth and regulated respiratory cycles and thus the loss of focus was further reduced. Compared with our initial attempts which were performed without the use of ventilation or ECG triggering, the combination of these two manipulations succeeded in the performance of stable *in vivo* imaging for a relatively longer period of time (approximately 5 minutes) during which we could obtain images of significantly higher quality. However since the artery was still free to move in space, a time dependent loss of focus occurred, which was

mainly expressed by a shift in the XY axis. Therefore, we were still not able to perform analysis of processes such as crawling or transmigration which demand stable imaging (in order to follow single cells) for longer time periods. In the studies available in the literature regarding the application of this technique, the imaging stability was tested only for short period of times (approximately 2 minutes)[118]. In the case of long-term recordings, imaging distortion and loss of focus was still present. Thus, analysis was performed only to the XY sections that were imaged in a comparable Z position and furthermore that were free of motional artifacts[93]. However, this selective use only of the better presented frames allows for descriptive analysis of cellular processes but cannot be applied in order to obtain quantitative information (such as crawling velocity, distance etc). In addition, in these studies analysis was performed in sequential time points only in the XY axis (normal time lapses) but not in 3D time lapse recordings (XYZ spatial axis and T temporal axis). Therefore, following this approach, the 3D reconstruction of the tissue over time, which is one of the most significant advantages of the two photon microscopy, could not have any application.

In order to make a step forward in the case of intravital TPLSM in carotid arteries we have established a new surgical model for stabilization of large vessels. The basic principle of this model was to construct a stable microenvironment for the vessel in order to minimise the movement artifacts in the XY and Z axis. This was achieved first by isolating the carotid arteries from the surrounding tissue by gently placing a fine plastic sheet underneath the vessel. In addition, the application of a custom build stage on the top of the vessels resulted in a reduced capacity of the arteries to move in space reducing their motion mainly in the Z but also in the XY axis. This surgical intervention in comparison with the application of ventilation and ECG triggered imaging enabled us to image the arteries in great resolution in the same area of the XY axis for significantly longer periods of time (approximately for 15 minutes). Furthermore, we succeeded in performing stable 4 dimensional (XYZ spatial axis, T temporal axis) analysis of the vessel and thus, in imaging at the same time all the layers of the arterial wall (media, intima, adventitia).

Our analysis regarding the blood flow conditions upon the application of our stage revealed linear flow in the common carotid arteries while distal to the carotid

bifurcation especially in the area of the external carotid artery the flow was mainly oscillatory during diastole. Although it cannot be excluded that this differentiation in the flow pattern in the external carotid artery is dependent on our preparation, our findings are consistent with observations in humans suggesting disturbed flow patterns in that area, directly connected to pro-atherosclerotic conditions[138,139].

We next questioned whether our surgical preparation itself can induce a relevant inflammatory reaction. Taking into consideration that neutrophils or inflammatory monocytes were not so far observed adhering on unstimulated endothelial cells we assumed that a vast accumulation of this kind of myeloid cells would imply a preparation dependent inflammatory reaction downstream to tissue injury. To address this question we have performed control experiments in the carotid arteries of C57Bl/6J, LysM^{eGFP} and CX3CR1$^{GFP/+}$ mice. The general outcome from these experiments was that the majority of the cells that interacted with the endothelium in the area of the carotid bifurcation, under steady state conditions, were patrolling monocytes. The differentiation between the different subset of monocytes and neutrophils was based on injection of fluorescent anti GR1 antibody which binds only to non inflammatory (patrolling monocytes) and to neutrophils but not to inflammatory monocytes. In addition we observed that the interactions of neutrophils with the endothelium typically took place in the area distal to the carotid bifurcation (external/ internal carotid artery) and not in the common carotid artery. This observation could be indicative of a mild inflammatory reaction intravascularly that could also be attributed to endothelial cell activation due to the oscillatory flow conditions in that area. Additionally the fact that the majority of the cells detected interacting with the endothelium are non inflammatory monocytes suggests that the vessel reserves the characteristics of steady state upon preparation.

8.5.1 Applications of novel stabilising model for TPLSM in large arteries

8.5.1.1 Detection of crawling and transmigration

We next questioned whether it could be possible to use our model in order to detect for the first time slow dynamic behaviour of leukocytes, such as crawling and

transmigration, in large arteries either in steady state conditions or in the inflammatory atherosclerotic environment. Regarding the steady state conditions, we have performed experiments in CX3CR1$^{GFP/+}$ mice while in the case of atherosclerosis in ApoE$^{-/-}$ mice and ApoE$^{-/-}$LysM^{eGFP} bone marrow chimeras. In the first case our experiments revealed the ability of patrolling monocytes to adhere and crawl under steady state conditions also in large arteries apart from their already described ability for crawling in venules and arterioles of the mouse skin, mesenterium and kidneys[32,44]. What is the role and biological relevance of this crawling procedure in steady state and whether this is connected with atherogenesis needs to be further investigated.

Apart from the case of monocytes in steady state also neutrophils were detected for the first time crawling in the presence of an atherosclerotic plaque in both ApoE$^{-/-}$ mice (were neutrophils were stained by injection of Ly6G 1A8 antibody) and ApoE$^{-/-}$ LysM^{eGFP} chimeras. The atherosclerotic lesions generally appeared either as auto-fluorescent areas or as black regions in higher imaging depths. Therefore, they could be differentiated from the luminal space either due to auto-fluorescence of this area or by injection of TRITC/FITC dextrans. In the last case the fluorescent signal from the dextrans intraluminally was disrupted in the areas where the plaque was present.

In the case of leukocyte migration into atherosclerotic lesions, we could occasionally detect neutrophil transmigration from the lumen in the plaque mainly in the area of the plaque shoulders. This is in agreement with previous *ex vivo* evidence of neutrophil intraplaque presence mainly in the shoulder of atherosclerotic lesions in mice[95]. Furthermore, earlier *in vivo* studies based on ECG and respiratory triggered TPLSM suggest luminal, rather than adventitial, recruitment of neutrophils in the lesions[93]. It has to be noted however that the mentioned results from *in vivo* experiments regarded carotid arteries of ApoE$^{-/-}$ mice fed with cholesterol diet only for 4 weeks. Therefore, the observed process of neutrophil luminal recruitment corresponds only in very early stages of atherogenesis and therefore our observations are the first *in vivo* evidence of neutrophil recruitment also in established atherosclerotic plaques. Whether crawling was a prerequisite for the transmigration of neutrophils in the arterial wall or not, could not be fully analysed

exactly because transmigration did not occur in a massive way. In addition in the cases where migration was detected, the neutrophils were already visualized in a process of transmigration without being clear whether they have previously crawled or not.

Interestingly, in experiments performed in Apoe$^{-/-}$LysM^{eGFP} chimeras we could also detect accumulation of neutrophils in the adventitial side of the wall in the vicinity of micro-vessels (vasa vasorum) present in the area. As in the case of luminal transmigration we could occasionally detect also adventitial transmigration in the inflamed wall. Previous studies, performed by means of conventional intravital microscopy, reported firm adhesion in the vasa vasorum in established mouse atherosclerotic plaques however there was no direct proof of per se adventitial migration in the lesion due to limitations of the applied techniques[117]. Our data for the first time provide direct *in vivo* indications of the ability of neutrophils for both luminal and adventitial transmigration in established atherosclerotic lesions. These results render our model an ideal tool for future *in vivo* analysis of the final steps of leukocyte migration also in the case of atherosclerosis using TPLSM.

8.5.1.2 Leukocytes presence and motility within plaques

Injection of Ly6G 1A8 antibody allows for in vivo imaging of the dynamic intraluminal behaviour of neutrophils in the presence of atherosclerotic plaque. However, the labelling ability of the antibody was limited only in the cells that were present intravascularly and not intraplaque. Therefore, it could not be used for *in vivo* analysis of the presence of neutrophils within lesions.

To investigate whether neutrophils but also other subsets of leukocytes could be detected within atherosclerotic lesions *in vivo*, we have performed experiments in ApoE$^{-/-}$LysM^{eGFP} and ApoE$^{-/-}$CX3CR1$^{GFP/+}$ bone marrow chimeras. As it is described in the literature however, irradiation of ApoE$^{-/-}$ mice results in reduced atherosclerotic plaque formation. This is attributed to the fact that ApoE is produced in the liver but also from other kind of cells such as macrophages. Therefore, in the case of bone marrow transplantation in ApoE$^{-/-}$ recipients from donors that are not of ApoE$^{-/-}$ origin apolipoprotein E can still be produced by macrophages resulting in clearance of

lipoproteins and therefore, in reduced atherosclerotic plaque formation[133]. To overcome this inconvenience we have performed the irradiation and bone marrow transplantation in ApoE$^{-/-}$ mice at the age of 16 weeks when atherosclerotic lesions are expected to be already present in an ongoing process of chronic inflammation[128]. Taking into consideration that monocytes and even more neutrophils are short lived cells[153] detection of this kind of cells within the plaque would imply recent recruitment. Furthermore, in order to circumvent the reduction in plaque formation and to visualize antigen presenting cells within the plaques we have crossed MHCII^{eGFP} with ApoE$^{-/-}$ mice. The exact origin of antigen presenting cells within the atherosclerotic plaques is not fully investigated. Although monocytes are believed to transform in dendritic cells and macrophages in atherosclerotic lesions, further studies suggest that these kind of cells are able for self-renewal in atherosclerosis suggesting also alternative origins[42]. Therefore, by performing bone marrow transplantation using as donors MHCII^{eGFP} mice in recipients with already established atherosclerotic plaques, we would probably be able to visualise only a small fraction of recently recruited antigen presenting cells (or of their progenitors).

The experiments performed in all of these mouse models confirmed that *in vivo* imaging of leukocytes within lesions is possible, however the imaging depth is limited in the area adjacent to adventitia. Thus, we cannot image leukocytes in the intimal area of established atherosclerotic plaques. From the leukocyte subsets analysed, neutrophils in ApoE$^{-/-}$LysM^{eGFP} bone marrow chimeras were highly motile. Although in the literature is described that they are mainly involved in initial steps of atherogenesis and in cases of instable (rupture prone) plaques[93,154], our studies reveal presence and an active behaviour of these cells also in the case of established stable lesions.

In summary our experiments provide for the first time a direct proof that TPLSM can be used for *in vivo* imaging of atherosclerotic plaques and for analysis of the presence and kinetics of different subsets of leukocytes within the lesions. In this context monocytes, antigen presenting cells and neutrophils were detected within established atherosclerotic plaques *in vivo*.

8.6 Crawling analysis

In the next part of our project we focused in analysis of leukocyte crawling during state state and inflammation and aimed in investigating the basic mechanisms that regulate this process in small vessels and carotid arteries.

8.6.1 Steady state

8.6.1.1 Crawling of monocytes in microvasculature and carotid arteries

To investigate which kind of leukocytes are able to crawl in the microvasculature of the mouse ear we have performed experiments in LysM^{eGFP} and CX3CR1$^{GFP/+}$ mice. Our studies showed that in the case of GFP+ neutrophils LysM^{eGFP} mice only very rare and transient interactions with the endothelial cells could be detected. These interactions were downstream to the blood flow resembling a rolling like fashion movement.Thus, we did not take into consideration this process as real crawling and neutrophils were not further analysed in steady state.

In contrast, GFP positive monocytes were as expected detected crawling in the microvasculature of CX3CR1$^{GFP/+}$ mice for long distances. This fraction of monocytes resembles the already described non classical patrolling monocytes which were observed crawling in venules and arterioles of mice in the absence of inflammatory stimuli[14]. Although these cells were analysed in the case of small vessels there is no study available regarding their presence and motility in unstimulated large arteries. Our *in vivo* experiments in carotid arteries of CX3CR1$^{GFP/+}$ mice showed that GFP positive monocytes could be observed crawling also in big arteries. Our main region of interest in that case was the carotid bifurcation which is an area prone to atherosclerosis. To test whether these cells are patrolling monocytes and not inflammatory, we have injected to the mice during our experiments the PE labelled GR1 antibody. In that way we confirmed that the majority of the cells imaged express CX3CR1 in high levels but do not express GR1, presenting phenotypic characteristics that refer to the non-inflammatory, patrolling subset of monocytes[14]. In addition our analysis showed that the crawling velocity and distance of these cells were comparable in both microvasculature and large arteries. Earlier studies in small

vessels report that patrolling monocytes are able for crawling not only downstream to the blood flow but also perpendicular and upstream following several paths (upstream, hairpin etc)[14]. However, this observation did not gain further attention so far. Our experiments showed that in both cases of microvasculature and carotid arteries the proportion of cells crawling downstream to the blood flow was similar with the proportion of cells crawling against the blood flow in an upstream/perpendicular fashion.

In total, our results reveal for the first time the potential of patrolling monocytes for crawling apart from the microvasculature also in large arteries. Furthermore they indicate that these cells apart from same phenotypic characteristics share also the same dynamic characteristics (regarding crawling direction, velocity and distance) in these different parts of the arterial tree.

8.6.1.2 Role of LFA-1 in monocytes crawling

The molecules that were analysed so far in previous studies regarding crawling of patrolling monocytes under steady state conditions were the beta 2 integrins LFA-1 and Mac-1[14]. Although the direct effect of blocking of these molecules was not analysed, it was shown that upon injection of anti LFA-1 antibody the population of crawling monocytes was reduced while injection of anti Mac-1 antibody had no effect in the number of crawling cells as well as in their crawling distance and velocity. Therefore, it was assumed that LFA-1 is the regulator of monocyte crawling under steady state while Mac-1 was thought to be dispensable. In our settings we were initially interested to analyse the direct effect of blocking of these beta-2 integrins in the crawling process of monocytes in the microvasculature and compare it with its long term effect. For that reason we applied an alternative model of analysis during which we focused in single cells that were tracked crawling during the injection of the blocking antibody (CSCTP analysis). Since LFA-1 is believed to regulate the crawling of patrolling monocytes, our initial experiments were performed in the context of blocking of this molecule. In that case a high percentage of monocytes analysed by CSCTP directly detached and only a few changed their crawling direction. These results show that although LFA-1 is considered to mediate monocytes crawling during steady state, injection of blocking antibodies against this integrin impairs

mainly adhesion. Furthermore, these data indicate that it is difficult to analyse *in vivo* the role of LFA-1 in the crawling behaviour of monocytes exactly due to its crucial role in adhesion. For that reason we have further focused in the analysis of the effect of blocking only of Mac-1 and not of LFA-1 in monocyte crawling in both the cases of small vessels and large arteries.

8.6.1.3 Role of Mac-1 in monocytes crawling

8.6.1.3.1 Microvasculature

We next hypothesized that Mac-1 might also be involved in the process of crawling of patrolling monocytes. To test our hypothesis we initially focused in analysing the direct effect of blocking of this integrin in the crawling process by applying the CSCTP for our analysis. Our experiments showed that blocking of Mac-1 resulted in a direct change in the crawling direction of a relatively high percentage of crawling cells while only a few detached. The effect in the crawling direction was more prominent in the upstream crawling population of cells. The majority of this subset directly turned crawling direction and followed a downstream to the blood flow path. Injection of IgG control isotype or of anti Mac-1 antibody and anti LFA-1 did not influence the crawling velocity of the patrolling monocytes.

In the next step we questioned whether the effect of blocking of Mac-1 in the crawling direction was only transient or it had a long lasting character. In order to address this question we have injected IgG control isotype or anti Mac-1 blocking antibody in two different groups of CX3CR1$^{GFP/+}$ mice and analysed the crawling behaviour of monocytes in different vessels in later time points without performing CSCTP. The detection of patrolling monocytes in the skin of the mouse ear was a demanding and long lasting procedure since in our experiments single cells crawled along the endothelium of a small number of vessels under steady state. To increase the number of cells analysed per experiment we increased the duration of our imaging up to 2 hours post injection in order to image a bigger number of vessels.

In our control group we could observe an equal proportion of cells crawling upstream or downstream to the blood flow. In contrast in the case of blocking of Mac-1 the majority of monocytes crawled downstream to the blood flow indicating reduced ability of these cells for upstream crawling. However, we did not observe any further

differentiation in the crawling characteristics of the patrolling monocytes (as these were analysed by crawling velocity, distance and linearity) in these groups of experiments. These findings are in agreement with the observations from other groups which suggest that blocking of Mac-1 integrin does not influence the crawling velocity and distance of patrolling monocytes[14]. In summary our studies showed that in contrast to what was so far believed, Mac-1 is actively involved in the process of crawling of patrolling monocytes by mediating their upstream crawling. The reason why previous studies did not detect the importance of Mac-1 in the role of crawling of monocytes could be that only factors such as crawling velocity, distance and number of crawling cells were analysed while per se the crawling direction did not gain much attention. The application of the CSCTP played a major role in the observation of the effect of blocking of Mac-1 in monocyte upstream crawling in steady state. However, a significant drawback in our approach is that this protocol can be applied for analysis only of one time point during which the blocking antibody is applied. Therefore, only one vessel can be analysed per mouse. This would further mean that especially in the case of patrolling monocytes a very small number of cells can be analysed per experiment.

8.6.1.3.2 Carotid arteries

In the case of the experiments performed in carotid arteries we observed that injection of blocking antibodies or of IgG isotype control led to unexpected instability of our imaging and loss of focus. Therefore, we were not able to apply the CSCTP. To analyse the effect of blocking of Mac-1 in the crawling process of patrolling monocytes we have performed two photon microscopy in carotid arteries of $CX3CR1^{GFP/+}$ mice shortly upon injection of anti Mac-1 antibody (when the mice were hemodynamically stable again). Following the same approach we performed experiments in a control group of $CX3CR1^{GFP/+}$ mice upon application of IgG isotype control. For our recordings we focused in the region of the carotid bifurcation and imaged for one hour. During this period of time we could often observe monocytes adhering and crawling in that area. Our experiments revealed that, as in the case of small vessels, blocking of Mac-1 resulted in a significant increase in the percentage of the downstream crawling monocytes suggesting that this beta 2 integrin regulates

the upstream crawling of these cells also in large arteries under steady state. Interestingly blocking of Mac-1 in carotid arteries led to a significant increase in the crawling velocity and linearity of monocytes although there was no effect in the same crawling characteristics in the microvasculature.

These findings suggest that monocytes are depending on Mac-1 for an active crawling on the endothelium of large arteries which allows them to move against the forces of the blood flow. When this molecule is blocked they are following the blood flow in a faster, more linear and passive way. This passive process seems to be more prominent under the high shear stresses of the large arteries than these of the small vessels. The fact that patrolling monocytes are still able to adhere and crawl under steady state conditions in both the microvasculature and the large vessels shows that Mac-1 is not the only molecule involved in this process of crawling and further investigation is needed in this direction.

8.6.2 Inflammation

8.6.2.1 Induction of sterile inflammation in microvasculature

A condition that gained a lot of attention the last years is sterile inflammation which is connected with conditions such as trauma and ischemia reperfusion injury as well as atherosclerosis[75]. Leukocytes are thought to follow the general steps of the migration cascade also in the case of sterile inflammation.

To create an environment of acute sterile inflammation in our experiments we have induced interstitial necrosis (through laser ablation) in the mouse ear in areas in the vicinity of post-capillary venules following an approach that has already been described in the literature[134]. In that way we could investigate the intravascular reaction of neutrophils to a plethora of signals released from the necrotic cells including danger associated molecular patterns (DAMPS). Furthermore, this would provide us with a more relevant model with atherosclerosis in large arteries which is characterized by intraplaque cellular necrosis and thus release of DAMPS. In that way a comparison of the mechanisms that regulate neutrophil crawling on the activated endothelium in small and large vessels could be possible. It has to be mentioned however, that post-capillary venules are significantly different as it matters

their structure and physiology from arteries. Thus, although the signals that lead to neutrophil recruitment could be the same in the case of acute sterile inflammation in venules and atherosclerosis in large arteries, the mechanisms that regulate cellular crawling and migration may be different.

In our experiments we used the laser of our microscope to induce interstitial necrosis in the vicinity of a venule in the mouse ear of C57Bl/6J mice and subsequently started imaging. Upon induction of interstitial injury we observed a significant increase in the number of crawling neutrophils (stained in vivo by Ly6G1 A8 antibody) as well as in the number of extravasated cells in comparison with the steady state. These results confirmed the inflammatory status of the venule in question and are in agreement with previous studies that describe leukocyte recruitment upon laser induced injury in the skin of the mouse ear[134]. In addition, we could observe that only a small percentage of cells crawled downstream to the blood flow as it was already reported in the literature in cases of acute inflammation in the microvasculature[63]. The higher percentage of upstream or perpendicular crawling cells was preserved during the whole duration of our experiment (1 hour). As it was already described in earlier studies the perpendicular crawling facilitates leukocytes to reach endothelial cell junctions which are thought to be favourable areas for transmigration. Additionally downstream crawling results in reduced transmigration[63]. In our experiments we could observe, in agreement with these results, that the majority of the cells that finally transmigrate are the cells that crawl upstream or perpendicularly to the blood flow and not downstream. These results indicate that the active process of perpendicular/ upstream crawling facilitates leukocyte migration.

8.6.2.2 Effect of blocking of Mac-1 integrin in the crawling of neutrophils during acute sterile inflammation

8.6.2.2.1 Direct effect

In a next step we questioned how blocking of Mac-1 integrin influenced the crawling behaviour of neutrophils under conditions of acute sterile inflammation in the skin of the mouse ear. To address this question we have performed experiments in C57Bl/6J

mice and have labelled neutrophils with injection of the Ly6G 1A8 antibody. By applying the CSCTP we could track cells continuously before and after injection of blocking antibodies against Mac-1 and therefore the direct effect in the crawling behaviour of neutrophils could be analysed. In our experiments only a small percentage of neutrophils changed direction or detached directly upon injection of the anti Mac-1 blocking antibody. In addition we did not detect any direct effect in the crawling distance and velocity of these cells. To better characterise the direct effect of injection of anti Mac-1 antibody, we have further analysed the forward migration index of the crawling cells in the X (xFMI) and Y (yFMI) axis. The forward migration index is an indicator of the efficiency of cells to crawl towards a direction and it has mainly been used in *in vitro* studies regarding leukocyte chemotaxis[155]. In our case a positive xFMI indicates upstream to the blood flow crawling while a negative value indicates downstream to the flow crawling. As it matters yFMI, a positive value indicates intravascular crawling towards the injury while a negative value against it. As it was shown in other studies intravascular chemotactic gradients induce intraluminal directional crawling of neutrophils towards the source of the chemotactic stimuli[50]. Therefore, we considered yFMI as an indication of the ability of cells to sense chemotactic gradients within the vessel and crawl towards their source which in our case was the area of the laser ablation. In note that the mathematical calculation of the FMI is not directly dependent on the absolute count of cells crawling towards a direction but represents only the efficiency of the cells to crawl towards this direction. Our analysis showed that blocking of Mac-1 did not have any significant direct effect either in the xFMI or yFMI of the cells analysed by CSCTP. This would indicate that blocking of Mac-1 does not impair in a direct way the ability of cells to crawl upstream to the blood flow and to sense intraluminally chemotactic gradients implying that other integrins such as LFA-1 may also regulate this process.

8.6.2.2.2 Analysis in the total population of crawling neutrophils per time period

Apart from the cells analysed by CSCTP we were also interested in the behaviour of the total population of cells in different time points. Therefore, we have taken into consideration for our further analysis the whole population of crawling neutrophils per

time period during our experiments. Following this approach we could observe that in the first time period (0-15 minutes) of recording there was a significantly higher percentage of neutrophils that crawled upstream or perpendicularly to the blood flow in both the cases of IgG isotype or anti Mac-1 injection (injection took place approximately in the seventh minute of recording). Interestingly however, in the next two time periods of recording (15-30 min and 30-45 min) equal percentages of neutrophils crawled upstream/perpendicularly and downstream to the blood flow in the group where Mac-1 was blocked. This implies a non direct effect of anti Mac-1 antibody in the crawling behaviour of neutrophils suggesting a possible role for this integrin in the regulation of upstream crawling. Previous studies performed in VAV1$^{-/-}$ mice showed that the majority of neutrophils in these mice crawled downstream to the blood flow in inflammatory conditions[63]. Blocking of Mac-1 in that case did not influence the crawling behaviour of these downstream crawling cells. However, in other studies performed in C57Bl/6J mice, which contain neutrophils able also for upstream crawling, blocking of Mac-1 significantly impaired the ability of netrophils to crawl. Again in that case this could imply a possible role of Mac-1 mainly for neutrophil upstream crawling.
In our experiments however, the majority of the cells in the group treated with anti Mac-1, regained an upstream/perpendicular crawling direction which was similar to the control experiments in the last time point (45-60 min) of our recordings.

Regarding the general crawling characteristics of neutrophils we observed that in the first time period (0-15 min) and last time period (45-60) of imaging, blocking of Mac-1 did not influence the general crawling velocity, distance and xFMI or yFMI suggesting that Mac-1 is dispensable for the crawling behaviour of neutrophils in the onset of the inflammatory response and in later timepoints.

However, in the second time period of recording (15-30 min) neutrophils were significantly more efficient for downstream crawling (as analysed by xFMI quantification) upon blocking of Mac-1. In addition, in the same time period, the crawling velocity and distance of neutrophils was significantly increased in the mice treated with anti Mac-1 blocking antibody. This would imply that during this period of time the blocking of Mac-1 leads to a more passive downstream crawling behaviour.

However, since neutrophils are still able to crawl other integrins are probably implicated in this process and compensate for the impaired Mac-1 function. In note that also previous studies performed in postcapillary venules indicated that LFA-1 is able to sustain significantly longer crawling distances than Mac-1 upon TNF-A induced inflammation[57]. The crawling direction however, was not analysed in that case.

In our experiments, we observed that the parameters of neutrophil crawling tended to be influenced in the same way that was described for the second time period also in the third period of recording (30-45 min). Interestingly however, this tendency was not expressed as a statistically important difference in comparison with the control group.This means that although in both these time points there is an equal percentage of cells crawling upstream/perpendicularly and downstream to the blood flow the cells gradually regain their efficiency for upstream crawling.

Regarding the ability of neutrophils to follow intravascularly chemotactic signals, our analysis showed that in the case of the control experiments neutrophils were mainly efficient for crawling towards the injury (positive yFMI) in all time periods, probably following intravascular chemotactic signals.

In the case of blocking of Mac-1 we could observe a tendency of neutrophils to crawl against the injury in the second (15-30 minutes) and third time period (30-45 minutes) however this was not expressed as a statistical important difference with the control experiments. This would imply that Mac-1 was redundant for neutrophil directed migration intravascularly in our experiments. In the literature however, it has been described that Mac-1,LFA-1 and a4 integrin play a significant role in the chemotaxis of neutrophils[156] . *In vivo* data from previous experiments performed in the liver in the context of sterile inflammation also suggest an important role for Mac-1 on neutrophils intravascular chemotaxis[60]. However in that case, in contrast to experiments performed in other tissue such as the cremaster muscle, adhesion of neutrophils was only Mac-1 dependent while LFA-1 was dispensable. This could imply that the mechanisms mediating neutrophil recruitment and probably also chemotaxis in the liver could be tissue or stimulus dependent and thus different from the microvasculature of the skin of the mouse ear. Furthemore it has been described in *in vivo* experiments that Mac-1 mediates neutrophil recruitment in response to

HMGB1 while *in vitro* studies showed that Mac-1 mediates chemotaxis in response to stimuli such as fMLP and C5a. However, it has also been described that depending on the stimulus other integrins such as LFA-1 and a4 integrin are also indispensable for neutrophil directed migration in response to molecules such as IL-8 and LTB4 while Mac-1 was redundant in that case[156]. In addition several integrins of the b1 family were also shown to be implicated in the process of neutrophil chemotaxis[157]. This information from the literature in addition to our results could indicate that although Mac-1 is important for neutrophil sensing and following chemotactic gradients it is not the only molecule implicated in this process in the context of sterile inflammation in the skin of the mouse ear.

In summary our results show that blocking of Mac-1 had no direct effect in any of the crawling characteristics of neutrophils analysed by CSCTP. This would imply that other integrins such as LFA-1 could sufficiently sustain the migratory potential in already crawling cells upon blocking of Mac-1. Interestingly however, in the case of neutrophils adhering in later time points (especially during the 15th to 30th minute of recording), the majority of neutrophils follow passively a downstream path with a relatively higher velocity for longer distances in comparison to the cells in our control experiments. These results could imply that Mac-1 plays an important role regarding neutrophil crawling direction under acute sterile inflammation only during the initiation of the crawling procedure, influencing mainly cells that adhered upon injection of anti Mac-1 antibody and not already crawling cells analysed by CSCTP. Interestingly however, the effects of anti Mac-1 antibody in neutrophil crawling were very transient (lasted maximum 30 minutes) and in the last time period of imaging the crawling parameters of neutrophils were similar in both the treated and the control group. This could be explained either by an up regulation of Mac-1 on neutrophils or by a total take over of LFA1 in the crawling process. Which of the two mechanisms is responsible for the phenomena that we observed is still not clear. Finally, in our experiments Mac-1 did not play an important role for the ability of cells to sense chemotactic signals intravascularly since the yFMI was similar in both the control and the treated group. It has to be mentioned however, that we could observe a tendency of neutrophils to be less efficient for intravascular crawling towards the injury

(expressed by negative values in the yFMI) upon blocking of Mac-1 especially during the time period of 30 minutes (15-45 minutes of recording) during which neutrophils were characterized by a higher efficiency of downstream crawling. These results could imply that although Mac-1 is not indispensable for neutrophil directed chemotactic crawling in cases of sterile inflammation however it also participates in this process.

8.6.2.2.3 Effect of blocking of Mac-1 in neutrophils crawling during atherosclerosis in carotid arteries

So far there is no available data in the literature regarding neutrophil crawling in large atherosclerotic arteries. The only direct information that we have regards initial steps of the migration cascade (rolling and adhesion) and the role of selectins in these processes[114,117]. Several studies however reveal a role of both Mac-1 and LFA-1 in the development of atherosclerosis and recruitment of leukocytes within the lesion[158-160].

In addition, studies based on bone marrow transplantation experiments reveal that the plaque size is reduced upon reconstitution with bone marrow from donors that are deficient for Mac-1 and LFA-1integrins[161]. However, which step of the migration cascade is influenced by Mac-1 in the case of atherosclerosis and in what way is not known.

So far all our knowledge regarding the dynamic behaviour of leukocytes during crawling and transmigration relied on experiments performed in post-capillary venules. Therefore, our initial goal was to investigate the crawling characteristics of neutrophils in atherosclerotic carotid arteries and compare them with the case of sterile inflammation in the post-capillary venules of the mouse ear.

In our experiments we could observe that in contrast to the microvasculature there was an almost equal percentage of upstream/perpendicularly and downstream crawling cells in atherosclerotic carotid arteries. Additionally, in the case of atherosclerosis the neutrophils were able to crawl with higher velocities and for longer distances in comparison with the microvasculature. These observations could be attributed to the differences in the shear stress conditions between these different

parts of the arterial tree. The basic aim of this part of the study was to test whether Mac-1 influenced neutrophils crawling in the same way that influenced the behaviour of neutrophils during sterile inflammation in the small vessels. Therefore, our initial intention was to follow the same imaging protocol with the case of small vessels. This included 4 time periods of imaging of 15 minutes each and anti Mac-1 or IgG injection during the first time period. Our first experiments however, showed that injection during imaging led to a loss of focus that was often accompanied by an abnormal electrocardiographical pattern. Although the mice could rapidly recover we were not able to perform CSCTP analysis. In order to overcome this limitation we have performed an initial baseline recording of 15 minutes which was stopped before any kind of injection. Subsequently, we injected IgG isotype control in one group of mice while a second one was treated with anti Mac-1 blocking antibody. The time needed for the mice to recover in order to regain imaging stability was variable. Therefore, in the case of the large vessels we performed analysis of the time points that coincide with the two time periods where we detected the major effects of blocking of Mac-1 in the small vessels. The same parameters such as crawling directionality, distance, velocity and xFMI were analysed also in the case of atherosclerosis as in the microvasculature. Prominent variations in the size and location of the plaques did not allow us to perform comparative analysis of the yFMI. Interestingly, in the case of atherosclerosis we did not detect any differentiation in any of the parameters analysed upon blocking of Mac-1 in comparison with our control experiments. These results indicate that Mac-1 is dispensable for neutrophils adhesion and crawling in established atherosclerotic plaques. However, it cannot be excluded that this integrin plays a significant role in the per se process of migration in the atherosclerotic lesion or that it influences neutrophils crawling in earlier time points in the atherosclerotic plaque formation. Whether the oscillatory conditions present in the areas of plaque formation also influence the role of Mac-1 during crawling and which molecules are responsible for this procedure in that case remains to be elucidated. It should however be noted, that apart from the previously described available data from the literature that connect Mac-1 with atherosclerotic plaque formation there is also a study which suggests that this integrin is redundant for development of atherosclerosis in mice[162].

Summary

The dynamic behaviour of leukocytes during their migration to sites of inflammation was so far analysed only in small vessels under conditions of acute inflammation. A critical step to the leukocyte migration cascade is considered to be crawling. This process is characterised by a slow motion of leukocytes along the activated endothelium. Interestingly it was shown that also under steady state conditions a specific subset of monocytes is able for crawling along the unstimulated endothelium of small vessels for long distances. The molecules that are mainly thought to mediate the process of crawling are the beta-2 integrins LFA-1 and Mac-1. However, the direct effect of blocking of these integrins in leukocytes crawling was not analysed so far either under steady state or inflammatory conditions.

On the other hand large arteries are characterised by instability due to the cardiac and respiratory cycle of the mice. This characteristic did not allow so far for any analysis of the crawling process with any available intravital technique either during steady state or inflammation, which refers to atherosclerosis. TPLSM is generally considered to be ideal for long term intravital microscopy due to its high penetration depth and low phototoxicity. However, the slow process of imaging of this kind of microscopy in combination with the unstable nature of large vessels, raise significant limitations to the performance of stable *in vivo* imaging with this technique. The available approaches for performing intravital two photon microscopy in murine carotid arteries are based either on cessation of the blood flow or on triggered imaging acquisition according to the heart and respiratory cycle. In the first case however, the physiological conditions within the vessel are impaired while in the second stable imaging cannot be achieved for long periods of time.

In this dissertation we provide a novel surgical approach for stabilisation of large arteries which allows us to perform stable long term *in vivo* imaging in these vessels using TPLSM. In addition we propose a new approach for analysis of the direct effect of blocking of beta-2 integrins in leukocyte crawling based on a protocol of continuous single cell tracking (CSCTP) during the application of the blocking antibodies.

Our results show that the application of our surgical model for in vivo imaging of carotid arteries can be successfully applied in order to visualize so far non investigated aspects of leukocyte dynamic behaviour such as crawling and transmigration in large vessels. In that context we could observe processes such us neutrophil crawling, luminal or adventitial transmigration and intraplaque motility in atherosclerosis as well as monocytes crawling during steady state.

Regarding the mechanisms that regulate the crawling of patrolling monocytes in venules and arterioles under steady state we could show that in both the cases of large arteries and microvasculature, Mac-1 regulates the upstream crawling of this kind of cells. In the case of inflammation in the microvasculature we have used a model of induced laser injury in the interstitial area of the mouse skin. This leads to a sterile inflammatory reaction which could be considered to be a relative condition to atherosclerosis. In our experiments we showed that in small vessels the effect of Mac-1 had no direct effect in the crawling process of neutrophils however it led to a transient higher efficiency for downstream crawling for approximately 15-30 minutes after the injection of blocking antibody against Mac-1. Our results indicate that different mechanisms could influence the recruitment of neutrophils in response to sterile inflammatory stimuli in different time points. Thus, analysis of the direct but also long term effect of blocking of beta-2 integrins is essential to fully elucidate their role in the crawling process. In the case of established atherosclerotic plaques however, Mac-1 was dispensable for the crawling of neutrophils.

Abbreviations

nm	Nanometer
3D	3 dimension
4D	4 dimension
ADP	Adenosine diphosphate
APCs	Antigen presenting cells
ApoE	Apolipoprotein E
ATP	Adenosine triphosphate
CAMs	Cell adhesion molecules
CCD	Charged coupled device
CCL	Chemokine (C-C motif) ligand
CCR	C-C chemokine receptor
CD	Cluster of differentiation
cm	Centimeter
COPD	Chronic obstructive pulmonary disease
CXCL	Chemokine (C-X-C motif) ligand
CXCR	CXC chemokine receptor
DAMPs	Danger associated molecular patterns
ECG	electrocardiographic
ESL-1	E-selectin ligand 1
FITC	Fluorescein isothiocyanate
FMIx	Crawling distance along the X axis
FMIy	Crawling distance along the Y axis
fMLP	[Formyl-Methionyl-Leucyl-Phenylalanine
FPR	*formyl peptide receptors*
GAGs	Glycosaminoglycans
G-CSF	Granulocyte colony-stimulating factor
GFP	Green fluorescent protein
GMP	Granulocyte/monocyte progenitor.
GPCRs	G protein coupled receptors
HMGB1	High mobility group box 1
HPK1	Hematopoietic progenitor kinase 1
ICAM-1	Intercellular Adhesion Molecule 1
IL-1	Interleukin 1
IP	Intraperitoneal
IV	Intravenous
JAM	Junctional adhesion molecule
LDL	Low density lipoprotein
LFA-1	Lymphocyte function-associated antigen 1
Mac-1	Macrophage-1 antigen
mApB1	Mouse Actin-binding Protein 1
M-CSF	Macrophage colony-stimulating factor
MDP	monocyte, macrophage and dendritic cell precursor
MHC II	Major histocompatibility complex
Min	Minutes
MMP9	Matrix metallopeptidase 9
NaCl	Sodium chloride

NFkB	Nuclear Factor kappa B
Nlrp3	NOD-like receptor family, pyrin domain containing 3
P2X	Purinergic receptors
PAF	Platelet activating factor
PCR	Polymerase Chain Reaction
PDGF	Platelet derived growth factor
PE	R-Phycoerythrin
PECAM-1	Platelet endothelial cell adhesion molecule
PMN	polymorphonuclear
PSGL-1	P-selectin glycoprotein ligand -1
RAGE	Receptor for Advanced Glycation Endproducts
ROI	Region of interest
ROS	Reactive oxygen species
TGFβ	transforming growth factor b
TLR	Toll like receptor
TNF-a	Tumor necrosis factor a
TPLSM	Two photon laser scanning microscopy
TRITC	Tetramethylrhodamine
VAV1	vav 1 guanine nucleotide exchange factor
VCAM 1	Vascular cell adhesion molecule 1
VEGF	Vascular Endothelial Growth Factor
VLA-4	Very Late Antigen-4
vLDL	Very low density lipoprotein
VVOs	Vesiculo-vacuolar organelles
xFMI	Forward migration index in the X axis
yFMI	Forward migration index in the Y axis
µl	microliter
µm	micrometer

List of tables

List of figures

References

1. Kolaczkowska, E. & Kubes, P. Neutrophil recruitment and function in health and inflammation. *Nature reviews. Immunology* **13**, 159-175 (2013).
2. Ingersoll, M.A., Platt, A.M., Potteaux, S. & Randolph, G.J. Monocyte trafficking in acute and chronic inflammation. *Trends in immunology* **32**, 470-477 (2011).
3. Ley, K., Laudanna, C., Cybulsky, M.I. & Nourshargh, S. Getting to the site of inflammation: the leukocyte adhesion cascade updated. *Nature reviews. Immunology* **7**, 678-689 (2007).
4. Phillipson, M.*, et al.* Intraluminal crawling of neutrophils to emigration sites: a molecularly distinct process from adhesion in the recruitment cascade. *The Journal of experimental medicine* **203**, 2569-2575 (2006).
5. Bevilacqua, M.P. Endothelial-leukocyte adhesion molecules. *Annual review of immunology* **11**, 767-804 (1993).
6. Ulbrich, H., Eriksson, E.E. & Lindbom, L. Leukocyte and endothelial cell adhesion molecules as targets for therapeutic interventions in inflammatory disease. *Trends in pharmacological sciences* **24**, 640-647 (2003).
7. Panes, J., Perry, M. & Granger, D.N. Leukocyte-endothelial cell adhesion: avenues for therapeutic intervention. *British journal of pharmacology* **126**, 537-550 (1999).
8. Ding, Z.M.*, et al.* Relative contribution of LFA-1 and Mac-1 to neutrophil adhesion and migration. *Journal of immunology* **163**, 5029-5038 (1999).
9. Dunne, J.L., Collins, R.G., Beaudet, A.L., Ballantyne, C.M. & Ley, K. Mac-1, but not LFA-1, uses intercellular adhesion molecule-1 to mediate slow leukocyte rolling in TNF-alpha-induced inflammation. *Journal of immunology* **171**, 6105-6111 (2003).
10. Chesnutt, B.C.*, et al.* Induction of LFA-1-dependent neutrophil rolling on ICAM-1 by engagement of E-selectin. *Microcirculation* **13**, 99-109 (2006).
11. Libby, P. Inflammation in atherosclerosis. *Arteriosclerosis, thrombosis, and vascular biology* **32**, 2045-2051 (2012).
12. Hansson, G.K., Robertson, A.K. & Soderberg-Naucler, C. Inflammation and atherosclerosis. *Annual review of pathology* **1**, 297-329 (2006).
13. Galkina, E. & Ley, K. Immune and inflammatory mechanisms of atherosclerosis (*). *Annual review of immunology* **27**, 165-197 (2009).
14. Auffray, C.*, et al.* Monitoring of blood vessels and tissues by a population of monocytes with patrolling behavior. *Science* **317**, 666-670 (2007).
15. Summers, C.*, et al.* Neutrophil kinetics in health and disease. *Trends in immunology* **31**, 318-324 (2010).
16. Iwasaki, H. & Akashi, K. Myeloid lineage commitment from the hematopoietic stem cell. *Immunity* **26**, 726-740 (2007).
17. Gordon, S. & Taylor, P.R. Monocyte and macrophage heterogeneity. *Nature reviews. Immunology* **5**, 953-964 (2005).
18. Martin, C.*, et al.* Chemokines acting via CXCR2 and CXCR4 control the release of neutrophils from the bone marrow and their return following senescence. *Immunity* **19**, 583-593 (2003).
19. Kantari, C., Pederzoli-Ribeil, M. & Witko-Sarsat, V. The role of neutrophils and monocytes in innate immunity. *Contributions to microbiology* **15**, 118-146 (2008).
20. Borregaard, N. & Cowland, J.B. Granules of the human neutrophilic polymorphonuclear leukocyte. *Blood* **89**, 3503-3521 (1997).

21. Wantha, S., *et al.* Neutrophil-derived cathelicidin promotes adhesion of classical monocytes. *Circulation research* **112**, 792-801 (2013).
22. Brinkmann, V., *et al.* Neutrophil extracellular traps kill bacteria. *Science* **303**, 1532-1535 (2004).
23. Phillipson, M. & Kubes, P. The neutrophil in vascular inflammation. *Nature medicine* **17**, 1381-1390 (2011).
24. Segel, G.B., Halterman, M.W. & Lichtman, M.A. The paradox of the neutrophil's role in tissue injury. *Journal of leukocyte biology* **89**, 359-372 (2011).
25. Smith, J.A. Neutrophils, host defense, and inflammation: a double-edged sword. *Journal of leukocyte biology* **56**, 672-686 (1994).
26. Jordan, J.E., Zhao, Z.Q. & Vinten-Johansen, J. The role of neutrophils in myocardial ischemia-reperfusion injury. *Cardiovascular research* **43**, 860-878 (1999).
27. Edwards, S.W. & Hallett, M.B. Seeing the wood for the trees: the forgotten role of neutrophils in rheumatoid arthritis. *Immunology today* **18**, 320-324 (1997).
28. Quint, J.K. & Wedzicha, J.A. The neutrophil in chronic obstructive pulmonary disease. *The Journal of allergy and clinical immunology* **119**, 1065-1071 (2007).
29. Soehnlein, O. Multiple roles for neutrophils in atherosclerosis. *Circulation research* **110**, 875-888 (2012).
30. Auffray, C., Sieweke, M.H. & Geissmann, F. Blood monocytes: development, heterogeneity, and relationship with dendritic cells. *Annual review of immunology* **27**, 669-692 (2009).
31. Pardali, E. & Waltenberger, J. Monocyte function and trafficking in cardiovascular disease. *Thrombosis and haemostasis* **108**, 804-811 (2012).
32. Geissmann, F., Jung, S. & Littman, D.R. Blood monocytes consist of two principal subsets with distinct migratory properties. *Immunity* **19**, 71-82 (2003).
33. Soehnlein, O., *et al.* Neutrophil secretion products pave the way for inflammatory monocytes. *Blood* **112**, 1461-1471 (2008).
34. Serbina, N.V., Jia, T., Hohl, T.M. & Pamer, E.G. Monocyte-mediated defense against microbial pathogens. *Annual review of immunology* **26**, 421-452 (2008).
35. Strauss-Ayali, D., Conrad, S.M. & Mosser, D.M. Monocyte subpopulations and their differentiation patterns during infection. *Journal of leukocyte biology* **82**, 244-252 (2007).
36. Sunderkotter, C., *et al.* Subpopulations of mouse blood monocytes differ in maturation stage and inflammatory response. *Journal of immunology* **172**, 4410-4417 (2004).
37. Kamei, M. & Carman, C.V. New observations on the trafficking and diapedesis of monocytes. *Current opinion in hematology* **17**, 43-52 (2010).
38. Nahrendorf, M., *et al.* The healing myocardium sequentially mobilizes two monocyte subsets with divergent and complementary functions. *The Journal of experimental medicine* **204**, 3037-3047 (2007).
39. Shi, C. & Pamer, E.G. Monocyte recruitment during infection and inflammation. *Nature reviews. Immunology* **11**, 762-774 (2011).
40. Ziegler-Heitbrock, L. The CD14+ CD16+ blood monocytes: their role in infection and inflammation. *Journal of leukocyte biology* **81**, 584-592 (2007).
41. van Furth, R. & Cohn, Z.A. The origin and kinetics of mononuclear phagocytes. *The Journal of experimental medicine* **128**, 415-435 (1968).

42. Hashimoto, D.*, et al.* Tissue-resident macrophages self-maintain locally throughout adult life with minimal contribution from circulating monocytes. *Immunity* **38**, 792-804 (2013).
43. Swirski, F.K.*, et al.* Identification of splenic reservoir monocytes and their deployment to inflammatory sites. *Science* **325**, 612-616 (2009).
44. Carlin, L.M.*, et al.* Nr4a1-dependent Ly6C(low) monocytes monitor endothelial cells and orchestrate their disposal. *Cell* **153**, 362-375 (2013).
45. Nourshargh, S., Hordijk, P.L. & Sixt, M. Breaching multiple barriers: leukocyte motility through venular walls and the interstitium. *Nature reviews. Molecular cell biology* **11**, 366-378 (2010).
46. Ley, K. The role of selectins in inflammation and disease. *Trends in molecular medicine* **9**, 263-268 (2003).
47. Alon, R.*, et al.* The integrin VLA-4 supports tethering and rolling in flow on VCAM-1. *The Journal of cell biology* **128**, 1243-1253 (1995).
48. Hynes, R.O. Integrins: bidirectional, allosteric signaling machines. *Cell* **110**, 673-687 (2002).
49. Schurpf, T. & Springer, T.A. Regulation of integrin affinity on cell surfaces. *The EMBO journal* **30**, 4712-4727 (2011).
50. Kinashi, T. Intracellular signalling controlling integrin activation in lymphocytes. *Nature reviews. Immunology* **5**, 546-559 (2005).
51. Allen, S.J., Crown, S.E. & Handel, T.M. Chemokine: receptor structure, interactions, and antagonism. *Annual review of immunology* **25**, 787-820 (2007).
52. Rossi, D. & Zlotnik, A. The biology of chemokines and their receptors. *Annual review of immunology* **18**, 217-242 (2000).
53. Bendall, L. Chemokines and their receptors in disease. *Histology and histopathology* **20**, 907-926 (2005).
54. Hamel, D.J., Sielaff, I., Proudfoot, A.E. & Handel, T.M. Chapter 4. Interactions of chemokines with glycosaminoglycans. *Methods in enzymology* **461**, 71-102 (2009).
55. Lodowski, D.T. & Palczewski, K. Chemokine receptors and other G protein-coupled receptors. *Current opinion in HIV and AIDS* **4**, 88-95 (2009).
56. Arnaout, M.A., Mahalingam, B. & Xiong, J.P. Integrin structure, allostery, and bidirectional signaling. *Annual review of cell and developmental biology* **21**, 381-410 (2005).
57. Sumagin, R., Prizant, H., Lomakina, E., Waugh, R.E. & Sarelius, I.H. LFA-1 and Mac-1 define characteristically different intralumenal crawling and emigration patterns for monocytes and neutrophils in situ. *Journal of immunology* **185**, 7057-7066 (2010).
58. Frommhold, D.*, et al.* RAGE and ICAM-1 differentially control leukocyte recruitment during acute inflammation in a stimulus-dependent manner. *BMC immunology* **12**, 56 (2011).
59. Diamond, M.S. & Springer, T.A. A subpopulation of Mac-1 (CD11b/CD18) molecules mediates neutrophil adhesion to ICAM-1 and fibrinogen. *The Journal of cell biology* **120**, 545-556 (1993).
60. McDonald, B.*, et al.* Intravascular danger signals guide neutrophils to sites of sterile inflammation. *Science* **330**, 362-366 (2010).
61. Schenkel, A.R., Mamdouh, Z. & Muller, W.A. Locomotion of monocytes on endothelium is a critical step during extravasation. *Nature immunology* **5**, 393-400 (2004).

62. Ryschich, E.*, et al.* Active leukocyte crawling in microvessels assessed by digital time-lapse intravital microscopy. *The Journal of surgical research* **135**, 291-296 (2006).
63. Phillipson, M.*, et al.* Vav1 is essential for mechanotactic crawling and migration of neutrophils out of the inflamed microvasculature. *Journal of immunology* **182**, 6870-6878 (2009).
64. Dixit, N., Yamayoshi, I., Nazarian, A. & Simon, S.I. Migrational guidance of neutrophils is mechanotransduced via high-affinity LFA-1 and calcium flux. *Journal of immunology* **187**, 472-481 (2011).
65. Jakob, S.M.*, et al.* Hematopoietic progenitor kinase 1 (HPK1) is required for LFA-1-mediated neutrophil recruitment during the acute inflammatory response. *Blood* **121**, 4184-4194 (2013).
66. Shulman, Z.*, et al.* Lymphocyte crawling and transendothelial migration require chemokine triggering of high-affinity LFA-1 integrin. *Immunity* **30**, 384-396 (2009).
67. Barreiro, O.*, et al.* Dynamic interaction of VCAM-1 and ICAM-1 with moesin and ezrin in a novel endothelial docking structure for adherent leukocytes. *The Journal of cell biology* **157**, 1233-1245 (2002).
68. Carman, C.V. & Springer, T.A. A transmigratory cup in leukocyte diapedesis both through individual vascular endothelial cells and between them. *The Journal of cell biology* **167**, 377-388 (2004).
69. Shaw, S.K., Bamba, P.S., Perkins, B.N. & Luscinskas, F.W. Real-time imaging of vascular endothelial-cadherin during leukocyte transmigration across endothelium. *Journal of immunology* **167**, 2323-2330 (2001).
70. Dvorak, A.M. & Feng, D. The vesiculo-vacuolar organelle (VVO). A new endothelial cell permeability organelle. *The journal of histochemistry and cytochemistry : official journal of the Histochemistry Society* **49**, 419-432 (2001).
71. Voisin, M.B., Probstl, D. & Nourshargh, S. Venular basement membranes ubiquitously express matrix protein low-expression regions: characterization in multiple tissues and remodeling during inflammation. *The American journal of pathology* **176**, 482-495 (2010).
72. Matzinger, P. Tolerance, danger, and the extended family. *Annual review of immunology* **12**, 991-1045 (1994).
73. Bianchi, M.E. DAMPs, PAMPs and alarmins: all we need to know about danger. *Journal of leukocyte biology* **81**, 1-5 (2007).
74. Kono, H. & Rock, K.L. How dying cells alert the immune system to danger. *Nature reviews. Immunology* **8**, 279-289 (2008).
75. Chen, G.Y. & Nunez, G. Sterile inflammation: sensing and reacting to damage. *Nature reviews. Immunology* **10**, 826-837 (2010).
76. van Beijnum, J.R., Buurman, W.A. & Griffioen, A.W. Convergence and amplification of toll-like receptor (TLR) and receptor for advanced glycation end products (RAGE) signaling pathways via high mobility group B1 (HMGB1). *Angiogenesis* **11**, 91-99 (2008).
77. Chen, C.J.*, et al.* Identification of a key pathway required for the sterile inflammatory response triggered by dying cells. *Nature medicine* **13**, 851-856 (2007).
78. Ross, R. Atherosclerosis--an inflammatory disease. *The New England journal of medicine* **340**, 115-126 (1999).

79. Ross, R. & Glomset, J.A. Atherosclerosis and the arterial smooth muscle cell: Proliferation of smooth muscle is a key event in the genesis of the lesions of atherosclerosis. *Science* **180**, 1332-1339 (1973).
80. Blann, A.D. Endothelial cell damage and the development or progression of atherosclerosis. *Clin Sci (Lond)* **97**, 119-121 (1999).
81. Davignon, J. & Ganz, P. Role of endothelial dysfunction in atherosclerosis. *Circulation* **109**, III27-32 (2004).
82. Bonetti, P.O., Lerman, L.O. & Lerman, A. Endothelial dysfunction: a marker of atherosclerotic risk. *Arteriosclerosis, thrombosis, and vascular biology* **23**, 168-175 (2003).
83. Vanhoutte, P.M. Endothelial dysfunction and atherosclerosis. *European heart journal* **18 Suppl E**, E19-29 (1997).
84. Stoletov, K.*, et al.* Vascular lipid accumulation, lipoprotein oxidation, and macrophage lipid uptake in hypercholesterolemic zebrafish. *Circulation research* **104**, 952-960 (2009).
85. Bochkov, V.N.*, et al.* Oxidized phospholipids stimulate tissue factor expression in human endothelial cells via activation of ERK/EGR-1 and Ca(++)/NFAT. *Blood* **99**, 199-206 (2002).
86. Gargalovic, P.S.*, et al.* The unfolded protein response is an important regulator of inflammatory genes in endothelial cells. *Arteriosclerosis, thrombosis, and vascular biology* **26**, 2490-2496 (2006).
87. Hansson, G.K. & Hermansson, A. The immune system in atherosclerosis. *Nature immunology* **12**, 204-212 (2011).
88. Van Vre, E.A., Ait-Oufella, H., Tedgui, A. & Mallat, Z. Apoptotic cell death and efferocytosis in atherosclerosis. *Arteriosclerosis, thrombosis, and vascular biology* **32**, 887-893 (2012).
89. de Souza, A.W., Westra, J., Limburg, P.C., Bijl, M. & Kallenberg, C.G. HMGB1 in vascular diseases: Its role in vascular inflammation and atherosclerosis. *Autoimmunity reviews* **11**, 909-917 (2012).
90. Kalinina, N.*, et al.* Increased expression of the DNA-binding cytokine HMGB1 in human atherosclerotic lesions: role of activated macrophages and cytokines. *Arteriosclerosis, thrombosis, and vascular biology* **24**, 2320-2325 (2004).
91. Kanellakis, P.*, et al.* High-mobility group box protein 1 neutralization reduces development of diet-induced atherosclerosis in apolipoprotein e-deficient mice. *Arteriosclerosis, thrombosis, and vascular biology* **31**, 313-319 (2011).
92. Ming, L.*, et al.* Simvastatin suppressed HMGB1-RAGE axis and atherosclerosis via mevalonate pathway. *Heart* **97**, A47 (2011).
93. Drechsler, M., Megens, R.T., van Zandvoort, M., Weber, C. & Soehnlein, O. Hyperlipidemia-triggered neutrophilia promotes early atherosclerosis. *Circulation* **122**, 1837-1845 (2010).
94. Naruko, T.*, et al.* Neutrophil infiltration of culprit lesions in acute coronary syndromes. *Circulation* **106**, 2894-2900 (2002).
95. Rotzius, P.*, et al.* Distinct infiltration of neutrophils in lesion shoulders in ApoE-/- mice. *The American journal of pathology* **177**, 493-500 (2010).
96. Zernecke, A.*, et al.* Protective role of CXC receptor 4/CXC ligand 12 unveils the importance of neutrophils in atherosclerosis. *Circulation research* **102**, 209-217 (2008).
97. Soehnlein, O. & Weber, C. Myeloid cells in atherosclerosis: initiators and decision shapers. *Seminars in immunopathology* **31**, 35-47 (2009).

98. Doring, Y., *et al.* Lack of neutrophil-derived CRAMP reduces atherosclerosis in mice. *Circulation research* **110**, 1052-1056 (2012).
99. Ionita, M.G., *et al.* High neutrophil numbers in human carotid atherosclerotic plaques are associated with characteristics of rupture-prone lesions. *Arteriosclerosis, thrombosis, and vascular biology* **30**, 1842-1848 (2010).
100. Swirski, F.K., *et al.* Ly-6Chi monocytes dominate hypercholesterolemia-associated monocytosis and give rise to macrophages in atheromata. *The Journal of clinical investigation* **117**, 195-205 (2007).
101. Swirski, F.K., *et al.* Monocyte accumulation in mouse atherogenesis is progressive and proportional to extent of disease. *Proceedings of the National Academy of Sciences of the United States of America* **103**, 10340-10345 (2006).
102. Johnsen, S.H., *et al.* Monocyte count is a predictor of novel plaque formation: a 7-year follow-up study of 2610 persons without carotid plaque at baseline the Tromso Study. *Stroke; a journal of cerebral circulation* **36**, 715-719 (2005).
103. Ylitalo, R., Oksala, O., Yla-Herttuala, S. & Ylitalo, P. Effects of clodronate (dichloromethylene bisphosphonate) on the development of experimental atherosclerosis in rabbits. *The Journal of laboratory and clinical medicine* **123**, 769-776 (1994).
104. Soehnlein, O., *et al.* Distinct functions of chemokine receptor axes in the atherogenic mobilization and recruitment of classical monocytes. *EMBO molecular medicine* **5**, 471-481 (2013).
105. Haka, A.S., Potteaux, S., Fraser, H., Randolph, G.J. & Maxfield, F.R. Quantitative analysis of monocyte subpopulations in murine atherosclerotic plaques by multiphoton microscopy. *PloS one* **7**, e44823 (2012).
106. Tacke, F., *et al.* Monocyte subsets differentially employ CCR2, CCR5, and CX3CR1 to accumulate within atherosclerotic plaques. *The Journal of clinical investigation* **117**, 185-194 (2007).
107. Stolla, M., *et al.* Fractalkine is expressed in early and advanced atherosclerotic lesions and supports monocyte recruitment via CX3CR1. *PloS one* **7**, e43572 (2012).
108. Combadiere, C., *et al.* Decreased atherosclerotic lesion formation in CX3CR1/apolipoprotein E double knockout mice. *Circulation* **107**, 1009-1016 (2003).
109. Lesnik, P., Haskell, C.A. & Charo, I.F. Decreased atherosclerosis in CX3CR1-/- mice reveals a role for fractalkine in atherogenesis. *The Journal of clinical investigation* **111**, 333-340 (2003).
110. Teupser, D., *et al.* Major reduction of atherosclerosis in fractalkine (CX3CL1)-deficient mice is at the brachiocephalic artery, not the aortic root. *Proceedings of the National Academy of Sciences of the United States of America* **101**, 17795-17800 (2004).
111. Huo, Y., Hafezi-Moghadam, A. & Ley, K. Role of vascular cell adhesion molecule-1 and fibronectin connecting segment-1 in monocyte rolling and adhesion on early atherosclerotic lesions. *Circulation research* **87**, 153-159 (2000).
112. Ramos, C.L., *et al.* Direct demonstration of P-selectin- and VCAM-1-dependent mononuclear cell rolling in early atherosclerotic lesions of apolipoprotein E-deficient mice. *Circulation research* **84**, 1237-1244 (1999).
113. Huo, Y., *et al.* The chemokine KC, but not monocyte chemoattractant protein-1, triggers monocyte arrest on early atherosclerotic endothelium. *The Journal of clinical investigation* **108**, 1307-1314 (2001).

114. Eriksson, E.E., Xie, X., Werr, J., Thoren, P. & Lindbom, L. Direct viewing of atherosclerosis in vivo: plaque invasion by leukocytes is initiated by the endothelial selectins. *FASEB journal : official publication of the Federation of American Societies for Experimental Biology* **15**, 1149-1157 (2001).
115. Galkina, E.*, et al.* Lymphocyte recruitment into the aortic wall before and during development of atherosclerosis is partially L-selectin dependent. *The Journal of experimental medicine* **203**, 1273-1282 (2006).
116. Kircher, M.F.*, et al.* Noninvasive in vivo imaging of monocyte trafficking to atherosclerotic lesions. *Circulation* **117**, 388-395 (2008).
117. Eriksson, E.E. Intravital microscopy on atherosclerosis in apolipoprotein e-deficient mice establishes microvessels as major entry pathways for leukocytes to advanced lesions. *Circulation* **124**, 2129-2138 (2011).
118. Megens, R.T.*, et al.* In vivo high-resolution structural imaging of large arteries in small rodents using two-photon laser scanning microscopy. *Journal of biomedical optics* **15**, 011108 (2010).
119. Zoumi, A., Lu, X., Kassab, G.S. & Tromberg, B.J. Imaging coronary artery microstructure using second-harmonic and two-photon fluorescence microscopy. *Biophysical journal* **87**, 2778-2786 (2004).
120. van Zandvoort, M.*, et al.* Two-photon microscopy for imaging of the (atherosclerotic) vascular wall: a proof of concept study. *Journal of vascular research* **41**, 54-63 (2004).
121. Megens, R.T.*, et al.* Two-photon microscopy of vital murine elastic and muscular arteries. Combined structural and functional imaging with subcellular resolution. *Journal of vascular research* **44**, 87-98 (2007).
122. Campagnola, P.J.*, et al.* Three-dimensional high-resolution second-harmonic generation imaging of endogenous structural proteins in biological tissues. *Biophysical journal* **82**, 493-508 (2002).
123. de Grauw, C.J., Vroom, J.M., van der Voort, H.T. & Gerritsen, H.C. Imaging properties in two-photon excitation microscopy and effects of refractive-index mismatch in thick specimens. *Applied optics* **38**, 5995-6003 (1999).
124. Yu, W., Braz, J.C., Dutton, A.M., Prusakov, P. & Rekhter, M. In vivo imaging of atherosclerotic plaques in apolipoprotein E deficient mice using nonlinear microscopy. *Journal of biomedical optics* **12**, 054008 (2007).
125. Megens, R.T.*, et al.* Presence of luminal neutrophil extracellular traps in atherosclerosis. *Thrombosis and haemostasis* **107**, 597-598 (2012).
126. Curtiss, L.K. ApoE in atherosclerosis : a protein with multiple hats. *Arteriosclerosis, thrombosis, and vascular biology* **20**, 1852-1853 (2000).
127. Pendse, A.A., Arbones-Mainar, J.M., Johnson, L.A., Altenburg, M.K. & Maeda, N. Apolipoprotein E knock-out and knock-in mice: atherosclerosis, metabolic syndrome, and beyond. *Journal of lipid research* **50 Suppl**, S178-182 (2009).
128. Nakashima, Y., Plump, A.S., Raines, E.W., Breslow, J.L. & Ross, R. ApoE-deficient mice develop lesions of all phases of atherosclerosis throughout the arterial tree. *Arteriosclerosis and thrombosis : a journal of vascular biology / American Heart Association* **14**, 133-140 (1994).
129. Jones, B.A., Beamer, M. & Ahmed, S. Fractalkine/CX3CL1: a potential new target for inflammatory diseases. *Molecular interventions* **10**, 263-270 (2010).
130. Jung, S.*, et al.* Analysis of fractalkine receptor CX(3)CR1 function by targeted deletion and green fluorescent protein reporter gene insertion. *Molecular and cellular biology* **20**, 4106-4114 (2000).

131. Faust, N., Varas, F., Kelly, L.M., Heck, S. & Graf, T. Insertion of enhanced green fluorescent protein into the lysozyme gene creates mice with green fluorescent granulocytes and macrophages. *Blood* **96**, 719-726 (2000).
132. Boes, M.*, et al.* T-cell engagement of dendritic cells rapidly rearranges MHC class II transport. *Nature* **418**, 983-988 (2002).
133. Linton, M.F., Atkinson, J.B. & Fazio, S. Prevention of atherosclerosis in apolipoprotein E-deficient mice by bone marrow transplantation. *Science* **267**, 1034-1037 (1995).
134. Ng, L.G.*, et al.* Visualizing the neutrophil response to sterile tissue injury in mouse dermis reveals a three-phase cascade of events. *The Journal of investigative dermatology* **131**, 2058-2068 (2011).
135. Stark, K.*, et al.* Capillary and arteriolar pericytes attract innate leukocytes exiting through venules and 'instruct' them with pattern-recognition and motility programs. *Nature immunology* **14**, 41-51 (2013).
136. Lammermann, T.*, et al.* Neutrophil swarms require LTB4 and integrins at sites of cell death in vivo. *Nature* **498**, 371-375 (2013).
137. Proebstl, D.*, et al.* Pericytes support neutrophil subendothelial cell crawling and breaching of venular walls in vivo. *The Journal of experimental medicine* **209**, 1219-1234 (2012).
138. Zarins, C.K.*, et al.* Carotid bifurcation atherosclerosis. Quantitative correlation of plaque localization with flow velocity profiles and wall shear stress. *Circulation research* **53**, 502-514 (1983).
139. Ku, D.N., Giddens, D.P., Zarins, C.K. & Glagov, S. Pulsatile flow and atherosclerosis in the human carotid bifurcation. Positive correlation between plaque location and low oscillating shear stress. *Arteriosclerosis* **5**, 293-302 (1985).
140. Olshansky, B., Sabbah, H.N., Hauptman, P.J. & Colucci, W.S. Parasympathetic nervous system and heart failure: pathophysiology and potential implications for therapy. *Circulation* **118**, 863-871 (2008).
141. Schweitzer, P. & Teichholz, L.E. Carotid sinus massage. Its diagnostic and therapeutic value in arrhythmias. *The American journal of medicine* **78**, 645-654 (1985).
142. Alexander, S. & Ping, W.C. Fatal ventricular fibrillation during carotid sinus stimulation. *The American journal of cardiology* **18**, 289-291 (1966).
143. M. SHOTTON, D. Confocal scanning optical microscopy and its applications for biological specimens. *Journal of Cell Science* **94**, 175-206 (1989).
144. Oheim, M., Michael, D.J., Geisbauer, M., Madsen, D. & Chow, R.H. Principles of two-photon excitation fluorescence microscopy and other nonlinear imaging approaches. *Advanced Drug Delivery Reviews* **58**, 788-808 (2006).
145. Potter, S.M. Vital imaging: Two photons are better than one. *Current biology : CB* **6**, 1595-1598 (1996).
146. Grzybowski, A. & Pietrzak, K. Maria Goeppert-Mayer (1906-1972): two-photon effect on dermatology. *Clinics in dermatology* **31**, 221-225 (2013).
147. Helmchen, F. & Denk, W. Deep tissue two-photon microscopy. *Nature methods* **2**, 932-940 (2005).
148. Potter, S.M. Vital imaging: two photons are better than one. *Current biology : CB* **6**, 1595-1598 (1996).
149. Sumen, C., Mempel, T.R., Mazo, I.B. & von Andrian, U.H. Intravital microscopy: visualizing immunity in context. *Immunity* **21**, 315-329 (2004).
150. Hickey, M.J., Bullard, D.C., Issekutz, A. & James, W.G. Leukocyte-Endothelial Cell Interactions Are Enhanced in Dermal Postcapillary Venules of MRL/faslpr

(Lupus-Prone) Mice: Roles of P- and E-Selectin. *The Journal of Immunology* **168**, 4728-4736 (2002).
151. Gavins, F.N. & Chatterjee, B.E. Intravital microscopy for the study of mouse microcirculation in anti-inflammatory drug research: focus on the mesentery and cremaster preparations. *Journal of pharmacological and toxicological methods* **49**, 1-14 (2004).
152. Koltsova, E.K.*, et al.* Dynamic T cell-APC interactions sustain chronic inflammation in atherosclerosis. *The Journal of clinical investigation* **122**, 3114-3126 (2012).
153. Kinashi, T. & Katagiri, K. Regulation of immune cell adhesion and migration by regulator of adhesion and cell polarization enriched in lymphoid tissues. *Immunology* **116**, 164-171 (2005).
154. Kanemitsu, N.*, et al.* CXCL13 is an arrest chemokine for B cells in high endothelial venules. *Blood* **106**, 2613-2618 (2005).
155. Foxman, E.F., Kunkel, E.J. & Butcher, E.C. Integrating conflicting chemotactic signals. The role of memory in leukocyte navigation. *The Journal of cell biology* **147**, 577-588 (1999).
156. Heit, B., Colarusso, P. & Kubes, P. Fundamentally different roles for LFA-1, Mac-1 and alpha4-integrin in neutrophil chemotaxis. *J Cell Sci* **118**, 5205-5220 (2005).
157. Harler, M.B., Wakshull, E., Filardo, E.J., Albina, J.E. & Reichner, J.S. Promotion of Neutrophil Chemotaxis Through Differential Regulation of β1 and β2 Integrins. *The Journal of Immunology* **162**, 6792-6799 (1999).
158. Mine, S.*, et al.* Oxidized low density lipoprotein-induced LFA-1-dependent adhesion and transendothelial migration of monocytes via the protein kinase C pathway. *Atherosclerosis* **160**, 281-288 (2002).
159. Suzuki, J.*, et al.* Inhibition of accelerated coronary atherosclerosis with short-term blockade of intercellular adhesion molecule-1 and lymphocyte function-associated antigen-1 in a heterotopic murine model of heart transplantation. *The Journal of heart and lung transplantation : the official publication of the International Society for Heart Transplantation* **16**, 1141-1148 (1997).
160. Sotiriou, S.N.*, et al.* Lipoprotein(a) in atherosclerotic plaques recruits inflammatory cells through interaction with Mac-1 integrin. *The FASEB Journal* (2006).
161. Merched, A., Tollefson, K. & Chan, L. Beta2 integrins modulate the initiation and progression of atherosclerosis in low-density lipoprotein receptor knockout mice. *Cardiovascular research* **85**, 853-863 (2010).
162. Kubo, N., Boisvert, W.A., Ballantyne, C.M. & Curtiss, L.K. Leukocyte CD11b expression is not essential for the development of atherosclerosis in mice. *Journal of lipid research* **41**, 1060-1066 (2000).

Acknowledgements

I would like to sincerely thank and express my gratitude to my supervisor Prof. Dr.med Steffen Massberg for his scientific and personal guidance. His high quality scientific knowledge and experience were very valuable for me. Without his support I would not be able to complete this study.

I would also like to thank Dr Alexander Khandoga for his collaboration and guidance through the period of my work in our laboratory. He introduced the “continuous single cell tracking protocol” and this project was shaped under his advice.

In addition I would like to thank Veronica Liegsatz who worked for her doctoral Thesis in this project prior to my arrival in our group. The experiments regarding the direct effect of blocking of Mac-1 in the crawling of patrolling monocytes under steady state conditions were performed in collaboration with her.

I would further like to thank Dr Michael Lorenz who provided valuable daily assistance and advice during the whole period of my dissertation research which allowed me to improve as a scientist.

I would also I like to thank all my colleagues in our laboratory for their scientific collaboration and the pleasant atmosphere that they create in our group.

Finally I would especially like to thank my parents Anastasia and Luigi and my brother Theocharis- Alessandro for their invaluable support and belief in me. Without them it would have been impossible to fulfil my dissertation.

Publications

Monocytes, neutrophils, and platelets cooperate to initiate and propagate venous thrombosis in mice in vivo.
von Brühl ML, Stark K, Steinhart A, Chandraratne S, Konrad I, Lorenz M, Khandoga A, Tirniceriu A, **Coletti R**, Köllnberger M, Byrne RA, Laitinen I, Walch A, Brill A, Pfeiler S, Manukyan D, Braun S, Lange P, Riegger J, Ware J, Eckart A, Haidari S, Rudelius M, Schulz C, Echtler K, Brinkmann V, Schwaiger M, Preissner KT, Wagner DD, Mackman N, Engelmann B, Massberg S.